THE UNIVERSITY OF CHICAGO

DIVISIVE NORMALIZATION AND THE FLEXIBLE RESOLUTION OF AMBIGUITY

A DISSERTATION SUBMITTED TO
THE FACULTY OF THE DIVISION OF THE SOCIAL SCIENCES
IN CANDIDACY FOR THE DEGREE OF
DOCTOR OF PHILOSOPHY

DEPARTMENT OF PSYCHOLOGY

BY
JAELYN R. PEISO

CHICAGO, ILLINOIS
AUGUST 2022

Se lo dedico a mis Abuelos.

Porque me amaste, todos.

TABLE OF CONTENTS

LIST OF FIGURES

ABSTRACT

Our visual systems usually construct a useful and unambiguous representation of the world. When the visual system is presented with multiple compelling interpretations of the same space, neural populations compete for perceptual dominance to resolve ambiguity. Spatial and temporal context can guide the build-up of perceptual experience. Recent evidence shows that ambiguous representations can be resolved by enhancing differences between objects in view, in addition to enhancing perceived similarity (so-called interocular grouping, Peiso and Shevell, 2020). This dissertation investigated the possible role of divisive normalization in the resolution of ambiguous neural representations. The reported experiments use rivalrous dichoptic stimuli presented in interocular-switch rivalry to evoke neural ambiguity and observer reports of perceptual experience. Four experiments manipulated either the feature relations within a rivalrous dichoptic signal (Experiment 1) or adjacent non-rivalrous regions (Experiments 2-4) to investigate the influence of spatiochromatic context on the resolution of ambiguity. Within a single trial, observers' reports revealed the duration that various stimuli resulted in similarity-enhanced or difference-enhanced percepts. Similarity-enhancement refers to the resolution of percepts that reduce the visual distinctiveness of (1) rivalrous regions from each other or (2) rivalrous regions from their shared background; conversely, difference-enhancement refers to the resolution of percepts that increase the visual distinctiveness of objects in view. The motivating theoretical framework integrated divisive normalization accounts of attention and figure-ground processing to explain the perceptual flexibility observed in binocular rivalry experiments. Four experiments supported the hypothesis that a context-dependent divisive-normalization mechanism acts on a rivalrous chromatic signal to alter the resolution of ambiguity.

CHAPTER 1

INTRODUCTION

The goal of perception is to reduce the inherent uncertainty in the sensory representations of a complex and dynamic world. In the early stages of visual processing, there is never a one-to-one correspondence between neural representations and the objects in the physical world. Sensory representations are inherently ambiguous, as two-dimensional retinal images are expanded into a three-dimensional representation of the world. Incomplete or low-quality visual information can evoke additional neural ambiguity. A veridical model of the physical world is impossible as the reflected light captured by photoreceptors is always of lower dimensionality than the physical object it represents. The uncertainty inherent in our sensory representations of our world is not a new idea. Plato's allegory of the cave (275 BCE) aptly characterizes the point at hand; our experienced reality is nothing more than shadows on the proverbial cave wall. Inherent in a lower-dimensional projection from a higher-dimensional space is a perspective, just like the cave wall must be illuminated from a single direction to produce an articulated shadow.

Even if the visual system could receive a three-dimensional signal, a one-to-one correspondence between physical objects and perception would be disadvantageous to organisms because simultaneously producing a high-fidelity representation of every visible part of a complex scene is computationally untenable. Consider walking down a busy street; you may visually represent *all* the nearby dogs (and maybe their humans), bicyclists, cars, and buildings, but at what cost? Lost representations could include the visible irregularities in the sidewalk or anything specific about the person walking next to you. Without cortical capacity constraints, there may be little need for attention and working memory to help allocate resources and maintain representations (Linden et al., 2003). The nervous system has a finite number of neurons at any given moment, each with a limited dynamic range (Barlow, 1981). Due to these constraints, visual systems have evolved to selectively enhance,

attenuate, and combine features building up a perceptual experience that can support action in the present moment.

From this perspective, ambiguity resolution is the goal of everyday visual perception. When stimuli are ambiguous, perception must remain flexible—having some processes for deciding which feature combinations are meaningful and updating this decision over time. Typically, sensory cues converge on a single percept, with little competing evidence. Perception can be quite fast in these cases, resolving a stable and unchanging perceptual representation of a novel natural scene in as little as 150ms (Vanmarcke and Wagemans, 2015). Perceptual biases enable timely and meaningful perception in the face of incomplete or ambiguous visual information. What processes support perceptual flexibility so that neural representations for the same stimulus can evoke different percepts?

This dissertation will draw on several paradigms to characterize visual ambiguity resolution in the context of ordinary perception. Specifically, figure-ground segregation, perceptual grouping, and attentional enhancement are considered in the context of perceptual biases. Divisive normalization is suggested to be the supporting computation, acting across levels of the nervous system to enhance the signal-to-noise ratio (SNR) by dividing a neuron's response by the pooled response of other stimulus-responsive neurons. Divisive normalization has been implicated as the computation that underlies attention's perceptual enhancement effects (Cohen and Maunsell, 2011; Lee and Maunsell, 2009; Reynolds and Heeger, 2009; Schwartz and Coen-Cagli, 2013). Finally, an account of ambiguity resolution relying on dynamic feature-linking is proposed. Here, normalization pools provide implicit linking between features across the visual scene. Normalization pools are not fixed and change depending on the observer's goals, the stimulus, or both (i.e., task demands).

1.1 Perceptual Organization

> Why We See Things and Not the Holes Between Them... In the first place, the segregation and unification which occurs will separate areas of different degrees of internal articulation, and according to our [Gestalt] law, the more highly articulated ones will become figures, the rest fusing together to form the ground. Look at any landscape photograph. You see the shape of the things, the mountains, and trees and buildings, but not of the sky (Koffka, 1935).

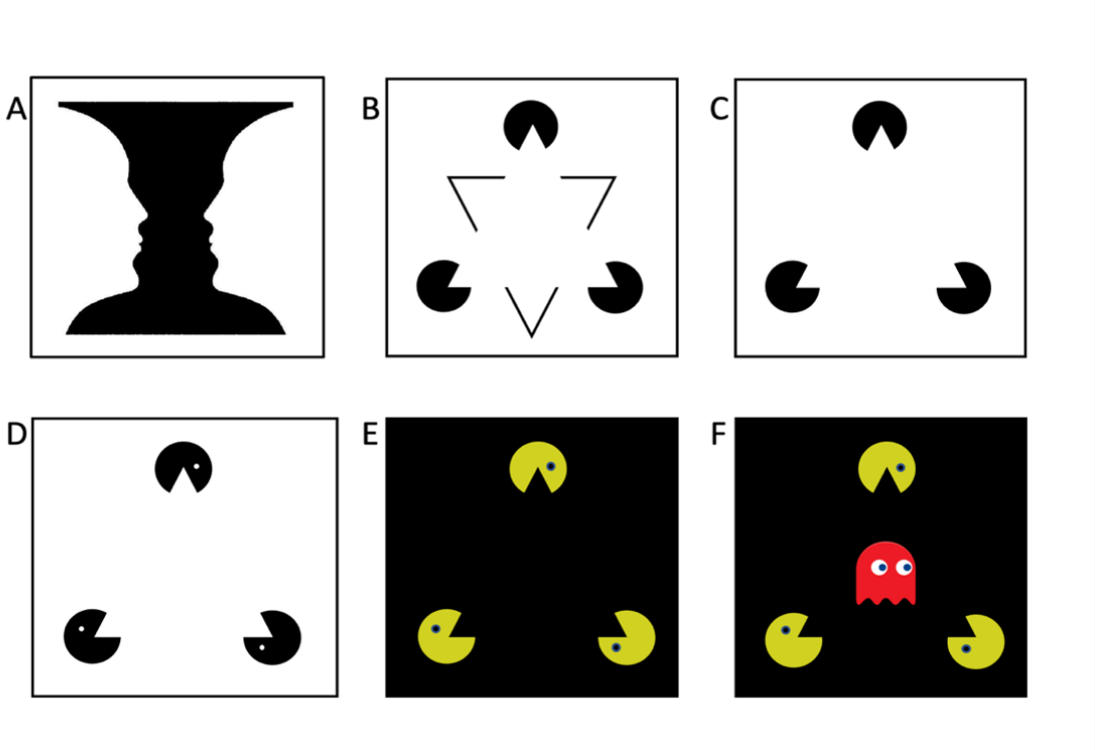

Figure 1.1: A) Rubin's Face, a bistable figure evoking near equal incidence of each figure. B) The Kanizsa triangle. C-F) Cues for one percept are removed (illusory triangle) and cues for another (Pac-Men as figures) are added.

Figure-ground segregation refers to the outcome of processes responsible for determining which region(s) of the visual field should be perceived as the background or ground; and which regions constitute the figure and should thus be prioritized in processing as the focus of perception. Classically, the study of figure-ground segregation emerged from the Gestalt

theorists, which described perceptual organization as a set of common cues that bias the perceptual grouping of objects and features in view. Here, cues such as continuity, similarity, proximity, and implied closure can lead the visual system to link certain features together and not others (Figure 1.1 A & B). This results in biases toward specific percepts, especially when multiple cues converge on the same conclusion (Koffka, 1935). For instance, in Koffka's mountain scene, several mountains group together based on their featural similarity and spatial proximity, evoking the percept of a continuous mountain range lining a continuous sky. These groupings provide perceptual continuity even if foreground trees parcel the mountain and sky into sections. Gestalt rules of perceptual organization can guide the creation of stimuli that evoke perceptually measurable neural ambiguity. Implicit in Koffka's musings about seeing the shape of the mountains and not the sky is the automaticity with which a figure is segregated from the ground. Figure-ground segregation is happening continuously, perceptually instantaneous, and not unique to vision (Rokni et al., 2014; Teki et al., 2011). Figure-ground segregation is influenced by bottom-up signals and can be modulated by top-down attention (Koffka, 1935; Poort et al., 2016; Toppino, 2003). There are many possible figures to enhance in most visual scenes each moment. The signals that are enhanced as figures and those suppressed as the ground can change dynamically with perceiver goals and fluctuations in attention (Huang et al., 2020). Figure-ground segregation is flexible—regions resolved as figures need not be all of the objects in the scene; many behaviorally irrelevant objects are selectively attenuated as the background. Additionally, figure-ground segregation is recurrently updated (Drewes et al., 2016; Lamme, 1995). This moment-by-moment segregation is imperative to both prediction and action.

Adaptive behavior requires perception to be selective. Perceptually grouped percepts are a functional and efficient representation of the world. When regions of the visual field are correlated by having similar features or feature conjunctions (e.g., color, contrast, and/or motion), perceptual groups are formed to improve perceptual efficiency. For example, the

capacity to perceptually group trees into a forest enables perceptual resources to be allocated elsewhere. When driving on a tree-lined road, a perceptual group can form out of the hundreds of individual trees that are visible. A continuous forest percept frees perceptual resources for enhancing signals from task-relevant stimuli, such as other cars and animals. Implicit in a grouped percept, such as a forest, is the loss of some differentiating information about individual parts that comprise it. For example, natural camouflage works well because the animal's features are grouped with the environment's features rendering it nearly undetectable. In this case, the visual system must enhance deviations from similarity to detect low-salience targets, like camouflaged animals.

In natural viewing, stimuli are often complex and have many time and space correlations. For example, a blue ball resting on the floor provides a form and color signal that is bound into one perceptual representation. If the ball is subsequently pushed, its features remain bounded as it moves across the floor in the direction of the applied force. In the absence of additional forces applied to the ball, it eventually comes to a stop. From a predictive coding perspective, the visual system uses these correlations alongside memory to form representations similar to statistical priors on the likelihood of candidate percepts, and these priors bias perception accordingly (Barlow et al., 1961). In the laboratory, researchers can carefully control stimulus properties and in doing so, manipulate the frequency of possible percepts. Consider the visual search paradigm, where targets can be rapidly identified if the perceptual task is easy due to more prominent differences between the target and distractors. When distractors are very similar or too numerous, attention must be deployed to search for a target serially, and this is marked by increases in reaction times (Treisman and Gelade, 1980; Wolfe, 2020). Similarity-enhancement due to grouping the target with the distractors interferes with perceptual efficiency, just as it does when searching for a camouflaged animal. The visual system can benefit from flexibly deploying perceptual biases depending on image properties and behavioral goals, as universally enhancing similarity or dissimilarity results

in visual representations that may be ineffective in supporting behavior.

Stimuli that are not completely perceptually resolved as a single perceptual representation are multistable. If a stimulus has only two stable perceptual representations, such as Rubin's vase (Figure 1.1 A), it is bistable. Multistability is easiest to demonstrate in bistable figures, such as Rubin's Face illusion (Figure 1.1 A) and the Kanizsa Triangle (Figure 1.1 B). Rubin's face illusion produces alternating percepts of either a vase or two faces over time (Kanizsa, 1976; Rubin, 1915). In this classic illusion, the vase is the dark figure in the center, and the negative white space formed by the edges of the vase's silhouette renders mirror images of faces in profile. Here, the main goal of perceptual organization is to segregate a figure (the object of perception) from the background. Enhancing the figure's signal and suppressing the ground signal enables action in a world where many stimuli compete to dominate perception.

Unlike Rubin's face illusion, not all multistable images lead to the near-equal frequency that observers perceive each candidate percept. In this case, the visual system accumulates unequal evidence for candidate percepts, and one percept is reliably selected by the visual system, as is the case with the Kanizsa triangle (Figure 1.1 B). Here, it is very difficult to perceive the objects at the triangle's vertices as the Pac-Man™ shaped figures that they are physically. Instead, the most frequent percept is of dark circles occluded by the light triangle, which also occludes an apparent second triangle outlined in black. Even when removing a cue, such as the second triangle (Figure 1.1 C), the image strongly promotes the triangle hypothesis; however, this is weakened by losing evidence for the triangle-on-top percept. The Kanizsa triangle takes advantage of the Gestalt principles of good continuation, closure, and depth through apparent occlusion to segregate the figure from the background—tipping the perceptual scale and biasing perception towards a white triangle atop three dark circles. By giving the Pac-Men eyes (white circles), it may become easier, but not easy, to perceive the Pac-Men as foreground figures (Figure 1.1 D). Now, let's enhance the Pac-Men as figure representation even more by rendering them in their associated color of yellow (Figure 1.1 E).

Finally, giving the Pac-Men their familiar ghostly prey (Figure 1.1 F) makes it less challenging to see the yellow circles as Pac-Men. The triangle formed by negative space frequently groups with the background and vanishes, albeit not permanently, from perception. Even when all the cues are stacked against the triangle percept (as in Figure 1.1 E), the Kanizsa triangle remains a strong illusion seeming to defy the added spatial and semantic evidence (for another example, see Peterson, 1999). The only way to completely remove the triangle percept is to rotate the triangle vertices away until the Pac-Man™ mouths do not contain a common region (Figure 1.2 B). When only two of the Pac-Men point to a common region (as in Figure 1.2 A), there is still enough evidence for a partial shape, and this percept will alternate with seeing the Pac-Men as foreground figures. In each moment, the visual system uses available evidence, including contextual clues and associations from memory (e.g., a yellow Pac-Man™ against a black background), to build the most useful representation of the visual field possible (Pylyshyn, 1999).

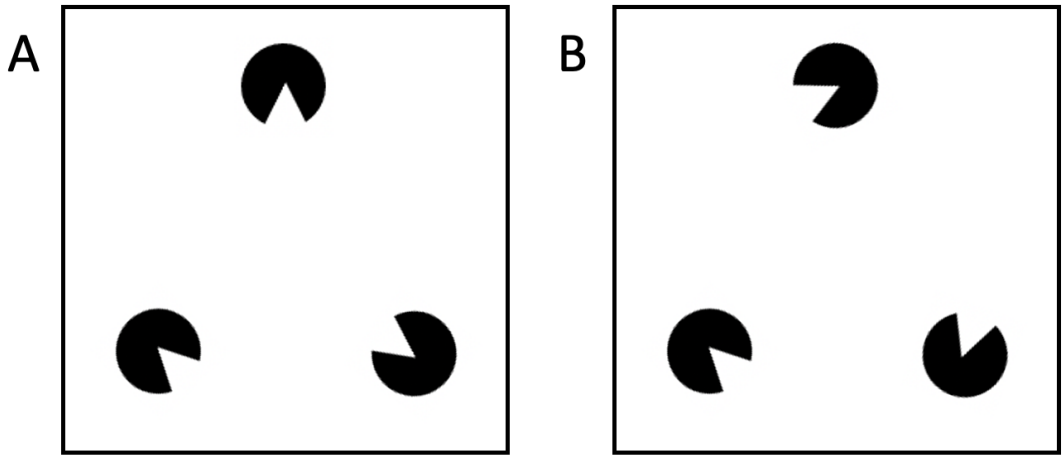

Figure 1.2: Pac-Man™ and Kanizsa triangle illusion. A) Despite ruining the triangle, a figure with at least two vertices still pops out from illusory contours. B) Illusory contours are abolished when none of the Pac-Men converge on a shared location.

Multistability has been frequently studied in perceptual grouping, binocular rivalry, and figure-ground segregation. In binocular rivalry, conflicting information is shown to cor-

responding regions of each eye, thus producing neural ambiguity. Two different physical objects in the world cannot occupy the same space at the same time. The visual system uses information from each eye alone and combines information across the two eyes to produce coherent percepts (Kovács et al., 1996). Similar to bistable figures, binocularly rivalrous stimuli evoke perceptual alternations between percepts. In conventional binocular rivalry, a meaningful percept (i.e., complete chimpanzee face) is available from monocular neural signals alone, which confounds coherency and eye-of-origin information (as in Figure 1.3 A & C). In patchwork rivalry, however, percept coherency and eye-of-origin information are dissociated (Kovács et al., 1996). In this case, a coherent percept requires selective integration from signals originating in both eyes (as in Figure 1.3 B & D). Coherence generally refers to the degree of statistical correlation (e.g., collinearity) across space and time (Ngo et al., 2000). For the example stimuli in Figure 1.3, patchwork presentation refers to presenting each eye with a mix of the possible dichoptic signal, such that neither eye ever has access to a complete chimpanzee face (Figure 1.3 B) or a uniformly colored dot array (Figure 1.3 D). Even with simple stimuli (e.g., Figure 1.3 C & D), the visual system reliably produces grouped percepts, resulting in perceptual alternations between all red and all green dots.

The unnatural experience of two entirely different images corresponding to the same area in space at the same time violates the visual system's expectation that objects occupying the same space at the same time are the same object. Such a violation introduces uncertainty, which interferes with stable perception (Hohwy et al., 2008; Hohwy, 2012). Drawing on a predictive coding perspective, the accumulation of evidence for the suppressed percept over time results in destabilizing the dominant percept, resulting in a switch between the two percepts (Hohwy et al., 2008). From this framework, conscious perception is the result of a prediction error minimization process. In binocular rivalry experiments, evidence strength is held constant for certain low-level features such as luminance contrast, while other features like chromaticity and orientation are systematically varied. The ambiguity evoked by binoc-

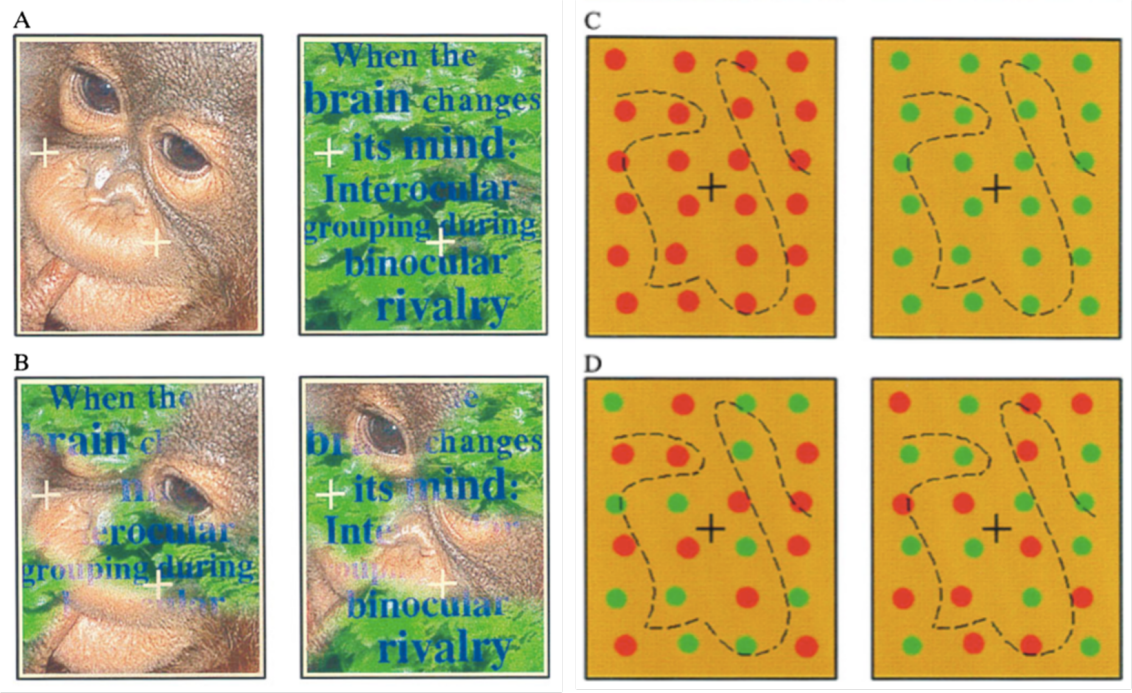

Figure 1.3: Conventional (A & C) & Patchwork Presentations (B & D). Images from (Kovács et al., 1996)© National Academy of Sciences.

ular rivalry may be different from other types of multistability since there are two signals for the same region of space. Despite this possible difference, the experience of binocular rivalry in everyday seeing makes it unlikely that ambiguity resolution of rivalrous stimuli relies on unique mechanisms (Brascamp and Shevell, 2021).

The perspective taken by this proposal is that the goal of all perceptual processing is ambiguity resolution (Geisler, 2011; Hohwy, 2012). Since everyday perception is ambiguity resolution, the present dissertation posits that the computations and mechanisms that support figure-ground segregation also underlie ambiguity resolution. Principally, it is suggested that the non-dominant percept(s) during rivalrous perception can be momentarily attenuated as the background. Here, attention samples active neural populations promoting different representations (Davidson et al., 2018). In doing so, attention dictates the landscape of candidate percepts—the resulting perceptual biases aid in reducing the infinite space of all possible pixel-by-pixel binocular combinations. The percepts experienced while

viewing rivalrous stimuli are only a subset of what is perceptually possible from the stimulus. This may provide phenomenological support for the role of attention in producing efficient representations by selecting which neural representations are sampled over time. Despite the apparent lack of top-down attentional modulation of perceptual experience during binocular rivalry (Meng and Tong, 2004), attention modulates alternation speed (Dieter et al., 2015), and inattention eliminates binocular rivalry altogether (Brascamp and Blake, 2012; Li et al., 2017; Zhang et al., 2011). This is compelling evidence that attention often contributes to perceptual disambiguation. The present work offers an extension of Barlow's feature-linking hypothesis (Barlow, 1981), which entails dynamic feature-linking depending on perceiver goals and fluctuations in attention. Dynamic feature-linking is posited to rely on flexible normalization pools (Schwartz and Coen-Cagli, 2013), where a neuron's response can be attenuated by cells with similar response profiles. Here, a neuron's response is normalized differentially depending on if the stimulus in its receptive field is currently being enhanced as a figure or, alternatively, suppressed as the background.

1.2 Flexible Normalization Pools & Dynamic Feature-Linking

In tandem, attention and adaptation make nearly all stimuli multistable (Kim et al., 2006). Attention destabilizes perception in the face of an unchanged stimulus by selectively enhancing some neural responses via gain modulation. Adaptation provides a recurrent recalibration of perception based on prevailing temporal statistics, reducing contrast gain for a dominant percept after sustained exposure. Adaptation can be operationally defined as a brief change in sensitivity or perception when exposed to a new stimulus and is marked by lingering aftereffects once the stimulus is absent (Webster, 2015). Despite being enhanced when attention is withdrawn, visual aftereffects produced by adaptation require initial conditions of spatial attention and visual awareness (Jung and Chong, 2014). In the absence of selective attention but not alertness, early visual populations still show contrast adapta-

tion substantiated by an elevation in contrast threshold. Adaptation of neural populations higher in the visual hierarchy (e.g., faces/IT and motion/MT) requires selective attention, and without it, the aftereffects are abolished (Moradi et al., 2005). During binocular rivalry, if one eye's image is moving (or a higher contrast) and the other is stationary, the moving (or higher contrast) stimulus will dominate perception. The eye receiving the weaker signal (low contrast or no motion) is suppressed, while the other eye's image dominates perception more frequently (Dieter et al., 2015). Attention-directed sensory adaptation only acts on the conscious percept. In effect, this enables adaptation via mutual inhibition to promote the oscillatory and synchronous dynamics by helping attention disengage from its current perceptual selection by building evidence for another percept. Electrophysiological support for this view comes from evidence that gamma-band oscillations (30-100 Hz), associated with fluctuations in attention, are correlated with the perceptual shifts reported in binocular rivalry and multistable figures, as well as fluctuations in attention-directed divisive normalization (Womelsdorf et al., 2006). Gamma band oscillations have also been implicated in the maintenance of neural representations, suggesting a role in visual working memory (Jokisch and Jensen, 2007; Roux and Uhlhaas, 2014).

Normalization models of attention posit that the same underlying computation that supports response normalization in the presence of multiple stimuli also supports gain modulation by attention (Lee and Maunsell, 2009). Neurons responding to a particular stimulus feature or region are normalized by the pool of similarly tuned neurons, and this reduces correlations in the neural representations between the neural representations of the attended figure and its surround, functionally improving the signal-to-noise ratio (SNR) (Barlow, 2001; Abbott and Dayan, 1999; Reynolds and Heeger, 2009). The presence of more than one stimulus in the visual field increases normalization strength by increasing the divisor. This is an intuitive account because the need for spatial attention is low when there is just one stimulus but very high as the number of distractors increases (Wolfe, 2020). Similarly, V1 neurons

are inhibited when their non-preferred stimulus is superimposed on their preferred stimulus. This remains true even when the non-preferred stimulus presented alone produces weak excitation or no response. This cross-orientation inhibition is also well-modeled using divisive normalization (Carandini et al., 1997). Both shifts in the focus of attention and changes in stimulus contrast can modulate the strength of normalization. However, attention acts on neural responses even when stimuli are constant (Lee and Maunsell, 2009). When attention is selectively applied to a stimulus, contrast gain is initially increased, while prolonged attention can impair sensitivity to the stimulus via adaptation (Ling and Carrasco, 2006). This account is consistent with conflicting repulsive and attractive adaptive shifts in cell tuning at short and long timescales, respectively.

Adaptation normalizes sensory response to expectation, allowing sensory information to integrate over multiple timescales. The visual system tracks stimulus correlations at different timescales. Long-term stimulus correlations from longer adapting periods cause the cell's tuning to shift toward the adaptor, inducing a percept more similar to the adaptor than the physical stimulus supports to aid in global color constancy (Werner, 2014). Conversely, short-term correlations from short adapting periods shift a cell's tuning away from the adaptor, as is common when experiencing afterimages. In repulsive shifts, the difference between the adapting stimulus and the percept is enhanced via a release of inhibition in color-responsive cells once the stimulus is removed. These repulsive shifts are important for enhancing differences among visual targets and change detection. The build-up of relevant information across multiple timescales enables the visual system to make the predictions necessary for rapid interaction with the environment.

Sensory adaptation's various effects may modulate normalization across the distributed hierarchy of the visual system (Aschner et al., 2018; Cronin et al., 2017). Specifically, noisy neuronal adaptation may drive the stochastic fluctuations in attention that underlie perceptual alternations in bistable stimuli (Dieter et al., 2015; Shpiro et al., 2009; van Ee,

2009). This experience is striking in binocular rivalry, where stochastic noise may play a role in the "traveling wave" frequently experienced between stable percepts (Wilson et al., 2001). Intuitively, attentional control, unconstrained by changes in the environment, would be maladaptive. Short-term adaptation may produce the oscillatory synchrony experienced in bistable perception by effectively biasing perception away from the system's most recent perceptual decisions (Braun and Mattia, 2010).

Attentional processes dictate the perceptual landscape by constraining the number of candidate percepts (Davidson et al., 2018), and adaptation destabilizes perception, thereby supporting the necessary flexibility (Kim et al., 2006; van Ee, 2009). Changes in the focus of attention at fine temporal and spatial scales would be challenging to detect if attention could not adjust a signal's normalization pool. For perception to be productively flexible, neuronal pools that act as the response divisor must dynamically change based on attention-directed normalization (Schwartz and Coen-Cagli, 2013). Dynamic normalization pools can account for enhancing similarity in neural populations through common divisors, resulting in grouped percepts. The subject of attentional focus is not normalized with the rest of the visual field, resulting in a smaller normalization pool and heightened population activity. This remains true in feature attention—here, cells responding to the selected feature are not normalized with the background, regardless of location (Cohen and Maunsell, 2011; Ni and Maunsell, 2019). Despite evidence pointing to the shared computation of normalization (Boynton, 2009; Lee and Maunsell, 2009; Reynolds and Heeger, 2009), fluctuations in neural activity due to feature versus spatial attention are uncorrelated, suggesting differences in underlying mechanisms and possible computational advantages of signal decorrelation (Cohen and Maunsell, 2011).

The theoretical perspective, here, is a neuron's normalization pool is dynamically guided by spatial attention and statistical dependencies (similarities) between image regions (Schwartz and Coen-Cagli, 2013). Flexible normalization pools alongside sensory adaptation may sup-

port a dynamic feature-linking account of perception. In Barlow's (1981) linking-features hypothesis, neural representations are linked together non-topographically, without spatial relations. In his original conceptualization, cells that respond to the same feature or feature conjunctions group together, resulting in a cogent similarity-enhanced percept. Here, uncertainty is reduced by rendering objects in view as more similar. Unconstrained similarity enhancement would make it difficult to see very fine details. A perceptual bias for enhancing the differences between similar objects is necessary for flexible perception, especially when these differences are small. With this in mind, this dissertation seeks to provide evidence that Barlow's linking features are supported by shared normalization pools; that is, features with a shared normalization pool have implicitly correlated fates, and thus a linking. Classically, when a stimulus is near a second identical stimulus, the normalization strength on each region is increased, thereby reducing the signal strength. However, if two stimuli are sufficiently different, they are not normalized together, and their differences may be perceptually enhanced. Divisive normalization, as it is classically held, suggests that normalization pools are fully stimulus-dependent so similar regions link and dissimilar regions do not. Normalization strength is dependent on feature similarity and behavioral goals by enhancing signals from particular features and spatial relations in the stimulus but not others (Schwartz and Coen-Cagli, 2013). Finally, adaptation enables the visual system to access sensory statistics over time (Wark et al., 2007). The visual system can have evidence-based temporal priors that independently track quickly changing and constant stimuli. Attentional fluctuations over time and space ensure that different neural populations will have variable levels of adaptation due to differences in adaptor onset and duration. Additionally, the extent of gain reduction due to adaptation depends on the difference between a neuron's response characteristics and the adaptor and the location in the neuron's receptive field (Solomon and Kohn, 2014). Attention and adaptation support efficient encoding by decorrelating neural signals across space and time, thereby reducing redundancy and maximizing information

capacity (Abbott and Dayan, 1999; Garcia-Diaz et al., 2012; Verhoef and Maunsell, 2017; Wang et al., 2003).

Theories of divisive normalization typically depend on center-surround receptive field antagonism (e.g., Schwartz and Coen-Cagli, 2013). The theoretical model offered here will treat divisive normalization as a canonical computation that can act at multiple levels, at the cell level, or on the distributed activity of many cells belonging to a population. Recent evidence of population coding in color perception (Emery et al., 2017; Wachtler et al., 2003) is consistent with the existing evidence of population coding for the perception of shape (Pasupathy and Connor, 2002), orientation (Ringach, 2010), and classically, the direction of motion (Georgopoulos et al., 1986). Population coding for shape is of particular interest, as shape-responsive cells share the ventral visual pathway with color, and there is evidence of cells sensitive to both features in area V4 (Bushnell et al., 2011; Kim et al., 2020). Psychophysical experiments with behavioral dependent measures are inherently probing population responses. Still, color-opponent cells in the cortex have been identified as serving separate perceptual organizational goals, as either spatial integrators or as spatial differentiators for color (Shapley et al., 2019). Since these computations directly relate to hypotheses about similarity-enhancement and dissimilarity-enhancement, the color-responsive cells that contribute to the population code for color appearance must also be considered. Despite the relative coarseness of behavioral measurements, response differences to stimuli designed to suit one cell type more than the other may be measurable.

1.3 Color-Opponency in Cortical Cells

The population code for color is built up from color-responsive cells with color-opponent response characteristics (Shevell and Martin, 2017). Single-opponent cells have receptive fields that are excitatory for one cone signal and inhibitory for an opponent cone signal. For example, a single-opponent cell may have an excitatory response for long-wavelengths

(L+) and an inhibitory response for medium-wavelengths (M−) for a stimulus in their receptive field. Single-opponent cells have spatially overlapping receptive fields (Figure 1.4 a & b). Unlike single-opponent cells, double-opponent cells (Figure 1.4 c) have two physically discrete sub-regions with opposite response profiles (e.g., L+/M− and L−/M+). Separate regions with coordinated single-opponency enable double-opponent cells to detect chromatic contrast while not being sensitive to a large uniform field at any chromaticity. The structure of their receptive fields specifies their roles in color perception. Single-opponent colors act to fill in continuous regions of color and are considered to be spatial integrators for color and without physically discrete sub-regions, these cells cannot detect chromatic contours. Double-opponent cells are classically represented with concentric receptive fields; however, recent evidence suggests that many double-opponent cells have elongated, asymmetrical receptive fields schematically similar to simple cells (Figure 1.4 d). Elongated cone-opponent receptive fields enable chromatic edge-detection through leveraging a multiplexed representation of color, orientation, and spatial frequency (Shapley et al., 2019; Shevell and Martin, 2017).

Double-opponent cells are implicated in differentiating the chromatic signal, making these cells a possible driver of divisive normalization. In particular, double-opponent cells have maximal responses to oriented, chromatic contours of relatively low spatial frequencies between one and four cycles-per-degree (cpd) of visual angle (Shapley and Hawken, 2011). By comparison, single-opponent cells are still orientation-selective but not contour-selective. Consider Figure 1.4 b; even though these receptive fields are smaller and *more* symmetrical, they will still show their maximal response for patches of long-wavelengths with 45° orientation. A single-opponent cell with one opponent sub-region cannot detect chromatic contours. Furthermore, a shift from a long-wavelength to middle-wavelength light in a 45° oriented line would have some intermediate effect on the cell, as the long-wavelengths will cause excitation and the middle-wavelengths will evoke inhibition at the site of the contour.

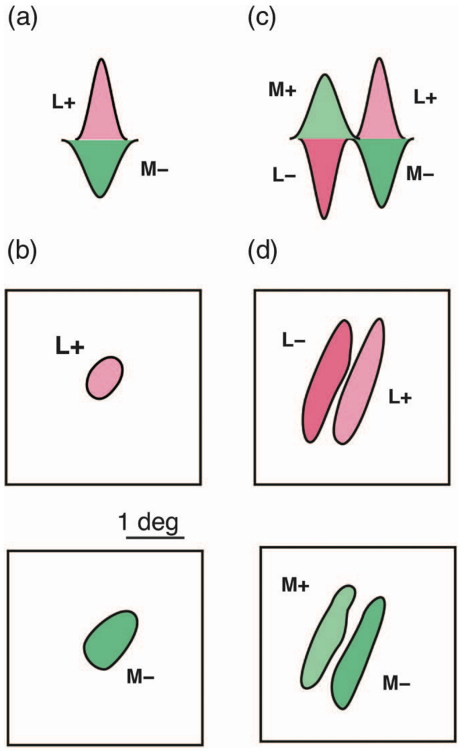

Figure 1.4: Cone-opponent receptive fields schematics. (a) Receptive field schematic for a single-opponent receptive field receiving excitatory input ($L+$), and inhibitory input ($M-$). (b) Isolating long and medium wavelength response profiles show largely overlapping, roughly symmetrical receptive fields. (c) Receptive field schematic for a double-opponent receptive field with two spatially discrete cone-opponent sub-regions. (d) Isolating long and medium wavelength response profiles reveals orientation-selective cone-opponent sub-regions. Figure from (Shevell and Martin, 2017).©

Here, single opponent cells cannot differentiate the current stimulus from any other stimulus with the same space-averaged signal (e.g., a square-wave grating and a checkered pattern). Consider a hypothetical single-opponent neuron that responds with the same intensity of excitation to L as the intensity of inhibition to M. In this case, a dichoptic display presented in Red/Green chromatic rivalry would have some neutral effect. Now consider a certain double-opponent (e.g., Figure 1.4 c) inheriting the response characteristics from the earlier single-opponent (Figure 1.4 a) cell as well as another single-opponent cell with the opposite response profile (L− and M+). For simplicity, we will consider the selectivity strength of the sub-regions to be equivalent and adjacent, with non-overlapping receptive fields (Figure 1.4

c). Unlike the single-opponent cells, these cells are selective for chromatic contours. Each sub-region has inverse response characteristics, allowing both sides of a chromatically-defined contour to be represented in the same neural unit. If we show this double-opponent cell a dichoptic, chromatically-rivalrous square-wave grating of its preferred frequency, it too will have a neutral effect. Here, the contour is still represented between boundaries as long as alternating phases do not contain the same information. Consider, for example, an L/M grating in rivalry with an M/L grating, where each eye's image is identical but offset by a single phase. In this specific case, double-opponent cells may not be able to encode the chromatic contour information inside the grating, as every cell will have the same binocular signal at every location. The detection of chromatic or luminance contour created at the boundary between the rivalrous signal and a stable background signal should be preserved. The experiments in this dissertation use stimuli that preserve contour information with alternating phases of a different chromaticity, rendering the chromatic signal ambiguous. Double-opponent cells act to enhance chromatic contours but may not be specialized for differentiating signals with ambiguous contour information. Neither double-opponent nor single-opponent cells may be individually responsible for establishing representations of the stimulus; however, the possibility of a particular color-responsive cell type driver will need to be ruled out.

1.4 Specific Research Aims

This dissertation explores the relationship between visual input and perceptual experience to characterize the perceptual flexibility in the resolution of ambiguous representations. Of particular interest was how the nervous system can enhance differences or similarities over time for a single, unchanged stimulus. Results are first reported for an experiment that provided novel evidence of a perceptual bias that disambiguates visual input by enhancing dissimilarity (Peiso and Shevell, 2020). The three additional reported experiments reveal

evidence of divisive normalization in resolving chromatically-ambiguous stimuli. In particular, this dissertation tests for evidence of divisive normalization in perceptual selection by leveraging existing models of attention, figure-ground segregation, and binocular rivalry. In addition to how rivalrous regions mutually influence the perceptual resolution (Experiment 1), the extent to which non-rivalrous stable regions of the visual field affect the resolution of rivalrous regions was explored (Experiments 2 and 3). By manipulating the rivalry status of the figure and background regions of dichoptic stimuli, Experiment 2 probes the reciprocity of normalization effects between the figure and the ground. Experiments 2 and 3 explored the influence of chromatically-defined spatial information on perceptual selection by manipulating the feature relations between the figure and background regions. To explore the influence of luminance contours on pooled divisive normalization, Experiment 4 manipulates the presence of luminance-defined edges. Finally, fully chromatic stimuli (i.e., without grey-appearing regions) address an open question regarding the influence of single and double-opponent cells in the resolution of a stable percept from an ambiguous neural signal.

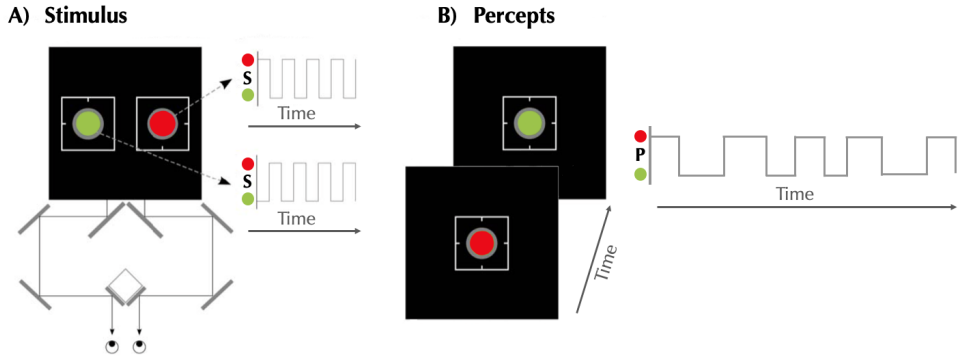

Figure 1.5: Schematic example of interocular-switch rivalry stimulus presentation time course and example perceptual outcome. (A) A stimulus in chromatic interocular-switch rivalry. Dotted arrows indicate that eyes always have different input and this input changes at a steady frequency over time. (B) Two possible fused percepts that alternate slower than stimulus swaps. Figure adapted from (Christiansen et al., 2017).©

The experiments comprising this dissertation manipulated neural ambiguity with dichoptic stimuli. Dichoptic stimulus presentation involves showing independent images to each eye. This is unlike typical viewing conditions, where the left and right eyes usually receive information from the same physical stimulus or the same region of the visual field. This method allows experimenters to independently manipulate the left and right eye's image and the extent to which they contain mutually convergent or divergent information. Divisive normalization is a canonical neural computation that acts across the distributed visual hierarchy (Aschner et al., 2018; Buschman and Kastner, 2015; Carandini and Heeger, 2012; Cronin et al., 2017). Accordingly, the extent to which perceptual organization is driven by "low" level neural representations (e.g., retina or Lateral Geniculate Nucleus (LGN)) or by "high" level representations (e.g., V4 or Inferior Temporal Gyrus) is not fixed (Carandini and Heeger, 2012; Beaudoin et al., 2007). However, due to evidence from macaque LGN that monocular cells are unaffected by rivalrous stimuli (Lehky and Maunsell, 1996), the response characteristics of cortical cells were considered in the theoretical motivation underlying the experimental design. Two methods are used to increase the frequency that the neural ambiguity is resolved by color-sensitive cortical cells. Presenting dichoptic stimuli in interocular-switch rivalry (ISR) reduces the role of monocular representations in early visual areas (Kovács et al., 1996; Logothetis et al., 1996; Slezak and Shevell, 2018). ISR entails swapping images between left and right eyes at a rate up to 6 Hz resulting in perceptual alternations similar in length to perceptual alternations in standard binocular rivalry. Perceptual experience spanning multiple swaps (Figure 1.5 B) eliminates the possibility that monocular suppression is the sole cause of the perceptual alternations evoked by rivalrous stimuli (Figure 1.5 A). Presentation faster than 6 Hz can lead to time-averaged percepts. In addition to ISR presentation, stimuli were presented in a patchwork configuration, such that measured percepts entailed integrating the left and right eyes' images (Figure 1.3).

CHAPTER 2

GENERAL METHODS

2.1 Apparatus

For all of the experiments presented here, stimuli were presented on a calibrated NEC MultiSync FP2141SB cathode ray tube (CRT) display, driven by an iMac computer. Observers viewed the CRT through an eight-mirror haploscope that displayed a different stimulus to corresponding retinotopic regions in each eye (Figure 2.1). Observers used a chin rest to ensure the path of light through the haploscope was approximately 115 cm long. To ensure the stable fusion of the two images and account for individual differences in interocular distance, observers adjusted the position of the final set of mirrors. Two Nonius lines were stably presented to each eye to aid the fusion of the two images. The left eye was presented with top and left Nonius lines, while the right eye was presented with bottom and right Nonius lines. A properly fused image had one fixation point and horizontally aligned left and right Nonius lines, and vertically aligned top and bottom Nonius lines.

2.2 Procedure

2.2.1 Photometry Protocol

Individualized isoluminant stimuli were generated for each observer to reduce the influence of luminance, or signals in the magnocellular visual pathway. To this end, each observer repeatedly performed heterochromatic flicker photometry (HFP). HFP is a method of measuring the spectral sensitivity of the human eye and can be used to define the human photopic luminosity function, V_λ (Lee et al., 1988; Wyszecki and Stiles, 1982). The HFP stimulus is a single region (i.e., disk) that is oscillated at 10-20 Hz between two different chromaticities. An observer is tasked with adjusting the intensity, typically of just one of the lights, until

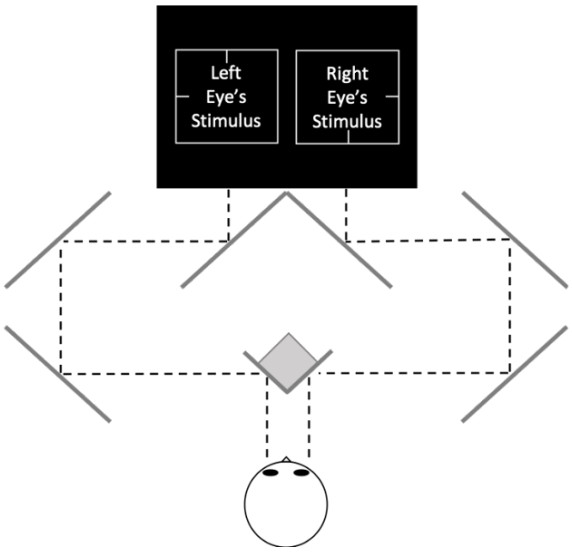

Figure 2.1: Mirror haploscope display. The CRT display is depicted as a black rectangle. The 8 mirrors are represented by grey 45° and 135° lines. Dashed lines represent the light paths.

the flicker is minimally perceptible. All observers performed five repetitions of HFP for three chromaticity pairs: red-appearing/green-appearing (R/G), blue-appearing/green-appearing (B/G), and blue-appearing/red-appearing (B/R) on each of three days. HFP performance was assessed by the reliability of the five within-day measurements, with an allowable daily standard deviation (SD) of ±1 SD across three days. The five measurements per color pair were averaged, yielding three means, one for each day. These daily means were then averaged together, and a final analytical check was performed by using R/G and B/G equiluminant ratios to calculate a theoretical B/R ratio. This calculated B/R ratio was compared to the measured B/R ratio, with allowable deviance of ±10%. Participants unable to obtain reliable HFP measurements were paid for their time and did not continue the study.

2.2.2 Experimental Protocol

Experimental protocols were identical across experiments. Only the number of trials, stimuli, and measured percepts changed. During each trial, observers were instructed to press and hold buttons on a gamepad for the duration that they experienced each measured per-

cept. The instructions were displayed on the screen using images to indicate target percepts and text instructions indicating the gamepad buttons corresponding to each target percept. Observers were instructed to withhold button presses for all percepts not indicated by the instructions, including partially resolved or piecemeal percepts. Total dominance durations were calculated by taking the average dominance duration of each of the measured percepts, including feature counterbalances, for each of three days. Standard errors of the mean were calculated using the mean total dominance durations for each experimental day. Each 70-second trial began with an instruction screen that indicated which button to press for each measured percept. To reduce the possible impact of differential adaptation between the two eyes from the onset ISR phase and onset effects (Carter and Cavanagh, 2007), measurements began after the initial 10 seconds, yielding a functional trial length of 60-seconds. Each observer completed four days of experimental trials, including a practice day. The set of experimental trials included all color and applicable orientation counterbalances. For all experiments, independence predictions were calculated from single-region rivalry trials. The first day was always a practice session, and these data were not submitted for analysis. Three experimental days followed, during which each observer completed the same set of experimental trials in random order.

2.3 Stimuli

All stimuli were generated in MATLAB® as indexed images for computationally efficient rendering. Chromatically defined stimuli were presented in ISR, swapping stimuli between the two eyes at a frequency of 3.75 Hz, or 7.5 swaps per second (Christiansen et al., 2017; Logothetis et al., 1996). Non-rivalrous regions, such as the fixation point and Nonius Lines, were held constant within a single trial. Finally, Experiments 2-4 exclusively presented stimuli in patchwork configurations since Experiment 1 found no statistically significant evidence that patchwork and conventional stimulus configurations produced different dominance times.

Across each of the four experiments, stimulus arrays shared the same arrangement, while features such as orientation, spatial frequency, chromaticity, and rivalry status were manipulated. Stimulus arrays had one of three arrangements: (1) a single rivalrous region 1.5° above fixation, (2) a single rivalrous region 1.5° below fixation, or (3) one rivalrous region 1.5° above fixation and one 1.5° below fixation (Figure 2.2 A). Rivalrous regions were always displayed within a 1.5° aperture. Single-rivalrous conditions (Figures 2.2 B & C) were used to determine independence predictions for the two rivalrous-region conditions (Figure 2.2), as described in the next subsection. All stimuli were presented inside 4.5° by 4.5° fusion boxes with Nonius lines. Fusion box edges were at a chromaticity metameric to the equal-energy spectrum and had luminance contrast with respect to their interior background. While peripheral and foveal vision may evoke different visual processes, the present experiments are not designed to address this.

2.3.1 Independence Predictions

Each region was measured independently in single rivalrous trials (Figure 2.2 B & C) to determine the chance probability of co-resolution of two adjacent rivalrous regions. Independence predictions leverage probability theory to calculate the chance probability of seeing a particular two-region percept as the joint probability (Figure 2.2 D) of seeing its component top (Figure 2.2 B) and bottom (Figure 2.2 C) regions from single-rivalrous trial measurement. The example calculation (Figure 2.2 D) for percept, A1, is provided, but the calculations for every measured percept can be easily understood by taking the joint probability of corresponding elements from B and C. For example, calculating the independence probability for measured percept, A3, is the product of the probabilities for B3 and C3.

Using this schematic, independence predictions were constructed for all experimental conditions for each of Experiments 1-4. Control conditions in Experiments 2 and 3 did not have independence predictions. Each stimulus (including all counterbalances) has two

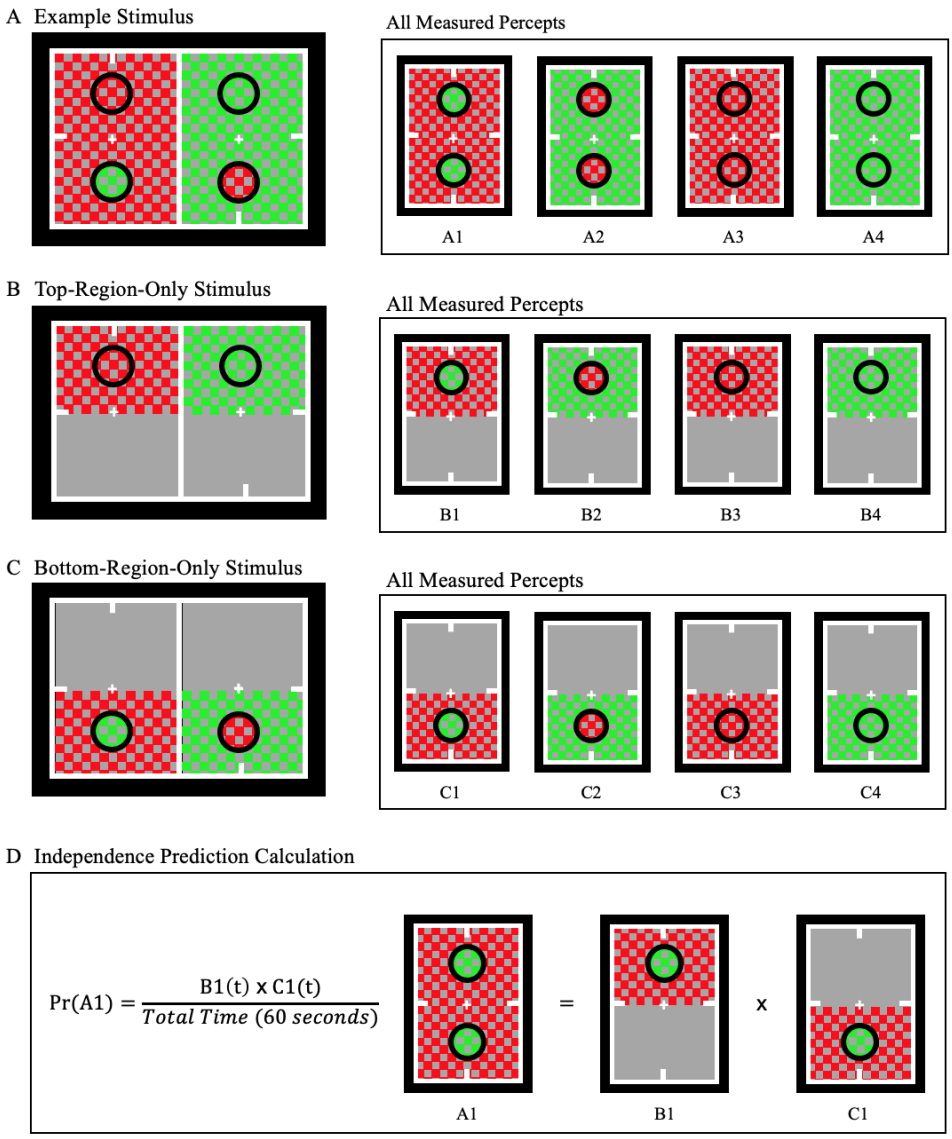

Figure 2.2: Example independence prediction. A) An example experimental condition with four measured percepts, A1-A4. B) The corresponding top-region-only stimulus and its four measured percepts, B1-B4. C) The corresponding bottom-only-region stimulus and its four measured percepts, C1-C4. D) The independence prediction calculation for percept A1, which is the joint probability of the average total dominance durations for the corresponding top and bottom percepts, B1 and C1.

corresponding independence trials, one bottom-only and one top-only trial. This calculation quantifies the expected value under the null hypothesis (H_0) that features are *not* linked by similarity to resolve ambiguity and instead are resolved independently (Shevell, 2019).

Rejecting H_0 is evidence of interocular grouping.

2.4 Data Preparation

Before conducting statistical analyses, total dominance-time proportions were arcsine-transformed and then averaged across three experimental days, improving conformity to normality assumptions (Kirk, 2013). The standard error of the mean was always calculated across three experimental days. Finally, the residual mean square error (MSERes) for a one-way ANOVA was used to perform planned comparisons.

2.5 Observers

Before participation, all observers (age 19–35) gave written informed consent as required by the University of Chicago's Institutional Review Board. Observers were screened for normal stereoscopic vision using the Titmus Stereo Test and for normal color vision using Ishihara Plates and Rayleigh matches made with a Neitz anomaloscope.

CHAPTER 3

EXPERIMENT 1

3.1 Rationale

Perceptual grouping contributes to the resolution of visual ambiguity of multiple spatially separate regions in view by enhancing their perceptual similarity (Alais and Blake, 1999; Kovács et al., 1996; Lee et al., 2018; Slezak and Shevell, 2018). Existing experimental evidence that supports the ubiquity of grouped percepts has frequently employed rivalrous stimuli (Figure 3.1 A) with the same rivalrous features in separate rivalrous regions (for exceptions, see: Slezak and Shevell, 2020; Slezak et al., 2018). The design of Experiment 1 provided a novel test of whether divisive normalization can contribute to perceptual resolution. The working hypothesis was that difference-enhanced percepts would become significantly more common when mutually imposed normalization forces are unequal between rivalrous regions (Figure 3.1 B) rather than equal (Figure 3.1 A). All the components of the rivalrous signal in Figure 3.1 A's example stimulus are the same; both regions are rivaling between a red-appearing and green-appearing 45° square-wave grating. Conversely, the rivalrous signals in Figure 3.1 B have one shared component (two green 45° gratings) and a unique component (red 45° or green 135° gratings). The shared components in the rivalrous signal should impose more mutual divisive normalization than the unique components. To this end, a dichoptic stimulus (Figure 3.1 B) had two rivalrous regions sharing one set of feature conjunctions (e.g., a green 45° square-wave grating above and below fixation) and one set of feature conjunctions that was unique to each region (e.g., a red 45° and a green 135°, above and below fixation, respectively). The resulting rivalry was between different features above and below fixation. One region was in chromatic rivalry (top region of Figure 3.1 B), and the other was in orientation rivalry (bottom region of Figure 3.1 B). Note that both regions had a signal for a green 45° oriented grating (top-right and bottom-left of Figure 3.1

B) and could be grouped. In the experimental runs, both grouped and difference-enhanced percepts were measured. Two other possible percepts were also measured on each trial (see Figure 3.2 C & D).

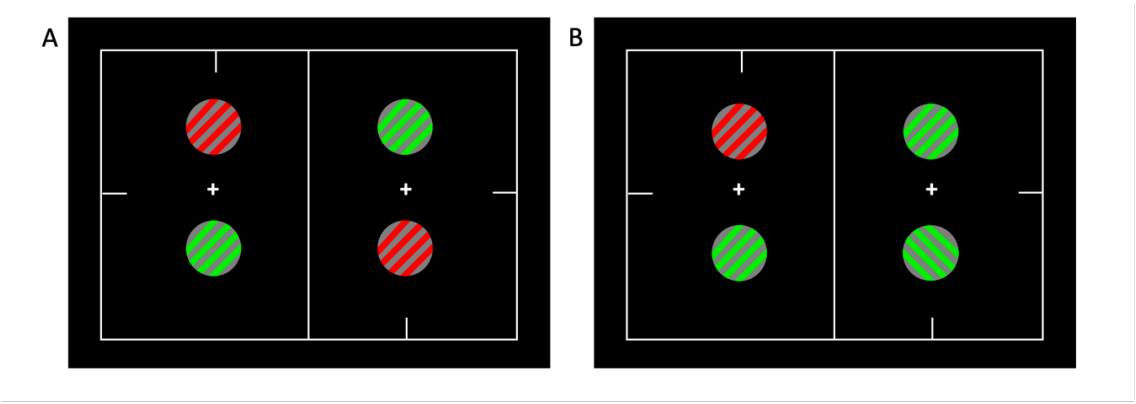

Figure 3.1: A) Rivalrous stimulus with identical rivalry in two regions. B) Rivalrous stimulus with different rivalry in two regions.

3.2 Stimuli

The stimuli for each experimental condition counterbalance were four cycles-per-degree (cpd) square-wave gratings. Single-grating conditions (Figure 2.2) were used to determine independence predictions for the two-grating conditions (Figure 3.1 B), as described in Chapter 2. A maximally similar percept (Figure 3.2 B) here refers to top and bottom regions resolving as identical in both orientation and color. A maximally different percept (Figure 3.2 A) refers to the top and bottom regions resolving as different across both features, specifically orthogonal orientations and different colors.

Stimuli were always presented in ISR at 3.75 Hz. The rivaling chromaticities for all conditions were set at [L/(L + M), S/(L + M)] values of [0.62, 1.00], referred to as "green," and [0.71, 1.00], referred to as "red" (MacLeod and Boynton, 1979). The "grey" value was [0.665, 1.00]. The unit of S/(L + M), which is arbitrary, was set to 1.0 for equal-energy-spectrum "white." All were presented at 5.0 cd/m^2 on a dark background called "black" ($\approx 0.3\ cd/m^2$).

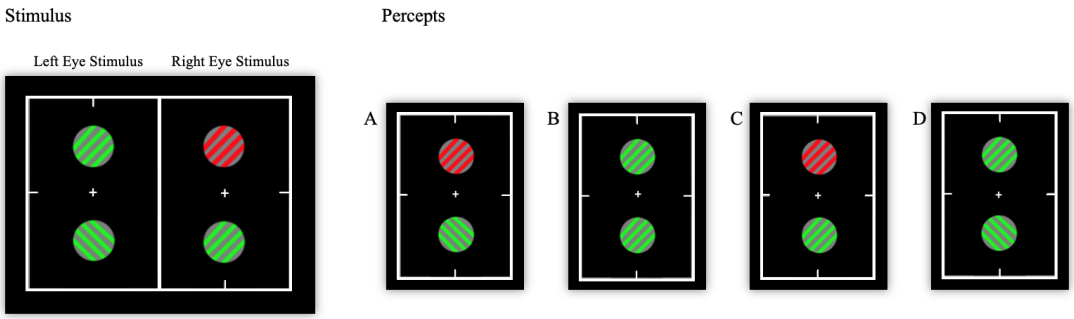

Figure 3.2: Left image is identical to figure 3.1B. A-D) show measured percepts (see text).

Rivalrous gratings were equiluminant and presented in the same retinotopic location; they could appear "red/grey" or "green/grey." Gratings in only orientation rivalry were the same chromaticity, both "red/grey" or "green/grey," but with orthogonal orientations (one at 45° and the other at 135°).

3.3 Predictions

Experiment 1 measured all of the physically possible non-piecemeal and non-fused (i.e., non-plaid) percepts. Although the most similarity and difference-enhanced percepts were critical to testing the working hypothesis of unequal divisive normalization, two additional percepts were measured (Figures 3.2 C & D). These percepts were included to explore more of the perceptual landscape, as the epochs of withheld response reflect all non-measured perceptual experiences (i.e., piecemeal combinations and plaid fusions). It was predicted that difference-enhanced percepts would dominate perception. In particular, a maximally different percept (Figure 3.2 A) may dominate perception more than predicted by chance (for prediction calculations, see Figure 2.2 D) and more than similarity-enhanced percepts. Observers were instructed to withhold their response to piecemeal and fused percepts, even though these percepts were sometimes experienced. Support for the divisive normalization hypothesis would be statistically significant increases in total dominance times for difference-

enhanced percepts relative to similarity-enhanced (grouped) percepts and to the expectations generated from an independence model.

3.4 Results

Prior to conducting analyses, total dominance times were averaged across trials in the same condition and then converted into a proportion of the 60-s trial.

Four two-grating (above and below fixation) percepts were measured:

1. Gratings that were different in every feature (Figure 3.2 A).
2. Gratings that were the same in every feature (Figure 3.2 B).
3. Gratings that were the same orientation but different colors (Figure 3.2 C).
4. Gratings that were different in orientation but had the same color (Figure 3.2 D).

Data were prepared as described in Section 2.4. A set of four planned orthogonal contrasts tested whether percept dominance proportions varied between conventional and patchwork stimulus presentations. Alpha was not corrected for multiple comparisons because an uncorrected test provided the most powerful and thus conservative test. Consistent with previous findings, none of the 16 comparisons (four contrasts x four observers) between patchwork and conventional presentation types was significant (Figure 3.4). Accordingly, the data were collapsed over presentation type and analyzed using four planned Bonferroni-corrected contrasts comparing measurements to the independence prediction calculated from single rivalrous trials (Figure 3.5).

Difference-enhanced percepts, with gratings above and below fixation different in both features (Figure 3.2 A), were *always* perceived more often than chance (independence) for every observer, however observer AS never resolved a single-grating percept so her data could not be compared to chance (Figure 3.4). Every other observer perceived difference-enhanced percepts significantly more than chance ($p < 0.001$). Only one subject showed significant evidence of interocular grouping (Obs. JA: $p < 0.05$). Average total dominance durations

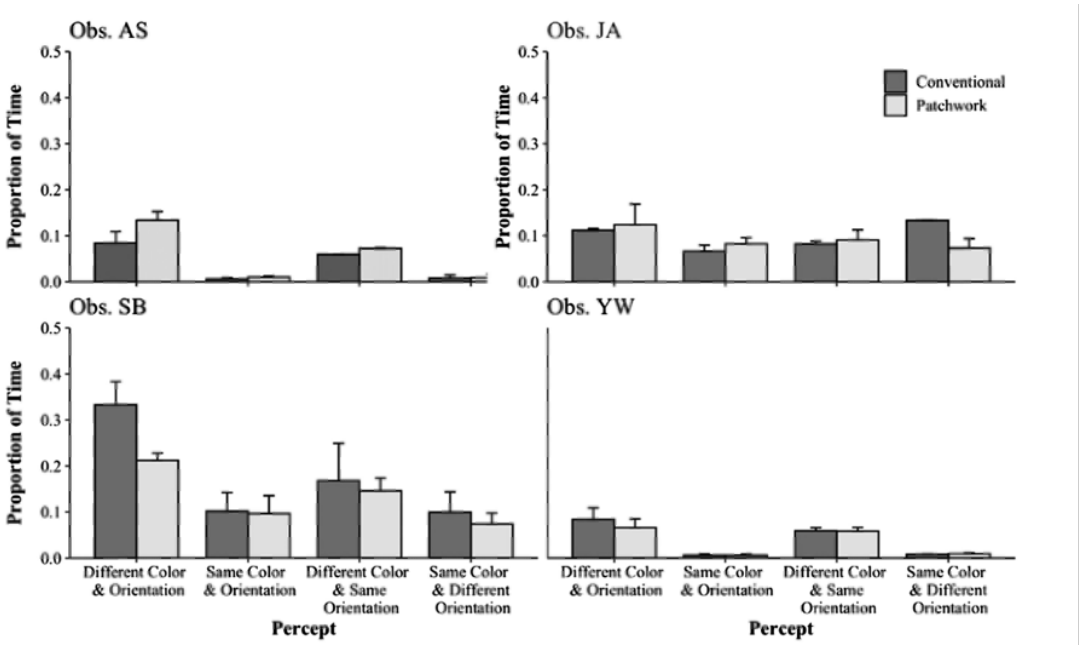

Figure 3.3: Results from four observers. The vertical axis is the proportion of a 60-s trial during which each of the four percepts was measured. The horizontal axis indicates the four measured percepts. Dark bars indicate conventional presentation and light bars indicate patchwork presentation.

for percepts of gratings, with the same orientation but different colors, were significantly above chance for all three analyzed observers ($p < 0.05$). Percepts of different orientation and same color gratings were seen above chance for one observer (JA: $p < 0.001$).

A post hoc comparison between gratings of the same versus different color above and below fixation was analyzed using a weighted contrast (Figure 3.5). All four observers produced significant contrasts, whereby dissimilarity-enhanced percepts had significantly higher average dominance times than similarity-enhanced percepts (Obs. AS, SB, & YW: $p < 0.001$; Obs. JA: $p < 0.05$). These results may suggest a dominant role of chromatic contrast in enhancing the difference signal in each location.

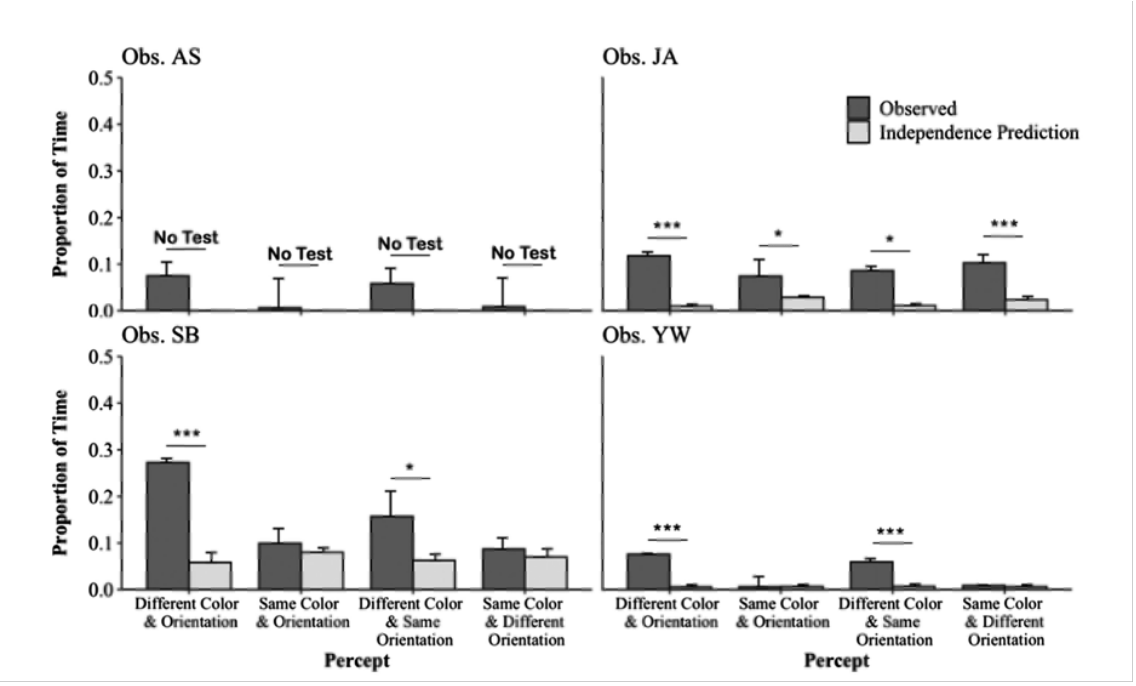

Figure 3.4: Results from four observers. The vertical axis is the proportion of a 60-s trial during which each of the four measured percepts was seen. The horizontal axis is the four measured percepts and their predicted values. Brackets indicate a significant contrast, where *, **, and *** indicate significance at $p < 0.05$, $p < 0.01$, and $p < 0.001$, respectively.

3.5 Discussion

Experiment 1 provided novel evidence that difference-enhanced percepts can be evoked using rivalrous stimuli. Additionally, Experiment 1 provided support for the role of divisive normalization in decorrelating statistically dependent signals. Specifically, the signal that was shared between rivalrous regions was perceptually attenuated. Additionally, the perceptual dominance of difference-enhanced percepts across all subjects provided support for the hypothesis that more normalization strength is imposed on the signal component that is shared between rivalrous regions, increasing the likelihood that a difference-enhanced percept will dominate perception.

Total dominance durations of intermediate percepts provided evidence that the chromatic signal plays a driving role in ambiguity resolution. Specifically, the percepts (Figure 3.2 C & D) of red and green gratings, irrespective of grating orientation, always occurred more

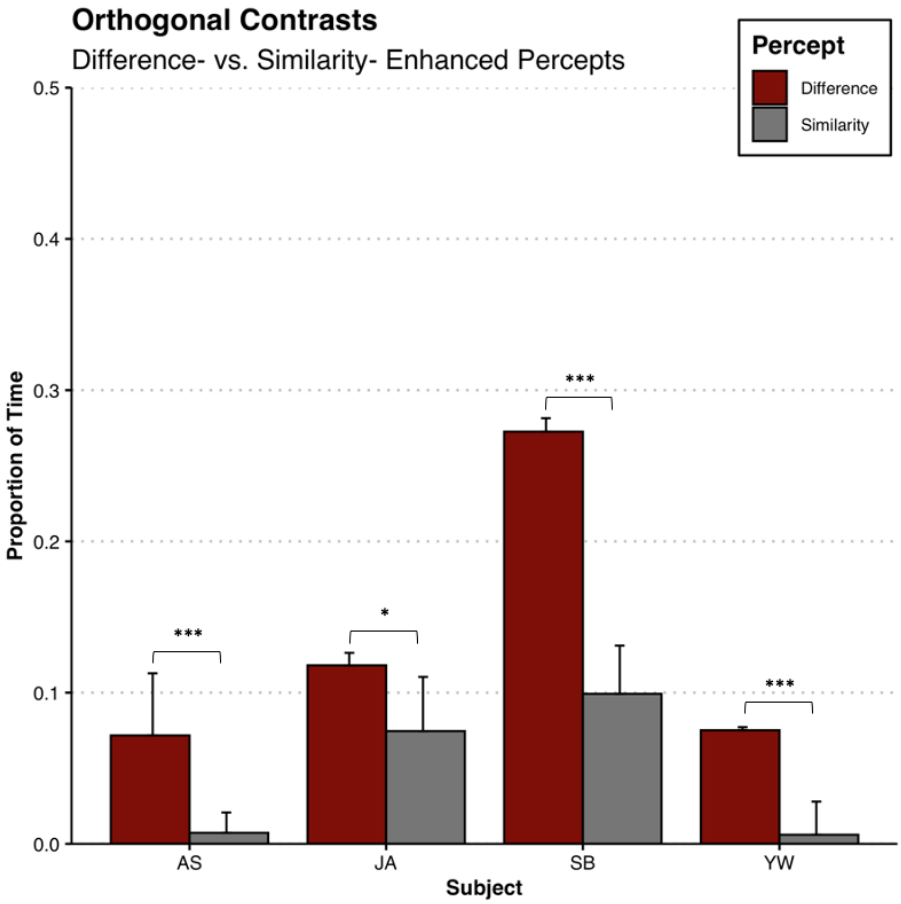

Figure 3.5: Results from four observers. The vertical axis is the proportion of a 60-s trial that each percept was seen. The horizontal axis is the four observers. Brackets indicate a significant contrast, where *, **, and *** indicate significance at $p < 0.05$, $p < 0.01$, and $p < 0.001$, respectively.

than the percepts with a shared color above and below fixation. These results can be explained by a divisive-normalization mechanism that implicitly links similar visual signals together by the pooled normalization of similarly-tuned neurons. Single-region rivalrous trials used in independence predictions were less perceptually stable for every subject than double-region rivalrous trials. Most subjects rarely resolved the measured percepts during single-grating trials (see Obs. AS, JA, & YW). This was consistent with anecdotal reports of persistent unstable perceptual experiences. Single-region rivalrous trials were collected to compute independence predictions; however, their perceptual instability may suggest that

context plays an essential role in ambiguity resolution. Adding a second rivalrous grating has a stabilizing effect on perception. A single object in the visual field does not require attention, and without the direction of spatial attention, normalization mechanisms may not reduce correlations or redundancies in the visual signal (Wolfe, 2020). Under normal viewing conditions, a single focal object without distractors would be perceptually stable. A dichoptic stimulus supplies twice the possible signal for a single region in space. In this way, the absence of context may interfere with perceptual selection by reducing the effect of attention-directed normalization. Experiment 2 was designed to address these remaining questions about the influence of context in ambiguity resolution.

CHAPTER 4

EXPERIMENT 2

4.1 Rationale

There is ample psychophysical evidence that context influences perception. Color perception itself is a prime example. Two distinct perceptual experiences can be produced by identical spectral mixes if each spectral mix is flanked by an appropriate hue (Figure 4.1). Induced pink and orange rings both appear reddish when viewed in isolation. Chromatic induction is a compelling example of the importance of context in color perception. Divisive-normalization mechanisms have been implicated as the supporting computation in color constancy, chromatic induction, cross-orientation suppression, and binocular rivalry (Murray et al., 2013; Said and Heeger, 2013; Webster and Mollon, 1995).

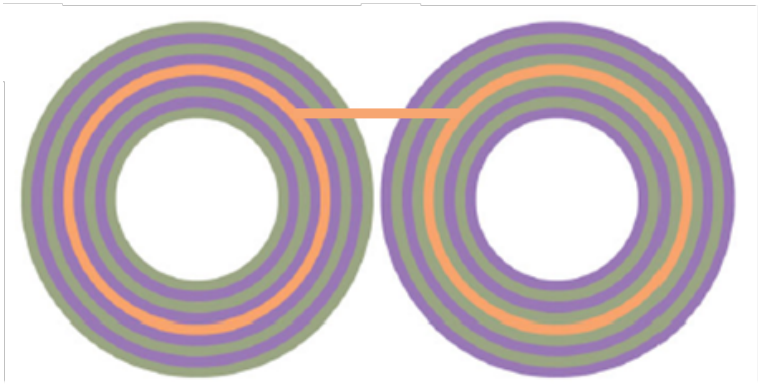

Figure 4.1: Rings are the physically identical (connecting bar) but produce different perceptual experiences. Adapted from (Monnier and Shevell, 2003).©

The present experiment sought novel evidence that stable, non-rivalrous regions of the visual field can influence the resolution of rivalrous regions. Specifically, the primary hypothesis (H_1) was that a non-rivalrous chromatic background could have a normalizing effect on rivalrous representations, selectively attenuating the perception of the color signal that also appears in the stable background. The visual system capitalizes on spatial extent as a cue for segregating figures from the ground (Peterson et al., 1991). Specifically, small areas

of the visual field that appear to be enclosed by a larger surround are more likely to be spontaneously perceived as the figure. Figure regions of the visual field evoke endogenous attention and more processing resources (Nelson and Palmer, 2007). However, it is an open question whether a stable figure can impose a similar strength normalization effect on the background. A possible perceptual benefit would be to increase a figure's saliency through chromatic contrast with the background. Suppose it does impose a normalization effect on the rivalrous background. Is this effect modulated by the relative area of the stable region, as a pooled normalization mechanism predicts? From a pooled normalization framework, the visual system leverages similarity in the visual field to form implicit links through pooled neural responses. If this is the case, adding a second rivalrous feature should not change the resolution of ambiguity compared to a similar stimulus configuration with one rivalrous feature.

A secondary hypothesis, (H_2), was that in the absence of a stable chromatic background, a pooled normalization mechanism would impose equal divisive strength across the pooled responses of cells tuned to each component of the rivalrous signal. Equal divisive normalization on component signals should evoke more similarity-enhanced percepts than difference-enhanced percepts. The perceptual outcome of a rivalrous figure and rivalrous background should be similar to the perceptual outcome of showing just rivalrous backgrounds, without figure regions evidenced by a chromatically contrasted region within a luminance-defined annulus. Experiment 2 addresses the two primary hypotheses (H_1 & H_2). Each of these primary hypotheses yielded several predictions. Five different conditions (A-E) were designed to test the predictions under each hypothesis. Due to this added complexity, each hypothesis will be addressed separately, with its corresponding set of predictions and results. At the end of the chapter, the discussion will integrate findings across the two hypotheses.

4.2 Stimuli

For all conditions with luminance-defined figure regions, gratings subtended 1.5° of visual angle and were surrounded by a black annulus (0 cd/m ^{2}) that increased the visual angle to 1.75°. All stimuli were presented inside square-shaped fusion boxes, which subtended 4.5° of visual angle, set to be the same luminance as the gratings near 15 cd/m^2. The peripheral background was black at 0 cd/m^2. The rivalrous chromaticities were defined using lsY values (MacLeod and Boynton, 1979) of [0.72, 0.3, 15] and [0.61, 0.3, 15], for red-appearing (called "red") and green-appearing (called "green") regions, respectively. Each square-wave grating oscillated at four cpd between a chromaticity, either red-appearing or green-appearing, and an equiluminant grey-appearing (called "grey") chromaticity [0.665, 1.0, 15]. When gratings and background regions had the same orientation, they were always presented in-phase. The bottom and top regions on top-only and bottom-only trials were a spatially uniform grey [0.665, 1.0, 15]. All trials were presented in ISR at 3.75 Hz (Christiansen et al., 2017; Logothetis et al., 1996). Additionally, the first ten seconds of each 70-second trial were discarded to avoid any onset asymmetry between the two eyes. The chromaticity, orientation, and regions in chromatic rivalry were manipulated to form five conditions.

4.3 Unequal Normalization Hypotheses

This section will address all hypotheses related to evoking difference-enhanced percepts under unequal divisive normalization of the rivalrous signal, influenced by a stable chromatic region. Condition A, the primary condition, was designed to investigate the prediction (P_{1A}) under H_1 that a stable, chromatic background will impose divisive normalization onto the signal it shares with the dichoptic signal. Two comparison conditions (Figure 4.2 B & C), were included to address open questions regarding the influence of the area of stable regions on normalization strength and to test an alternative explanation for difference-enhanced

percepts respectively. To address this hypothesis, comparisons between Conditions A and B were made (Figure 4.2 A & B). Condition C (chromatic & orientation rivalry) was included to compare to Condition A, addressing the possibility of a different saliency-enhancing mechanism that amplifies signals based on mutual dissimilarity. This would be contrary to a divisive-normalization mechanism that acts by linking signals by similarity, which can dynamically yield difference-enhanced and similarity-enhanced percepts to the same stimulus over time.

4.3.1 Conditions

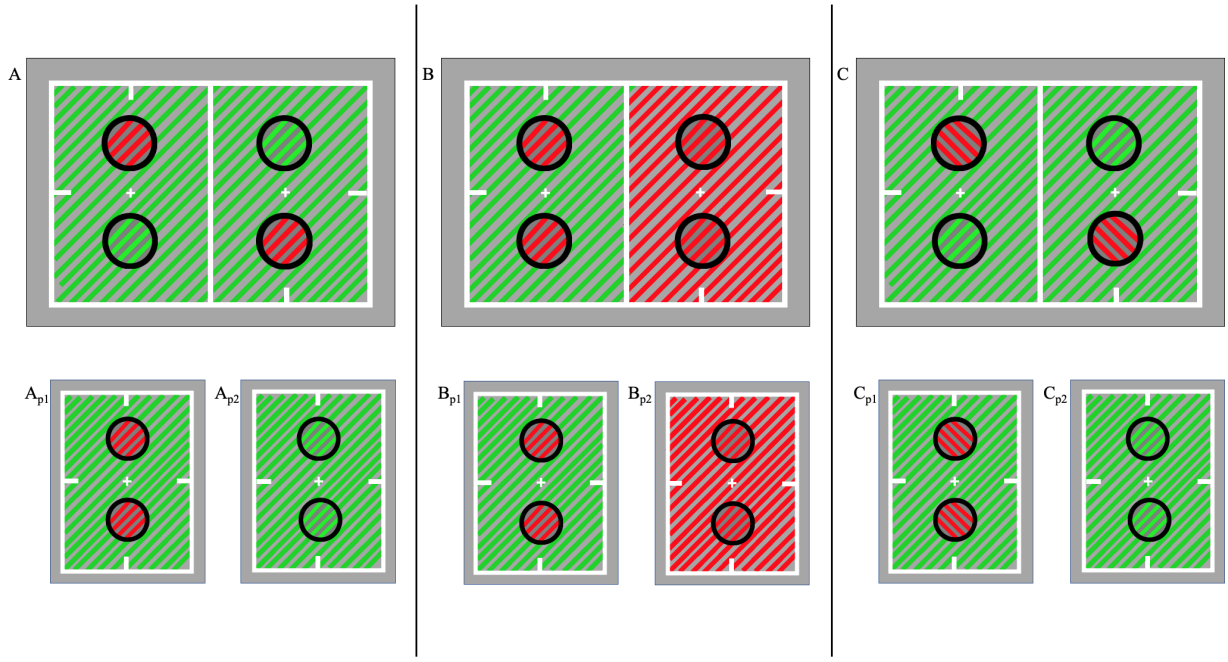

Figure 4.2: Conditions and percepts. Top row: left and right eye images for Conditions A-C. Bottom row: measured percepts for each condition.

Condition A: Rivalrous Gratings & Stable Background

Condition A's stimulus configuration (Figure 4.2 A) entailed red/green rivalrous (45° *or* 135°) gratings with a stable green or stable red background of the same orientation as rivalrous

gratings. This yielded four trial counterbalances for this condition: (1) red/green rivalrous 45° gratings on a stable green 45° background, (2) red/green rivalrous 135° gratings on a stable green 135° background, (3) red/green rivalrous 45° gratings on a stable red 45° background, and (4) red/green rivalrous 135° gratings on a stable red 135° background. Each of these trial types had two single-grating conditions used to calculate independence predictions for each region (Section 2.3.1), yielding eight single-grating conditions.

Condition B: Stable Gratings & Rivalrous Background

Condition B's stimulus configuration (Figure 4.2 B) reversed the rivalry status between figure and ground seen in Condition A. As in Condition A, all regions in stimuli (rivalrous backgrounds and stable gratings) had the same grating orientation (45° *or* 135°). Here, dichoptic gratings were non-rivalrous (stable green or red) and the background was presented in red/green chromatic rivalry. This yielded four trial counterbalances for this condition: (1) stable green 45° gratings on a 45° red/green rivalrous background, (2) stable green 135° gratings on a 135° red/green rivalrous background, (3) stable red 45° gratings on a 45° red/green rivalrous background, and (4) stable red 135° gratings on a 135° red/green rivalrous background. These four trial counterbalances yielded eight single-grating conditions (Section 2.3.1).

Condition C: Rivalrous Orthogonal Gratings & Stable Background

Condition C's stimulus configuration (Figure 4.3 C) entails red/green chromatically rivalrous 45° *and* 135° gratings in orientation rivalry, on a stable chromatic background. This yielded four trial counterbalances for this condition: (1) red 135° gratings rivaling green 45° gratings on a stable green 45° background, (2) red 45° gratings rivaling green 135° gratings on a stable green 135° background, (3) red 45° gratings rivaling green 135° gratings on a stable red 45° background, and (4) red 135° gratings rivaling green 45° gratings on a stable red 135°

background. As in Conditions A and B, four trial counterbalances yielded eight single-grating conditions (Section 2.3.1).

4.4 Results

Analyses were conducted within subjects using planned orthogonal contrasts. Since all predictions were directional, a non-parametric group analysis considering the one-tailed binomial probability of the observed results by chance under the null hypothesis (H_0) was used. The one-tailed binomial probability $\Pr(X \geq k) = \sum_k^n \binom{n}{k} p^k (1-p)^{n-k}$ of k or more successes on n trials under the null hypothesis (H_0).

4.4.1 Results: Unequal Normalization Hypotheses

Hypothesis 1 holds that stable, chromatic backgrounds influence the resolution of chromatically-ambiguous rivalrous regions by selectively imposing divisive normalization on the chromatically-identical component of the rivalrous signal. To test this hypothesis, data were prepared (Section 2.4) and analyzed using two sets of planned orthogonal contrasts (Figure 4.3) comparing the resolution of gratings as the same color ("Same") or as a different color ("Difference") than the background. For example, the total dominance duration that an observer resolved the gratings as green on a green background was compared to the resolution of green gratings on a red background.

P_{1A}: Comparisons Within Condition A

The first prediction under H_1 (P_{1A}) of increased divisive normalization on one component of a rivalrous visual signal will result in more difference-enhanced percepts than similarity-enhanced percepts. This set of planned orthogonal contrasts compared total average dominance durations between percepts within Condition A (Figure 4.2 A).

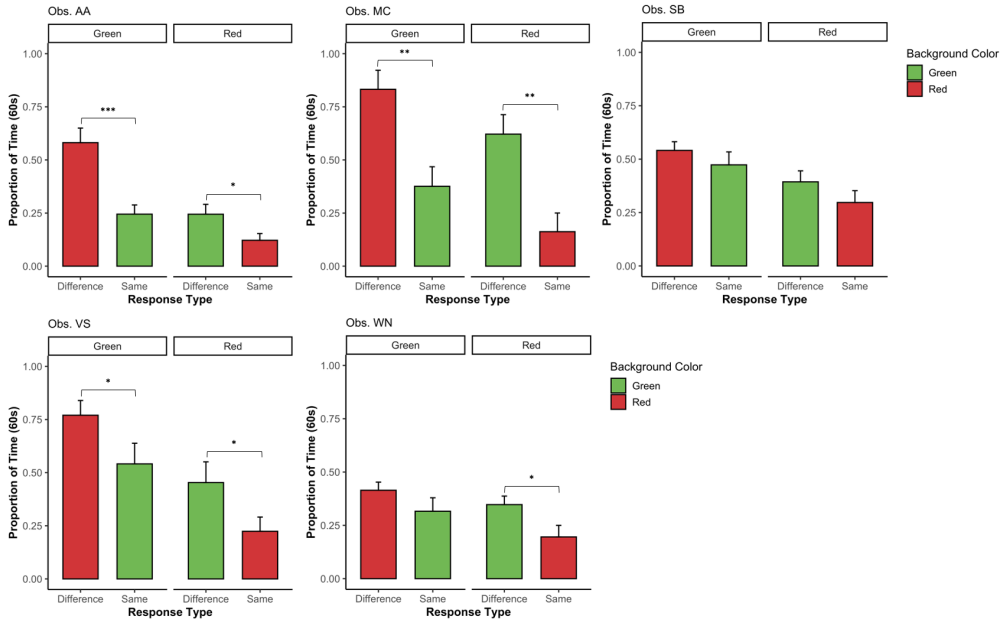

Figure 4.3: Planned contrasts for five subjects investigating P_{1A}. The vertical axis is the proportion of a 60-s trial that each percept was seen. The top horizontal axis groups results by resolved color of the rivalrous regions (figures), "Green" (left) and "Red" (right). The bottom horizontal axis indicates the response type ("Difference" or "Same"). Finally, bar color indicates the stable color (background) for each measurement. Brackets indicate a significant contrast, where *, **, and *** indicate significance at $p < 0.05$, $p < 0.01$, and $p < 0.001$, respectively.

Seven of the ten contrasts performed (two per observer) produced statistically-significant evidence supporting divisive normalization in the resolution of ambiguous gratings. The remaining three contrasts were in the predicted direction but failed to reach statistical significance (Obs. SB: p's > 0.11; Obs. WN $p = 0.104$). Despite this, every observer *always* resolved gratings to be a different color than their background more than the same color as their background. This pattern of results has the probability of $1/2^{10}$ ($p < 0.001$) of occurring by chance under H_0. These results provide statistically-significant support for H_1 and the predicted influence of divisive normalization in ambiguity resolution.

P_{1B}: Comparisons Within Condition B

Implicit in P_{1B} and P_{1AB} (next section) is an argument about figure-ground segregation. One of the primary configural cues to figure-ground segregation is the spatial extent of candidate figure and ground regions. Evidence that the ratio between stable and rivalrous regions influences normalization strength may also provide support for the role of divisive-normalization mechanisms in figure-ground segregation. This suggests that area-dependent divisive normalization underlies Gestalt observations that small, enclosed areas inform figure segregation. Additionally, small and large images on the retina and increasing convergence with retinal eccentricity may correspond to small and large normalization pools, respectively. To test P_{1B}, the average total dominance durations from Condition B (stable figure, rivalrous background) were analyzed using two planned orthogonal contrasts (Figure 4.4), comparing the resolution of the background color when it is the same or a different color than the stable figure.

Of the ten planned contrasts (two per subject), none achieved statistical significance (all p's > 0.1), and only four of the ten comparisons were in the predicted direction. These findings are consistent with P_{1B} in that stable figures did not impose a reliable divisive effect on rivalrous backgrounds. An early goal of perception is to segregate and enhance a figure from the background; Condition B provided configural cues (enclosed, small non-ambiguous figures) to figure-ground segregation. Given an easy-to-segregate figure, divisive normalization (an attention-directed mechanism) may not act on a peripheral background signal. These regions may be similarity-enhanced, thereby freeing up resources for figural processing.

P_{1AB}: Comparisons Between Conditions A & B

The third prediction (P_{1AB}), under H_1, was that stable backgrounds (Condition A) would impose a more reliable divisive effect on rivalrous regions than stable figures (Condition B).

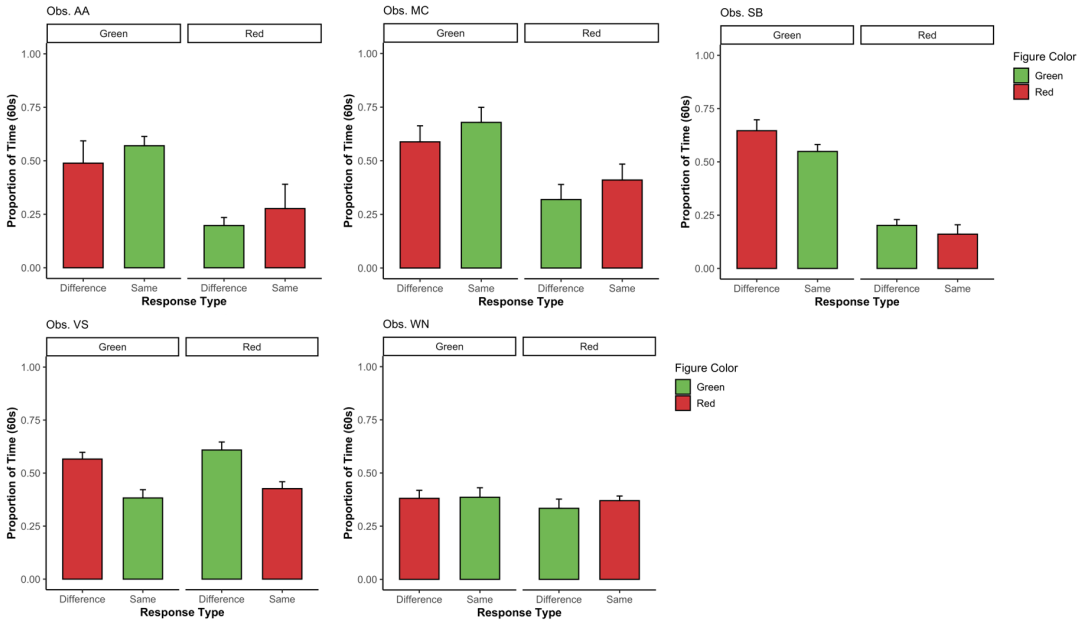

Figure 4.4: Planned contrasts for five subjects investigating P_{1B}. The vertical axis is the proportion of a 60-s trial that each percept was seen. The top horizontal axis groups the data by the resolved color of the rivalrous region (background), "Green" (left) and "Red" (right). The bottom horizontal axis indicates the response type ("Difference" or "Same"). Finally, bar colors indicate the stable color (figure) for each measurement.

Specifically, normalization strength was expected to be weaker for Condition B, resulting in less difference-enhancing and more similarity enhancement. Accordingly, average total dominance durations from Conditions A and B were analyzed using four planned orthogonal contrasts (Figure 4.5).

Of the 20 planned contrasts, only ten were statistically significant and in the predicted direction. Six of the ten remaining comparisons were in the predicted direction, and the remaining four were in the opposite direction of the prediction. Using the one-sided binomial probability $\Pr(X \geq k)$ of observing 16 (k) or more successes on 20 (n) trials is equal to $p = 0.0059$. This provided evidence that the relative size of stable and rivalrous regions influences the normalization strength of stable regions on rivalrous regions.

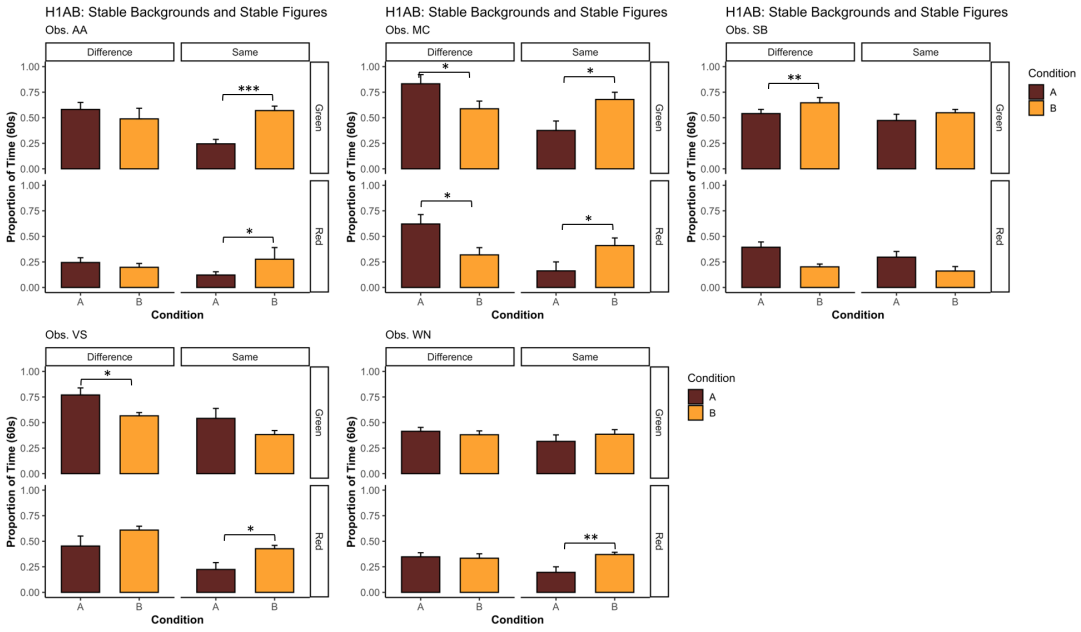

Figure 4.5: Planned contrasts for five subjects investigating P_{1AB}. The primary vertical axis is the proportion of a 60-s trial that each percept was seen. The right vertical axis groups results by the stable color of the background ("Green" or "Red"). The top horizontal axis groups results by the resolved color of the rivalrous region (figures), "Difference" (left) and "Same" (right). The bottom horizontal axis and bar color indicate the Condition (A or B). Brackets indicate a significant contrast, where *, **, and *** indicate significance at $p < 0.05$, $p < 0.01$, and $p < 0.001$, respectively.

P_{1AC}: Comparison Between Conditions A & C

The fourth prediction (P_{1AC}), under H_1, was the addition of a second rivalrous feature (i.e., orientation rivalry) will not significantly affect the normalization strength on the signal component shared between the stable background and rivalrous figures. H_1 holds that normalization pools form by linking similar signals across the visual field; increasing the differences between the shared and unshared feature conjunction should not affect the resolution of ambiguity. Significant statistical differences between these conditions would suggest that another saliency-increasing mechanism that acts on a difference signal between components may be at play. Accordingly, average total dominance durations from Conditions A and C were tested using four planned orthogonal contrasts (Figure 4.6).

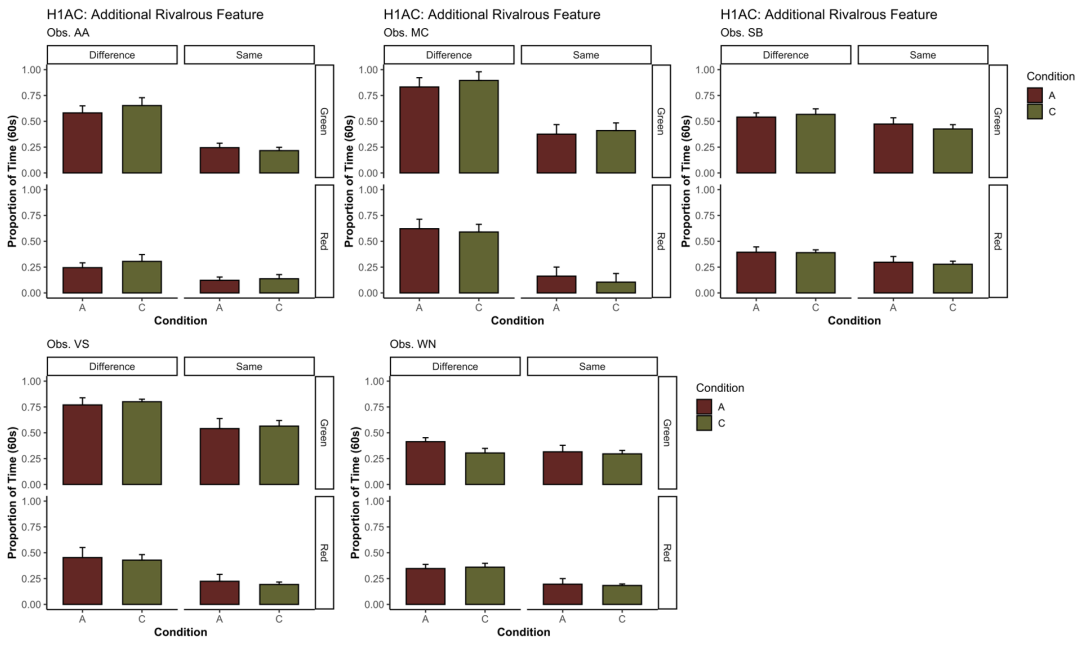

Figure 4.6: Planned contrasts for five subjects investigating P_{1AC}. The primary vertical axis is the proportion of a 60-s trial that each percept was seen. The right vertical axis groups results by the stable color of the background ("Green" or "Red"). The top horizontal axis groups results by the resolved color of the rivalrous region (figures), "Difference" (left) and "Same" (right). The bottom horizontal axis and bar color indicate the Condition (A or C).

None of the 20 planned comparisons was significant. As predicted by H_1, divisive normalization acts exclusively on similar components of the rivalrous signal, and will not be significantly changed by adding a second rivalrous feature, as long as one component of the rivalrous signal was identical to the stable background.

4.5 Equal Normalization & The Lost Figures Hypothesis

This section will address all predictions under hypothesis H_2 related to perceptual selection under conditions of equal divisive normalization. H_2 posits that visual regions with identical binocular signals will be linked by the pooling of neural signals responding to the same components. In the absence of a stable chromatic region, perception was predicted to resolve as similarity-enhanced due to equal divisive normalization strength on all feature conjunctions.

Despite equal normalization strength, each eye's image has evidence of a chromatically contrasted grating because all stimuli were presented in patchwork, where a similarity-enhanced or difference-enhanced percept requires binocular integration. Here, a normalization mechanism is posited to act primarily at the binocular level, as the binocular signal is the site of the neural ambiguity. Before integrating the disparate visual signals at the binocular level, the component monocular signals are not ambiguous. The working hypothesis was that divisive normalization aids in figure-ground selection by generating unequal normalization strength based on the relative amount of component signals. Despite monocular evidence of a figure, the figure may be lost at the binocular signal and not reliably enhanced by divisive normalization. Conditions D and E (Figure 4.7) were specifically designed to investigate the predictions under H_2. Comparisons with Conditions A and B (Figure 4.2) will also be made.

This hypothesis (H_2) yielded several predictions: (1) Condition D should evoke significantly more similarity-enhanced than difference-enhanced percepts (P_{2D}). (2) A comparison between Condition A (stable background) and D (rivalrous figures & rivalrous background) should reveal significantly more difference-enhanced percepts in Condition A relative to Condition D and significantly more similarity-enhanced percepts in Condition D relative to Condition A (P_{2AD}). (3) A comparison between Conditions D (rivalrous figure & rivalrous background) and E (rivalrous background) will not be statistically different (P_{2DE}). (4) A comparison between Condition B (stable figure, rivalrous background) and Condition E may reveal a visual processing asymmetry in normalization effects when the figure was the stable region, not the background. Here, the resolution of the background may not be influenced by the presence of a stable figure, resulting in similar results in Conditions B and E (Figure 4.9).

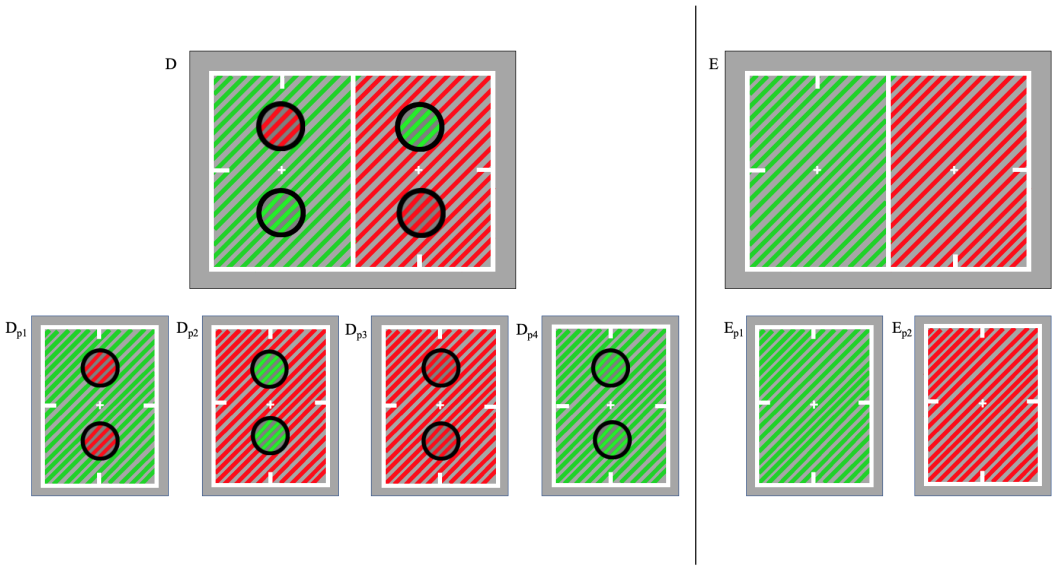

Figure 4.7: Conditions and percepts. Top row: left and right eye images for Conditions D and E. Bottom row: measured percepts for each new condition.

4.5.1 Conditions

Condition D: Rivalrous Gratings & Background

Gratings and the background were all in identical chromatic rivalry with the same orientation. Gratings were placed on their backgrounds in a patchwork arrangement, such that each eye received both color gratings (one above & one below fixation) on either a green or red square-wave background. This yielded two trial types for this condition, 45° and 135° trials, and four single grating trials, one top and one bottom per trial. For top-only trials, the bottom region was set to be grey; the inverse arrangement was used for bottom-only trials.

Condition E: Rivalrous Background Only

This condition was included to compare to Condition D. Stimuli in Condition E were red/green rivalrous background that was either 45° or 135° gratings. This yielded two trial types, one for each orientation. This condition was intended as a control, so no top-only or

bottom-only trials were included. Observers indicated the duration that they perceived the background as all green or all red.

4.5.2 Results: The Lost Figure Hypothesis

H_2 holds that with a uniform chromatic signal across the rivalrous stimulus, all the cell responses to the same signal components (i.e., red or green) should be pooled together and impose a spatially uniform normalization effect. The pooling of similar signals provided an implicit link between regions sharing the same features. Rivalrous gratings presented on rivalrous backgrounds are predicted to evoke similarity-enhanced percepts of either a green grating on a green background or a red grating on a red background.

P_{2D}: Comparisons within Condition D

The spatiochromatic configuration of Condition D was such that each eye had a non-ambiguous representation of a chromatically-contrasted grating within a luminance-defined annulus. Binocular representations of this stimulus would have identical, albeit rivalrous, chromatic signal at every location. In accord with the lost figure hypothesis (P_{2D}), similarity-enhanced percepts will dominate perception.

Of the four planned orthogonal contrasts (one per observer), all four showed significantly more similarity-enhanced percepts (Figure 4.8). One observer (MC) never reported difference-enhanced percepts and showed a ceiling effect for similarity-enhancement, so this result was not analyzed with the planned contrasts. Still, the implication of the measurements is the same as for the other observers. These contrasts are evidence consistent with equal divisive normalization across pooled neural responses with identical chromatic signals at every location. A possible implication of this finding is that similar normalization across the visual field may impede the normalization process from segregating a figure.

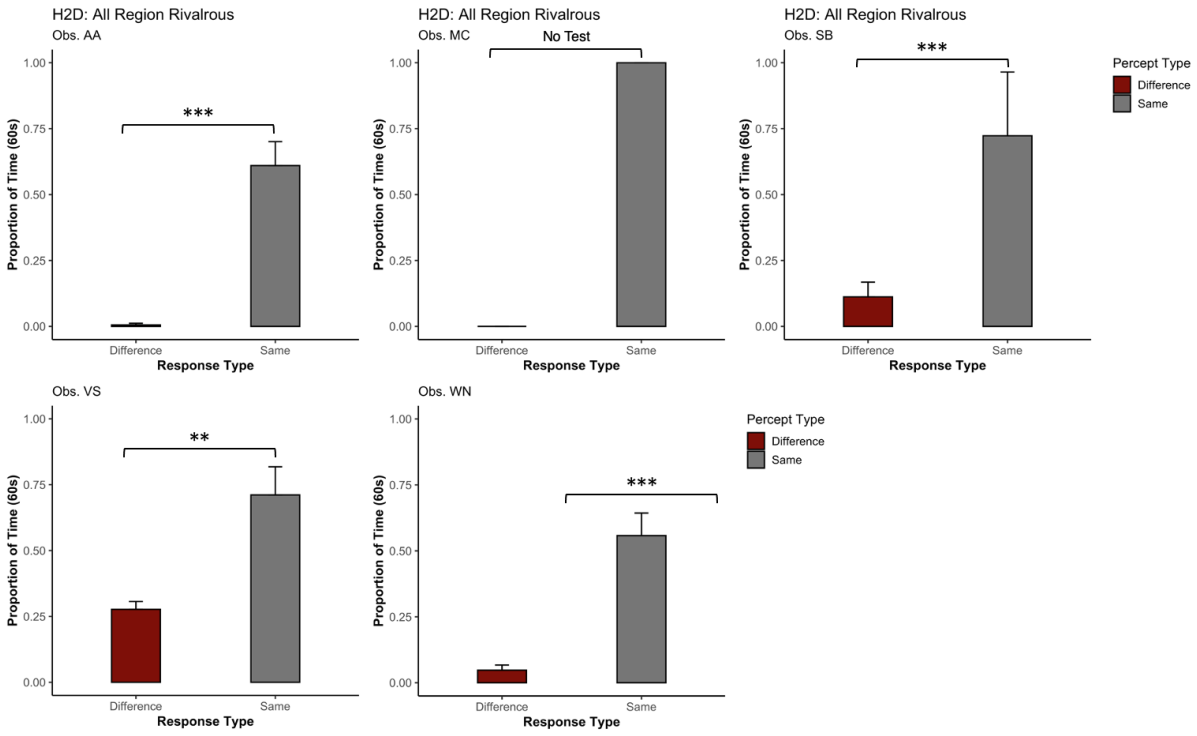

Figure 4.8: Planned contrasts for five subjects investigating P_{2D}. The vertical axis is the proportion of a 60-s trial that each percept was seen. The horizontal axis indicates the response type ("Difference" or "Same"). Brackets indicate a significant contrast, where *, **, and *** indicate significance at $p < 0.05$, $p < 0.01$, and $p < 0.001$, respectively.

P_{2DE}: Comparisons between Conditions D & E

The binocular signal evoked by Conditions D and E was identical; every region was in red/green chromatic rivalry. There are two configural differences between Conditions D and E: Condition D has (1) luminance-outlined rivalrous regions and (2) a patchwork arrangement. Experiment 2 used a patchwork configuration to reduce the influence of eye-of-origin information and individual monocular signals. Here, the goal was to capture how monocular representations may contaminate perceptual resolution by comparing it to a condition that would be theoretically the same at the binocular level. Unfortunately, due to an oversight during experimental design, these data cannot disentangle the effects evoked by patchwork

configuration or the presence of annuli. Additionally, the prediction for this comparison was informed by the response properties of double-opponent cells. Despite equal normalization often resulting in the loss of figure signal, it was predicted that the representation is partially preserved by double-opponent cells that are sensitive to luminance and chromatic contrast present in Condition D but not Condition E. Taken together, the a priori prediction was that the results would be weak, but that Condition E may show more similarity-enhanced percepts relative to Condition D (Figure 4.9).

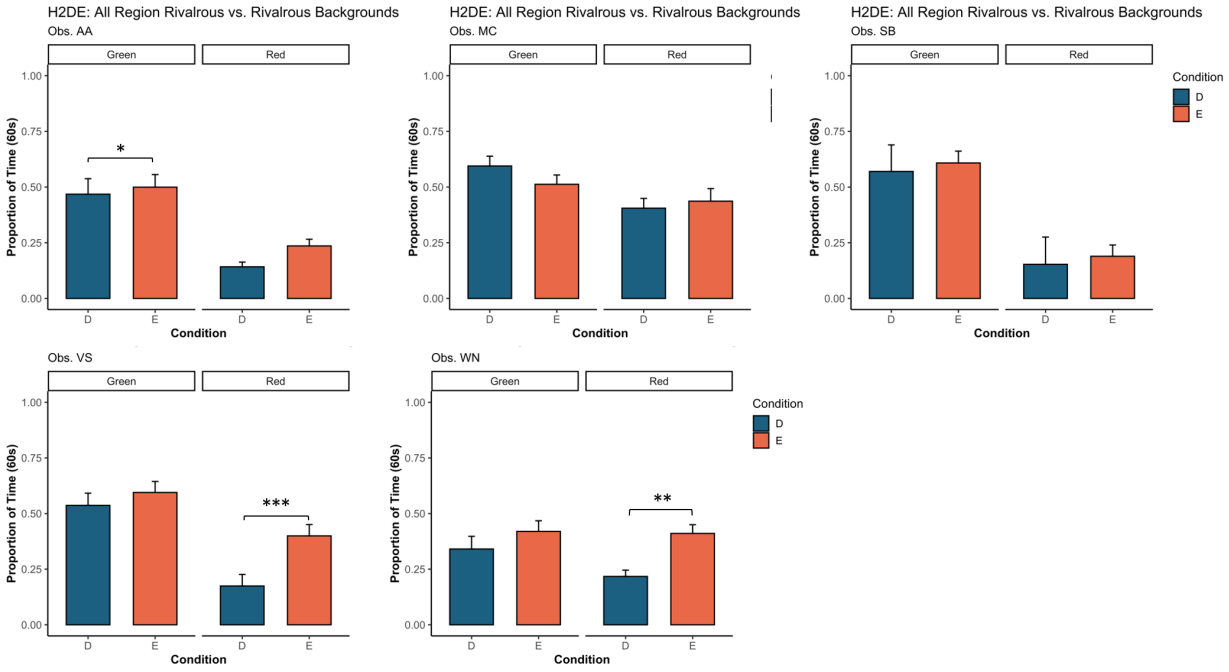

Figure 4.9: Planned contrasts for five subjects investigating P_{2DE}. The vertical axis is the proportion of a 60-s trial that each percept was seen. The bottom horizontal axis indicates the Condition (D or E). The top horizontal axis organizes bars by response type ("Green" or "Red"). Brackets indicate a significant contrast, where *, **, and *** indicate significance at $p < 0.05$, $p < 0.01$, and $p < 0.001$, respectively.

Since Condition E did not have luminance-bounded (annuli) rivalrous regions (see Figure 4.7 E), only all-green or all-red percepts from Condition D were included in comparisons. Of the ten planned orthogonal contrasts performed, only three achieved statistical significance. It should be noted that while this is weak evidence, all three significant results were for the

same contrast, comparing all-red percepts in Condition E to all-red percepts in Condition D and in the same direction. In fact, of the ten comparisons made, nine out of ten were in the predicted direction. This pattern of results (n = 10, k = 9) has the chance probability $\Pr(X \geq k)$ of $p = 0.0107$ of occurring under the H_0. These results provide tentative support for the hypothesis that the presence of annuli or patchwork configuration may act as weak figure-ground segregation cues that slightly reduce the extent to which center and surround signals are pooled together.

P_{2BE}: Comparisons between Conditions B & E

This comparison between Conditions B and E was not planned a priori. Instead, the between-condition comparison P_{1AB} and within-condition comparison P_{1B} inspired a post hoc investigation. The comparison between Conditions A and B revealed significant evidence of more difference-enhancing in Condition A (rivalrous figure & stable background) than in Condition B (stable figure & rivalrous background). The comparison between similarity-enhanced and difference-enhanced percepts within Condition B was inconsistent and not significant. To make comparisons to Condition E (rivalrous backgrounds only), Condition B means reflect the total dominance durations for each background color, irrespective of the stable grating color or percept type ("difference-enhanced" or "similarity-enhanced"). The prediction for the comparison between Condition B (stable gratings & rivalrous background) and Condition E (rivalrous background only) was that they would *not* be statistically different.

Of the ten orthogonal contrasts, none produced significant differences. This is consistent with the prediction but provides only tentative evidence that the resolution of a rivalrous background is not influenced by a dichoptically stable figure region. Taken together with evidence from P_{1AB}, advantages to figural processing may be an emergent feature of pooled divisive-normalization.

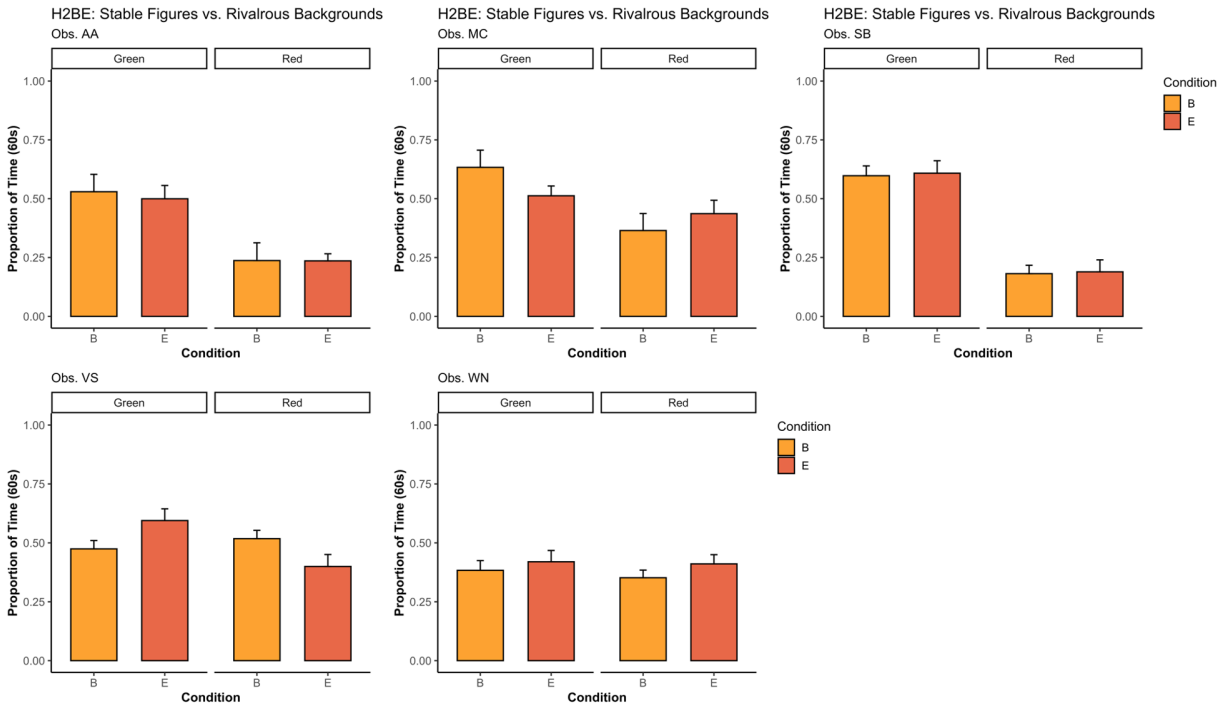

Figure 4.10: Exploratory, post hoc contrasts for five subjects investigating P_{BE}. The vertical axis is the proportion of a 60-s trial that each percept was seen. The bottom horizontal axis and bar colors indicate the Condition (B or E). The top horizontal axis organizes bars by resolved color; "Green" (left) or "Red" (right).

P_{2AD}: Comparisons between Conditions A & D

Condition A (stable background) was designed to evoke unequal divisive normalization on a rivalrous figure's component signals. Conversely, Condition D (rivalrous background & figure) was designed to evoke equal divisive normalization on both component signals of a rivalrous figure. Under H_1 and H_2, the prediction (P_{2AD}) was that Condition D would evoke significantly more similarity-enhanced percepts but significantly fewer difference-enhanced percepts relative to Condition A.

Of the ten planned orthogonal contrasts conducted (two per observer), 9 were statistically significant, and all ten were in the predicted direction (Figure 4.10). Recall that observer MC never reported a difference-enhanced percept during Condition D trials; accordingly, no

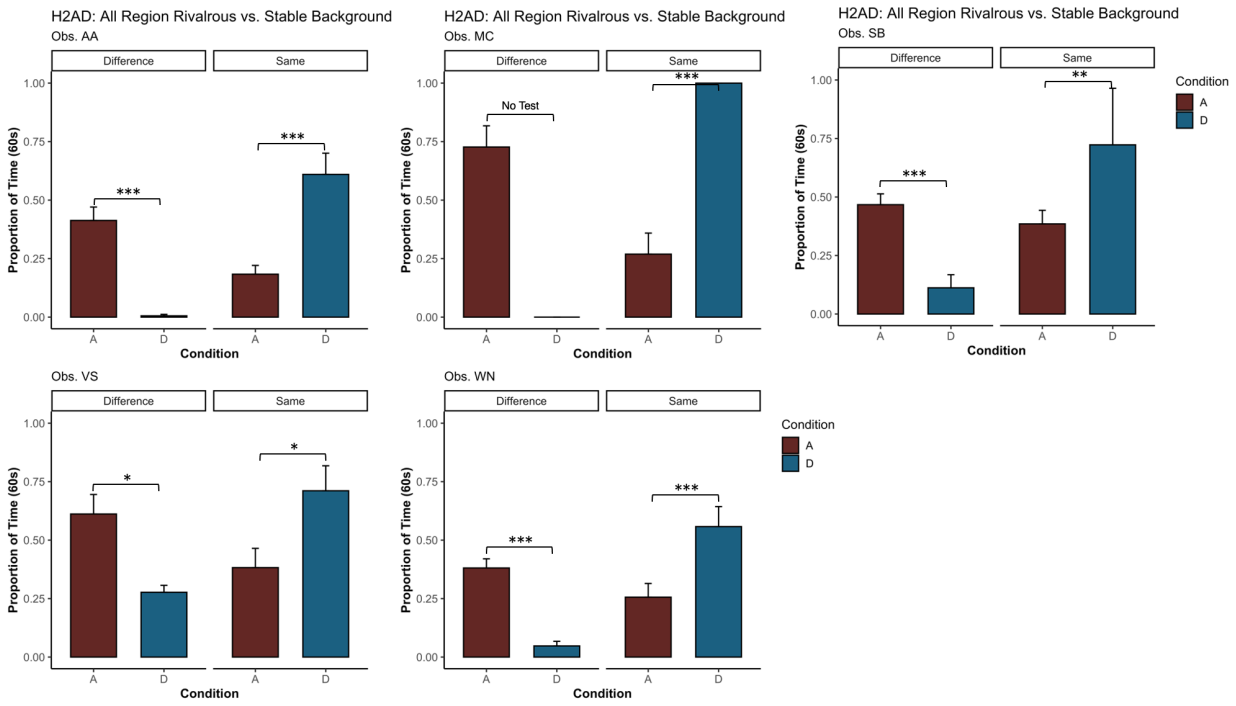

Figure 4.11: Planned contrasts for five subjects investigating P_{2AD}. The vertical axis is the proportion of a 60-s trial that each percept was seen. The bottom horizontal axis and bar color indicate the Condition (A or D). The top horizontal axis organizes bars by response type ("Difference" or "Same"). Brackets indicate a significant contrast, where *, **, and *** indicate significance at $p < 0.05$, $p < 0.01$, and $p < 0.001$, respectively.

comparisons were made to the absence of observations. In addition to corroborating the main effects of these individual conditions, the contrast for P_{AD} highlights a perceptual reversal in ambiguity resolution that depends on the relationship between figures and the surround.

4.5.3 Independence Predictions: Conditions A-D

As described in the general methods, independence predictions were calculated using top and bottom trials (Section 2.3.1). Independence predictions provide a measure of interocular grouping, and violations of independence reveal perceptual bias which, in this case, is the above chance occurrence of top and bottom gratings resolving as identical. Independence predictions should be treated with caution in Experiments 2-4. Unlike Experiment

1, where the primary manipulation was within the rivalrous signal (i.e., rivalry types above and below fixation), the remaining experiments manipulated the stable region adjacent to rivalrous regions. Comparisons between observations and independence predictions cannot index the extent to which a stable background influences the resolution of rivalrous regions. These predictions can only indicate the expectation under an independence model that top and bottom regions will resolve together. The manipulation of stable background chromaticity was a known increase in the statistical dependencies between rivalrous and background regions. In line with a normalization pool explanation of interocular grouping, it was expected that single-grating trials used to calculate independence predictions would show very similar resolution rates due to the influence of the background. Since the joint probability of two equally likely independent events is always less than the probability of just one of these events, it was expected that these comparisons would be rarely significant, but likely in the predicted direction, where observations occurred for longer average dominance durations than their predictions.

Condition A: Observations vs. Predictions

Of the 20 planned contrasts, one observer (Obs. WN) produced three significant results (p's < 0.05) and all other comparisons were not significant but were in the predicted direction. This has the chance probability of occurring under H_0 of $p = (0.5)^{20}$.

Condition B: Observations vs. Predictions

Of the 20 planned contrasts, only one was significant (Obs. WN, $p < 0.05$) but all 20 were in the predicted direction. As before, this has the chance probability of occurring under the null hypothesis of $p = (0.5)^{20}$.

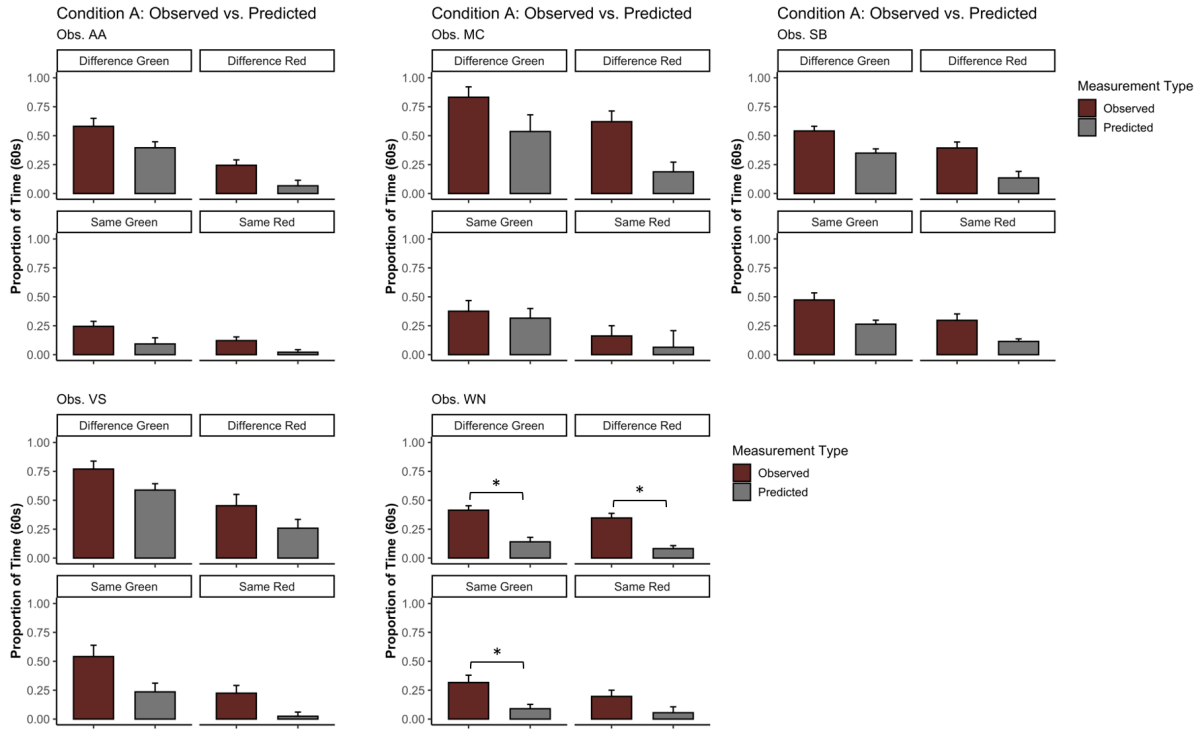

Figure 4.12: Planned contrasts for five subjects comparing observations in Condition A to their independence predictions. The vertical axis is the proportion of a 60-s trial that each percept was seen. Bar colors indicate the measurement type ("Observed" or "Predicted"). The top horizontal axes organize bars by response type ("Difference" or "Same") and background color ("Green" or "Red"). Brackets indicate a significant contrast, where *, **, and *** indicate significance at $p < 0.05$, $p < 0.01$, and $p < 0.001$, respectively.

Condition C: Observations vs. Predictions

Of the 20 planned contrasts, two were significant (Obs. WN, p's < 0.05), but all 20 were in the predicted direction, with the chance probability of occurring under the null hypothesis of $p = (0.5)^{20}$.

Condition D: Observations vs. Predictions

Of the 20 planned contrasts, one was significant (Obs. WN, $p < 0.05$). Thirteen of the remaining comparisons were in the predicted direction, with the chance probability of oc-

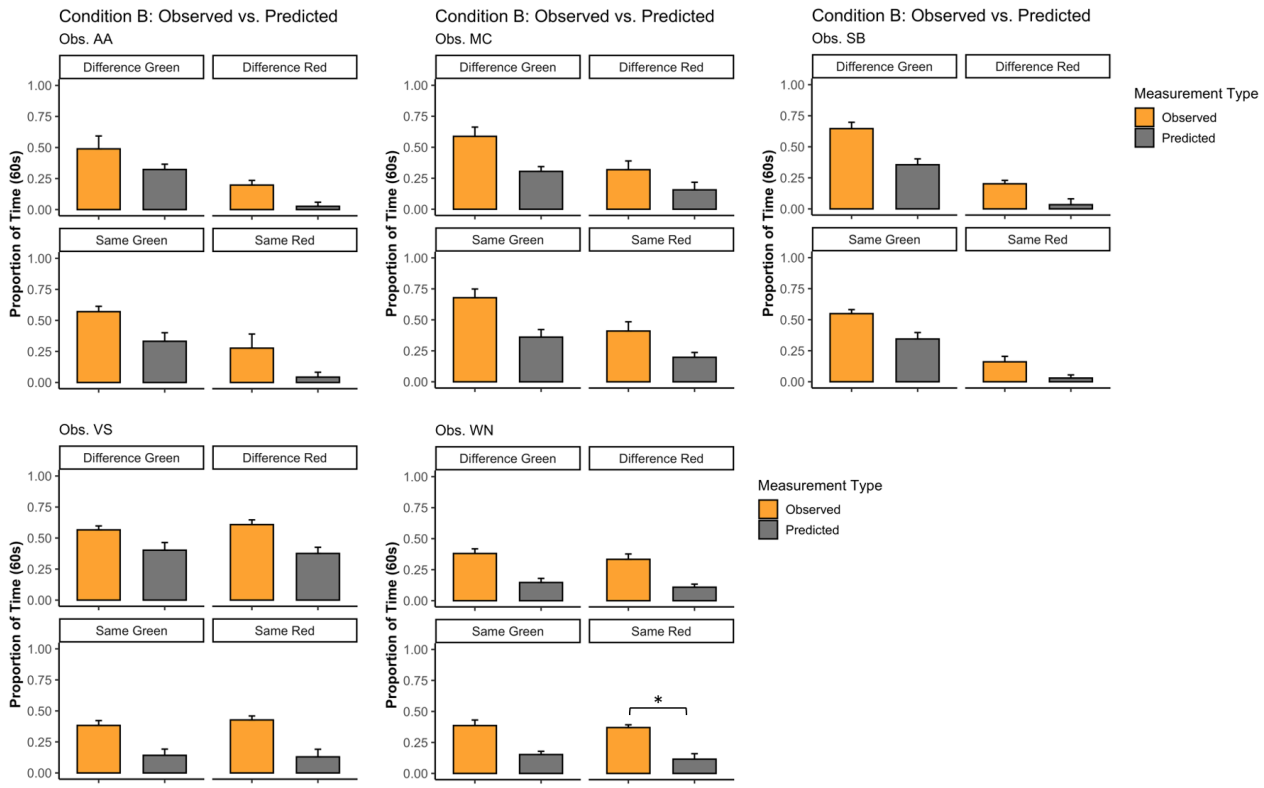

Figure 4.13: Planned contrasts for five subjects comparing observations in Condition B to their independence predictions. The vertical axis is the proportion of a 60-s trial that each percept was seen. Bar colors indicate the measurement type ("Observed" or "Predicted"). The top horizontal axes organize bars by response type ("Difference" or "Same") and background color ("Green" or "Red"). Brackets indicate a significant contrast, where *, **, and *** indicate significance at $p < 0.05$, $p < 0.01$, and $p < 0.001$, respectively.

curring under the null hypothesis of $p = 0.057$. Several observers (Obs. AA, MC, VS, and WN) never or rarely reported difference-enhanced percepts, so these low-measurement comparisons were considered failures under a binomial sign test.

4.6 Experiment 2 Discussion

Overarching hypotheses related to equal and unequal normalization yielded seven specific hypotheses and predictions. Of the seven a priori predictions, all seven provide evidence consistent with divisive normalization in ambiguity resolution. In particular, a stable back-

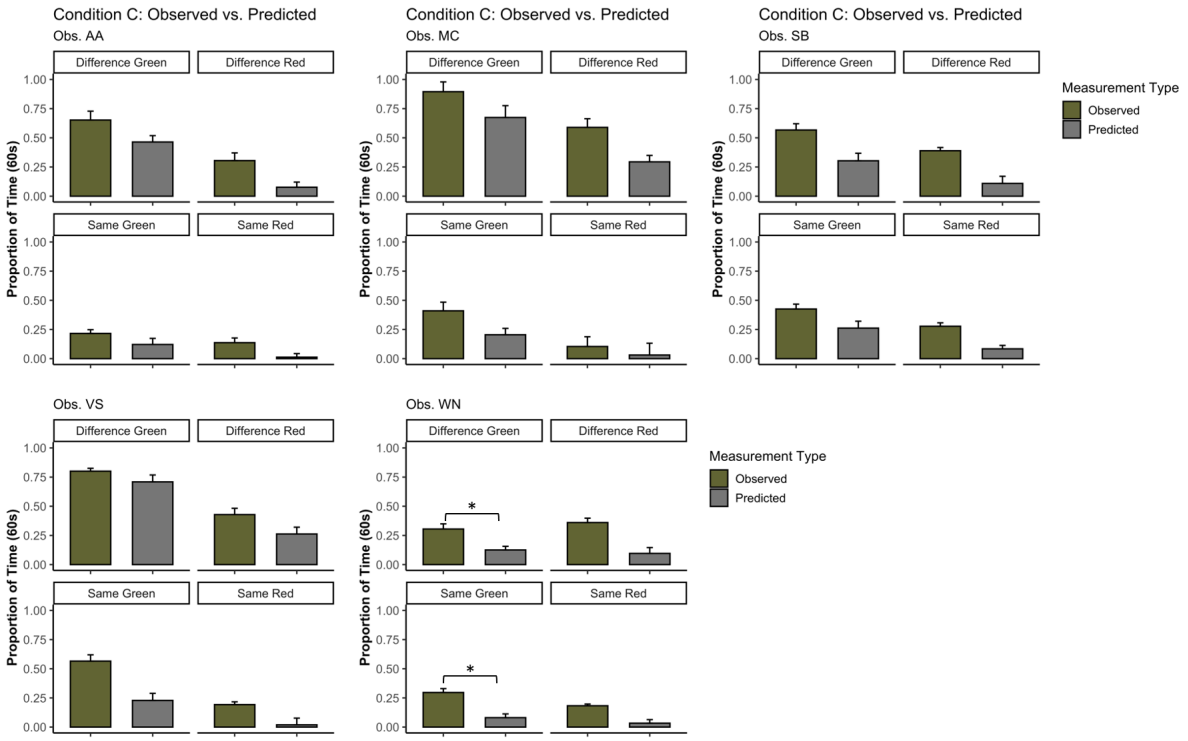

Figure 4.14: Planned contrasts for five subjects comparing observations in Condition C to their independence predictions. The vertical axis is the proportion of a 60-s trial that each percept was seen. Bar colors indicate the measurement type ("Observed" or "Predicted"). The top horizontal axes organize bars by response type ("Difference" or "Same") and background color ("Green" or "Red"). Brackets indicate a significant contrast, where *, **, and *** indicate significance at $p < 0.05$, $p < 0.01$, and $p < 0.001$, respectively.

ground influencing the resolution of ambiguous figures to maximize distinctiveness is novel evidence of a divisive-normalization mechanism acting on rivalrous representations. Experiment two revealed a visual processing asymmetry such that divisive normalization, an attention-directed mechanism, has a stronger influence on the resolution of rivalrous figures than rivalrous backgrounds. Experiment 2 also provides support for the role of divisive normalization in figure-ground segregation and may implicate figure-ground segregation as the process of resolving neural ambiguity, regardless of its source (e.g., typical viewing or rivalrous dichoptic viewing; Schwartz and Coen-Cagli, 2013; Sanchez-Giraldo et al., 2019). Finally, Experiment 2 corroborates and extends Experiment 1's finding that identical signals

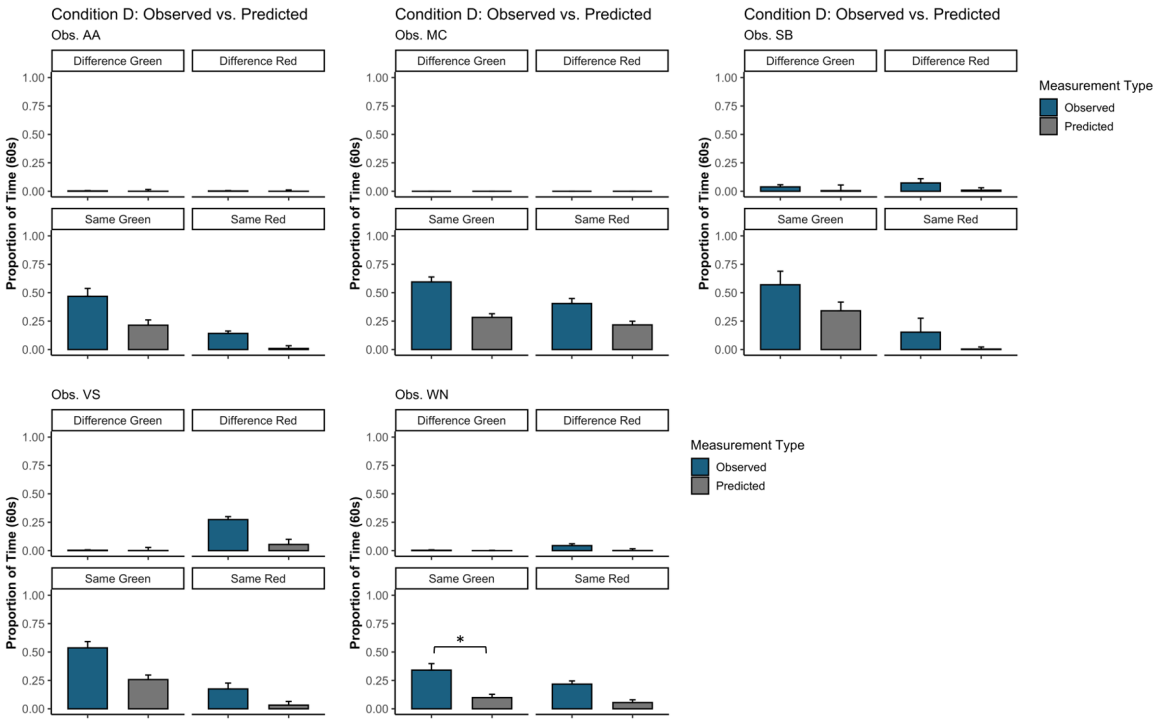

Figure 4.15: Planned contrasts for five subjects comparing observations in Condition D to their independence predictions. The vertical axis is the proportion of a 60-s trial that each percept was seen. Bar colors indicate the measurement type ("Observed" or "Predicted"). The top horizontal axes organize bars by response type ("Difference" or "Same") and background color ("Green" or "Red"). Brackets indicate a significant contrast, where *, **, and *** indicate significance at $p < 0.05$, $p < 0.01$, and $p < 0.001$, respectively.

in the visual field are linked together by a pooled response tuned to the same feature conjunctions. In this way, the most common signal has the largest response pool, so it would impose the most divisive normalization, thereby reducing the strength of prevalent signals and allowing other signals with a smaller response pool to be perceived.

Since stimuli in Experiments 1 and 2 were four cpd square-wave gratings, it was impossible to address cell-type hypotheses. A single-opponent cell would integrate over stimulus areas taking the space average, resulting in desaturated representations of chromatic stimuli due to averaging in grey phases. Double-opponent cells show their peak response to oriented patterns in the range of 2 cpd (Shapley and Hawken, 2011; Shapley et al., 2019). Since

double-opponent cells have been implicated in perceptually enhancing chromatic contrast for spatiochromatic patterns compared to uniform fields with the same space-average cone contrast (Shapley et al., 2019), the following experiment will consider both checkered pattern and uniform stimuli in the context of divisive normalization.

CHAPTER 5

EXPERIMENT 3

5.1 Rationale

Cone-opponent cells in the cortex, single and double-opponent, are implicated in processing chromatic signals. Single-opponent cells are thought to integrate over space, and large, uniform patches of color evoke their max response. Conversely, double-opponent cells are sensitive to spatiochromatic variations and provide their maximum response to chromatic stimuli with oriented spatiochromatic patterns that vary around two cpd (Shapley et al., 2019). Experiment 2 provided evidence of a divisive-normalization mechanism acting on rivalrous chromatic signals but was not designed to dissociate the influences of different cell types. The relative roles of each cell in processing a chromatic signal are exemplified by the perceptual difference between a uniform patch and a checkered pattern patch with the same space-averaged chromatic signal (Figure 5.1). The checkered pattern percept is stronger and more well-differentiated from the background despite having the same amount of signal across the same space. A normalization mechanism that can act to differentiate less common signals may rely more heavily on one cell type, and this may produce a detectable perceptual difference.

The present experiment explores the possibility of a particular class of opponent cell drivers and hypotheses related to the spatiochromatic-selectivity of a normalization mechanism. Hypotheses related to spatiochromatic-selectivity will shed light on the extent to which a normalization process is sensitive to the spatial distribution of the signal. If the relative amount of each chromatic signal is the primary influence on normalization strength, then a stimulus with a spatiochromatic pattern may split the normalization pools further. Specifically, patterned stimuli may evoke weaker divisive normalization due to a diluted chromatic signal. Two Conditions (A & B) were designed to differentiate between possible

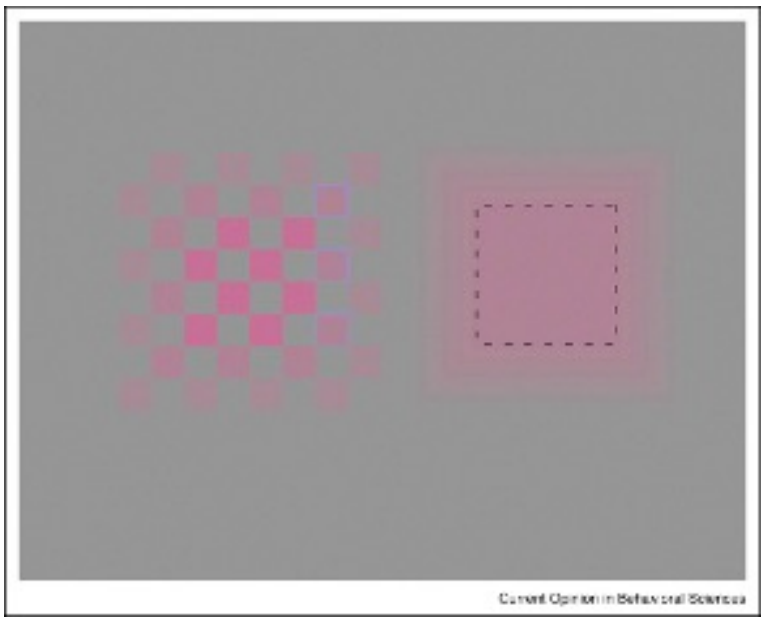

Figure 5.1: A pink–grey checkered pattern (left) and a central pink square (right) have the same space-average but the red-pink checkered pattern appears more colorful. Image adapted (contrast increased 70%) from Current Opinion in Behavioral Sciences© (Shapley et al., 2019).

driving cell types. An additional two (C & D) were designed to further assess the hypothesis from Experiment 2 that the relative area of stable to rivalrous regions can explain normalization strength. Finally, two additional stimuli were designed as control Conditions (E & F). Condition E is a stimulus with a space-averaged background, and Condition F introduces a stimulus with a neutral-colored (grey) background.

All comparisons were planned a priori, with an updated version of the hypothesis (H_1) from Experiment 2, which stated that a stable chromatic region would divisively normalize a rivalrous signal, resulting in the perceptual resolution of a color-differentiated percept. Under the updated hypothesis (H_1), the strength of divisive normalization imposed by a stable region onto a rivalrous region depends on each signal's relative strength. Here chromatic strength can be considered saturation after performing a space-average over stimulus. Grey regions of patterned stimuli should evoke an intermediate response from color-opponent cells. Specifically, single-opponent cells will average over a spatiochromatic pattern yielding a signal

for a color that is desaturated compared to its chromatic component. A double-opponent cell should be selective for chromatic contrast between grey and chromatic regions. Finally, a new hypothesis, H_3 considers whether a normalization mechanism acting on a chromatic signal will increase in strength as the background chromaticity gets closer in chromaticity space (MacLeod and Boynton, 1979) to one of the rivalrous signals. Experiments 1 and 2 cannot determine the extent to which divisive normalization may require identical signals or if the process is more continuous. Identical signals across a natural scene are rare, so the chromatic normalization mechanism is posited to be flexible, acting on the chromatic signal (relative cone activation) before it becomes a perceived color.

5.2 Stimuli

For all conditions, rivalrous figures subtended 1.5° of visual angle and were surrounded by a black annulus (0.25cd/m$^{2)}$ that increased the visual angle to 1.75°. All Stimuli were presented inside square-shaped fusion boxes with subtended 4.5° of visual angle, set to be the same luminance as the gratings near 15 cd/m^2. The peripheral background was set to be black at 0 cd/m^2. The rivalrous chromaticities were defined using lsY values of [0.72, 0.3, 14.95] and [0.61, 0.3, 14.95], for red-appearing (called "red") and green-appearing (called "green") regions, respectively. Stimuli were either a two cpd (with grey phases) checkered pattern or uniform. The bottom and top regions on top-only and bottom-only trials were a spatially uniform grey [0.665, 1.0, 14.95]. All trials were presented in ISR at 3.75 Hz (Christiansen et al., 2017; Logothetis et al., 1996). Additionally, the first ten seconds of each 70-second trial were discarded to remove eye-of-origin information. This experiment used six conditions (A-F) to make four planned comparisons.

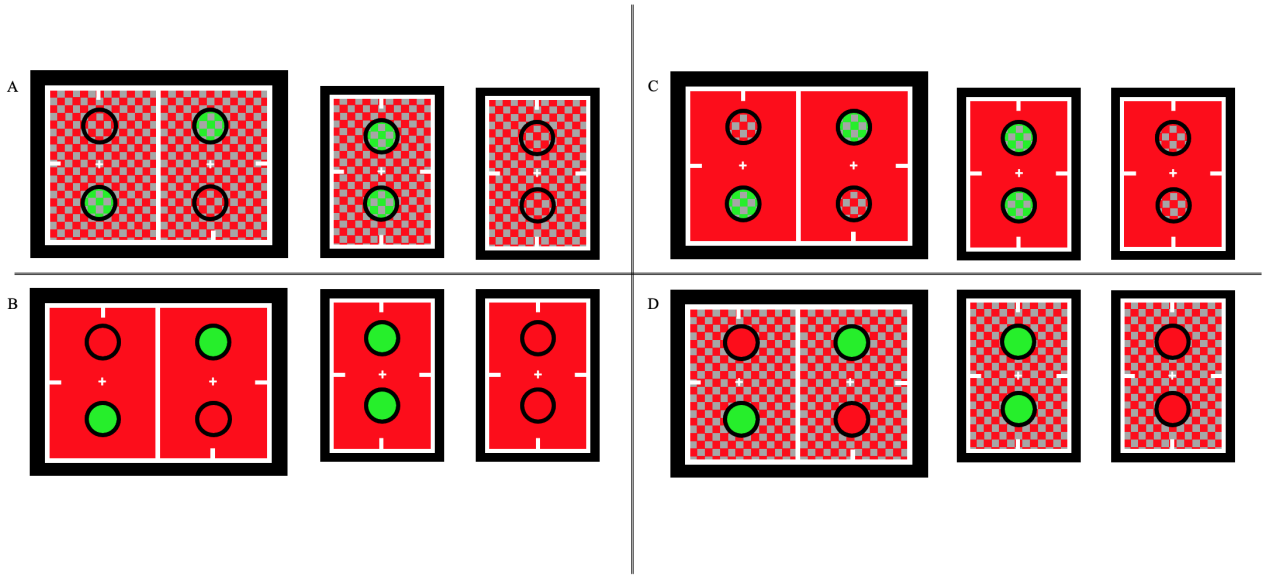

Figure 5.2: Conditions and percepts. Top row: left and right eye images and measured percepts for Conditions A and C. Bottom row: left and right eye images and measured percepts for Conditions B and D. Note: only red background stimuli are depicted but all conditions also appeared with green backgrounds.

5.2.1 Conditions

Condition A: All Checkered Pattern

Condition A's stimulus configuration (Figure 5.2 A) entails red/green rivalrous checkered pattern figures with a stable green or stable red checkered pattern background. This yielded two trial counterbalances for this condition: (1) red/green rivalrous checkered pattern on a stable green checkered pattern background and (2) red/green rivalrous checkered pattern on a stable red checkered pattern background. Each trial type had two single-grating conditions (see Section 2.3.1) used to calculate independence predictions for each region, yielding four single-grating trials.

Condition B: All Uniform

Condition B's stimulus configuration (Figure 5.2 B) entails red/green rivalrous disks with a stable green or stable red checkered pattern background. This yielded two trial counterbalances for this condition: (1) red/green rivalrous disks on a stable green background and (2) red/green rivalrous disks on a stable red background. Each trial type had two single-grating conditions (see Section 2.3.1) used to calculate independence predictions for each region, yielding four single-grating trials.

Condition C: Checkered Pattern with Uniform Background

Condition C's stimulus configuration (Figure 5.2 C) entails red/green rivalrous checkered pattern figures with a stable green or stable red uniform background. This yielded two trial counterbalances for this condition: (1) red/green rivalrous checkered pattern on a stable green background and (2) red/green rivalrous checkered pattern on a stable red background. Each trial type had two single-grating conditions (see Section 2.3.1) used to calculate independence predictions for each region, yielding four single-grating trials.

Condition D: Disks with Checkered Pattern Background

Condition D's stimulus configuration (Figure 5.2 D) entails red/green rivalrous disks with a stable green or stable red checkered pattern background. This yielded two trial counterbalances for this condition: (1) red/green rivalrous disks on a stable green checkered pattern background and (2) red/green rivalrous disks on a stable red checkered pattern background. Each trial type had two single-grating conditions (see Section 2.3.1) used to calculate independence predictions for each region, yielding four single-grating trials.

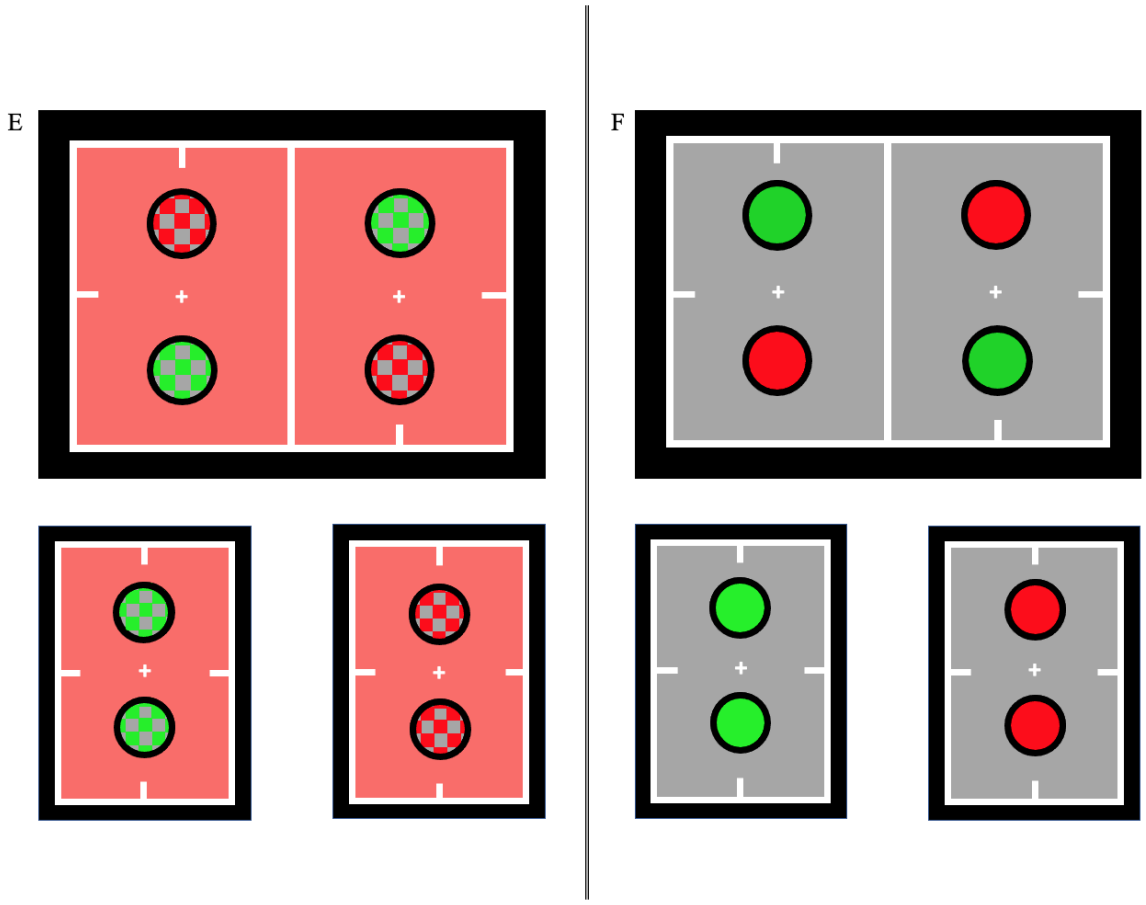

Figure 5.3: Conditions and percepts. Left: left and right eye images and measured percepts for Condition E. Right: left and right eye images and measured percepts for Condition F.

Condition E: Checkered Pattern with Space Average Background

Control Condition E's stimulus configuration (Figure 5.3 E) entails red/green rivalrous checkered pattern figures with a stable green or stable red space-average background. This yielded two trial counterbalances for this condition: (1) red/green rivalrous checkered pattern on a stable space-averaged green background and (2) red/green rivalrous checkered pattern on a stable space-averaged red background. Space-averaged chromaticities were constructed by averaging over grey/green and grey/red checkered patterns.

Condition F: Disks with Grey Background

Condition F (Figure 5.3 F) is also a control condition and entails red/green rivalrous disks on a stable isoluminant grey background. The isoluminant grey background was the same chromaticity as the grey phases in patterned stimuli. There were no trial counterbalances for this condition, and single-rivalrous trials were not included.

5.3 Results

Analyses were conducted within subjects using planned orthogonal contrasts. Since all predictions were directional, a non-parametric group analysis considered the one-tailed binomial probability of the observed results by chance under the null hypothesis (H_0). The one-tailed binomial probability $\Pr(X \geq k) = \sum_k^n \binom{n}{k} p^k (1-p)^{n-k}$ of k or more successes on n trials under H_0.

5.3.1 P_{AB}: Comparison between Conditions A & B

This comparison (Figure 5.4) tests the difference between total average dominance durations for patterned and uniform stimuli. Importantly, these conditions have the same *ratio* between figure and background chromatic signal. So, while a checkered pattern introduces intermittent grey regions driving the entire chromatic signal down by half, the amount of signal in the figure and background regions, compared to Condition B (Figure 5.2 B), is half. If Condition B (all uniform) evokes more difference-enhanced percepts than Condition A (all checkered pattern), this would suggest a divisive-normalization mechanism that depends on the amount of similar signal driving the effect. If Condition A (Figure 5.2 A) evokes more difference-enhanced percepts, double-opponent cells might be implicated in divisive normalization. In light of Experiment 2's results, the prediction was that uniform stimuli would impose greater divisive normalization due to pooling over larger groups

of color-selective neurons. The prediction is that Condition A (all checkered pattern) will evoke more similarity-enhanced and less difference-enhanced percepts relative to Condition B (all uniform).

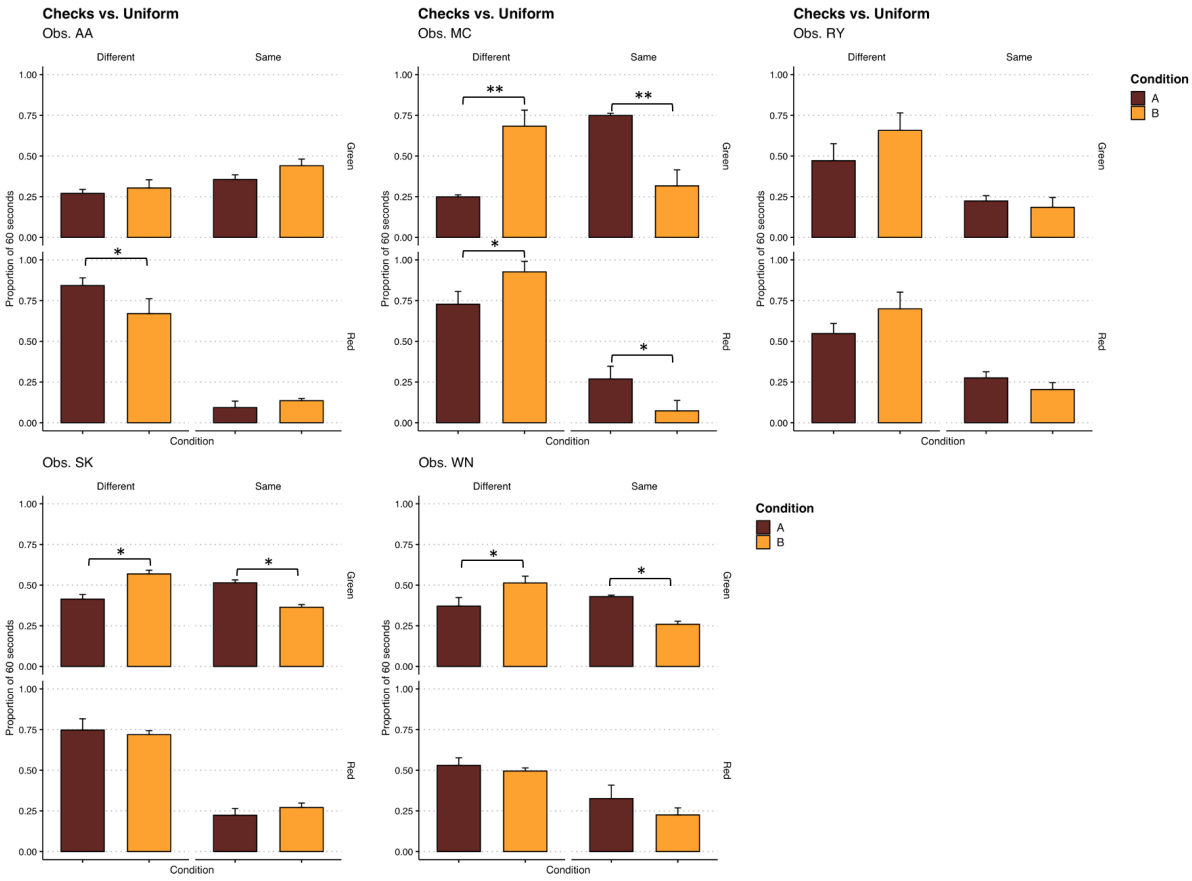

Figure 5.4: Planned contrasts for five subjects investigating P_{AB}. The vertical axis is the proportion of a 60-s trial that each percept was seen. The top horizontal axis groups results by response type ("Different" or "Same"). The bottom horizontal axis and bar color indicate the Condition (A or B). Brackets indicate a significant contrast, where *, **, and *** indicate significance at $p < 0.05$, $p < 0.01$, and $p < 0.001$, respectively.

Of the 20 (four per subject) planned comparisons (Figure 5.4), only nine were significant and of these eight were in the predicted direction. Overall, 14 of the 20 comparisons were in the predicted direction, where Condition A showed less difference-enhancing and more similarity-enhancement than Condition B. The one-tailed binomial probability 14 (k) successes on 20 (n) trials is 0.058 $\Pr(X \geq k)$. Additionally, one observer (AA) accounted

for half of the inconsistent results. This provided weak evidence that divisive normalization strength is modulated by the strength of chromatic signal rather than pattern-selectivity.

5.3.2 $P_{AC|BD}$: Comparisons between Conditions A vs C & B vs D

To further assess the influence of possible pattern selectivity, comparisons (P_{AC}) and (P_{BD}) investigated the strength of normalization of a matching and non-matching pattern between figure and background regions. Condition C (Figure 5.2 C); checkered pattern figure and uniform background and Condition A (all checkered pattern) have identical rivalrous signals but different backgrounds. To the same end, a planned comparison is made between Condition D (uniform figure and checkered pattern background) and Condition B (all uniform). If divisive normalization is pattern-selective, then Conditions A and B should have higher total average dominance durations for difference-enhanced percepts and lower total average dominance time for similarity-enhanced percepts relative to Condition C and D, respectively. Alternatively, suppose the divisive-normalization mechanism is dependent on the amount of chromatic signal in the background. In that case, conditions with a uniform background (B & D) should impose more divisive normalization than A and C, which have patterned backgrounds. The prediction for $P_{AC|BD}$ was that a normalization mechanism is not pattern-specific and uniform backgrounds impose stronger divisive normalization.

Of the 20 planned comparisons (Figure 5.5) between Conditions A and C, only six were statistically significant. Of the six significant results, three were in the predicted direction, and the other three were in the opposite direction (Obs. AA). Fourteen (k) of the 20 (n) trials were in the direction of the hypothesis, with the probability, $Pr(X \geq k) = 0.058$ of occurring by chance under H_0. This provided corroborating but weak evidence that divisive normalization is primarily modulated by the strength of chromatic signal than truly pattern-selective.

The prediction under H_1 for Conditions B (all uniform) and Condition D (uniform figure

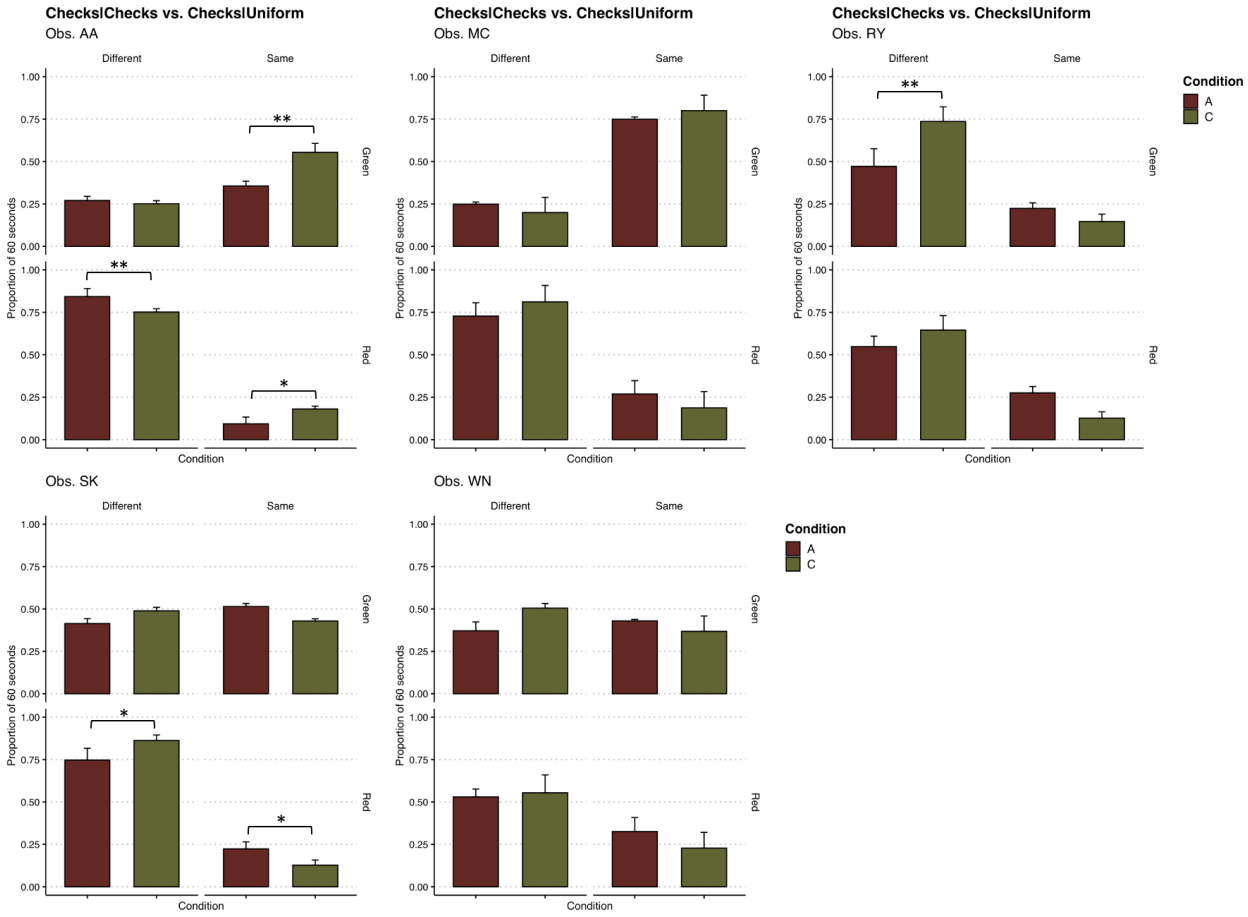

Figure 5.5: Planned contrasts for five subjects investigating P_{AC}. The vertical axis is the proportion of a 60-s trial that each percept was seen. The top horizontal axis groups results by response type ("Different" or "Same"). Right vertical axis is background color ("Green" or "Red"). The bar color indicates the Condition (A or C). Brackets indicate a significant contrast, where *, **, and *** indicate significance at $p < 0.05$, $p < 0.01$, and $p < 0.001$, respectively.

and checkered pattern background) was identical to comparisons between A and C (Figure 5.6), except the direction of prediction switches, such that Condition B (all uniform) should impose more divisive normalization due to a uniform background. For this comparison, only four planned comparisons were significant, but 17 of the 20 comparisons are in the predicted direction, with the chance probability of occurrence under the null of $p = 0.001$. $P_{AC|BD}$ that uniform background should impose more divisive normalization than patterned backgrounds was supported, although condition differences were minor.

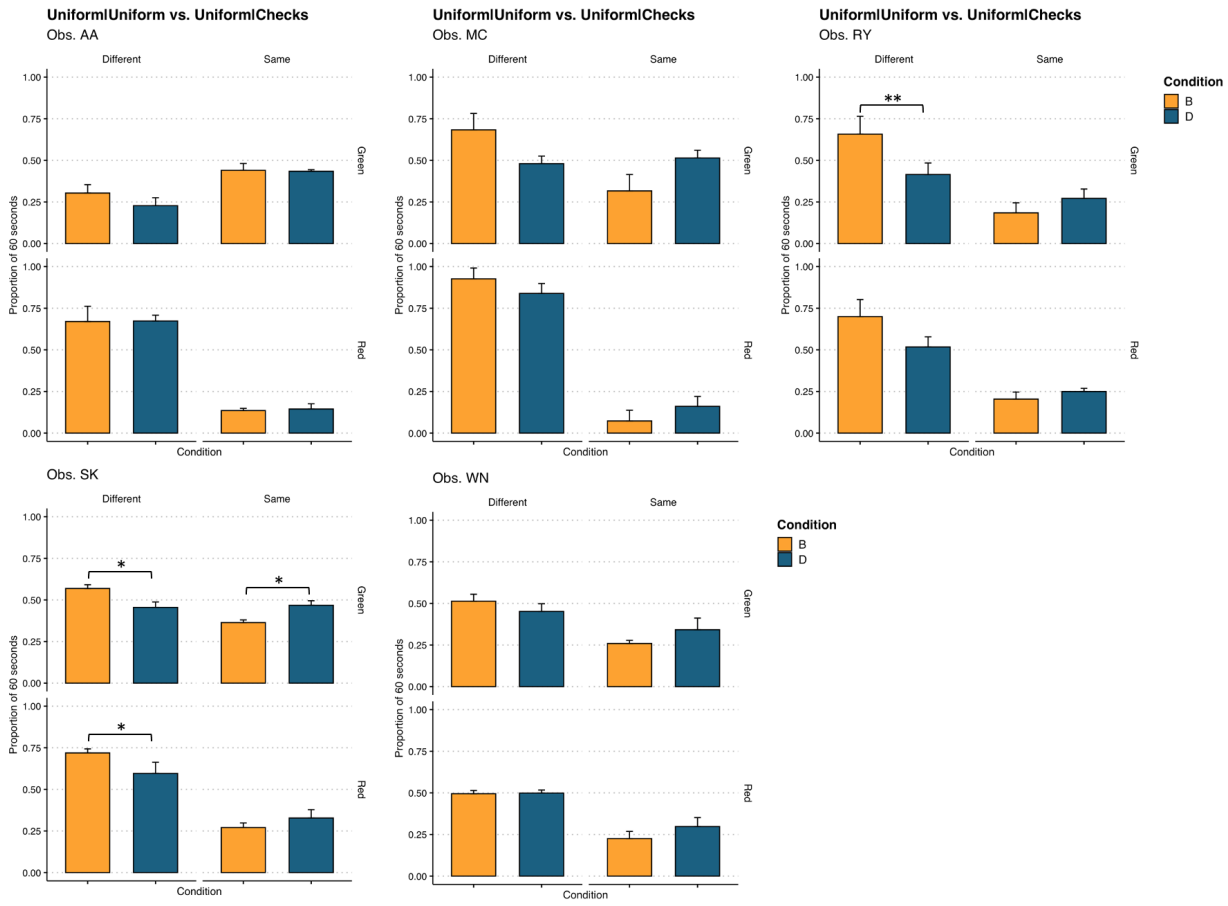

Figure 5.6: Planned contrasts for five subjects investigating P_{BD}. The vertical axis is the proportion of a 60-s trial that each percept was seen. The top horizontal axis groups results by response type ("Different" or "Same"). Right vertical axis is resolved color ("Green" or "Red"). The bar color indicates the Condition (B or D). Brackets indicate a significant contrast, where *, **, and *** indicate significance at $p < 0.05$, $p < 0.01$, and $p < 0.001$, respectively

Taken together, comparisons P_{AB} and $P_{AC|BD}$ provided weak evidence in support of the hypothesis that a divisive-normalization mechanism is modulated by the strength of the chromatic signal rather than being pattern-selective.

5.3.3 P_{AE}: Comparison between Conditions A & E

The comparison between A and E tested the hypothesis that single-opponent cells may integrate over patterned backgrounds and hold space-averaged representations. Specifically,

if single-opponent cells are implicated in a normalization process, Conditions A's (all checks) and E's (checks on space-average) results should be similar. P_{AE} is that control Condition E's results will not be statistically different from Condition A.

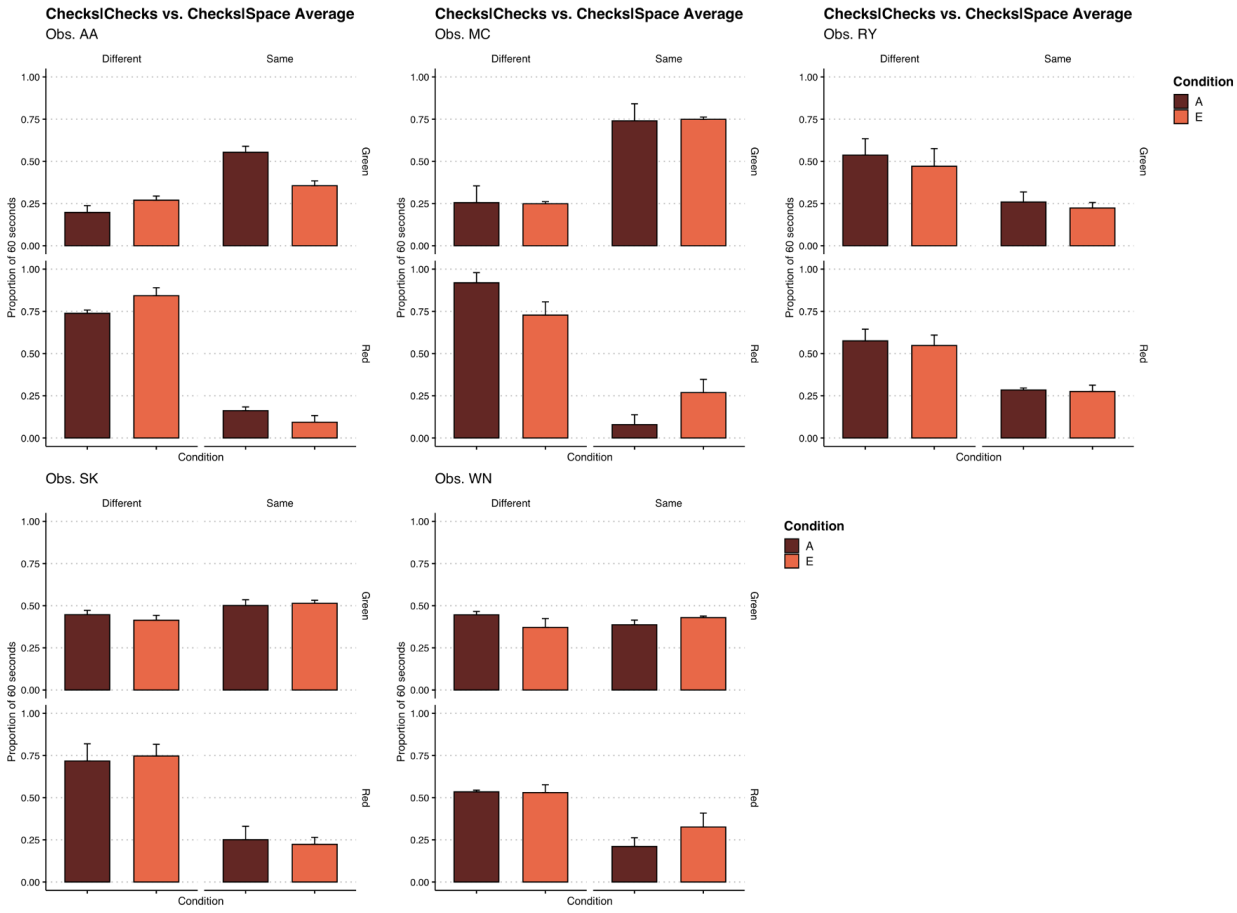

Figure 5.7: Planned contrasts for five subjects investigating P_{AE}. The vertical axis is the proportion of a 60-s trial that each percept was seen. The top horizontal axis groups results by response type ("Different" or "Same"). Right vertical axis is resolved color ("Green" or "Red"). The bar color indicates the Condition (A or E). Brackets indicate a significant contrast, where *, **, and *** indicate significance at $p < 0.05$, $p < 0.01$, and $p < 0.001$, respectively.

Of the 20 planned comparisons, four were significant. The remaining 16 show minimal differences and may provide weak support for the hypothesis that single-opponent cells play a role in divisive normalization. Specifically, single-opponent cells may be the cells being pooled over and divisively normalized.

5.3.4 P_{AF}: Comparison between Conditions A & F

It is unlikely that normalization pools are formed based on identical signals. The hypothesis for H_3 is simple; if divisive normalization is acting on chromatic signals, then a grey chromaticity should impose an intermediate normalization response because it is equidistant from red and green-appearing chromaticities. P_{AF} under H_3 was of a specific pattern of results that resemble a staircase rising in a specific direction. Specifically, a particular color percept (e.g., green) occurs the least surrounded by the same color (green) and occurs the most surrounded by an opponent color (red), with grey providing the intermediate step.

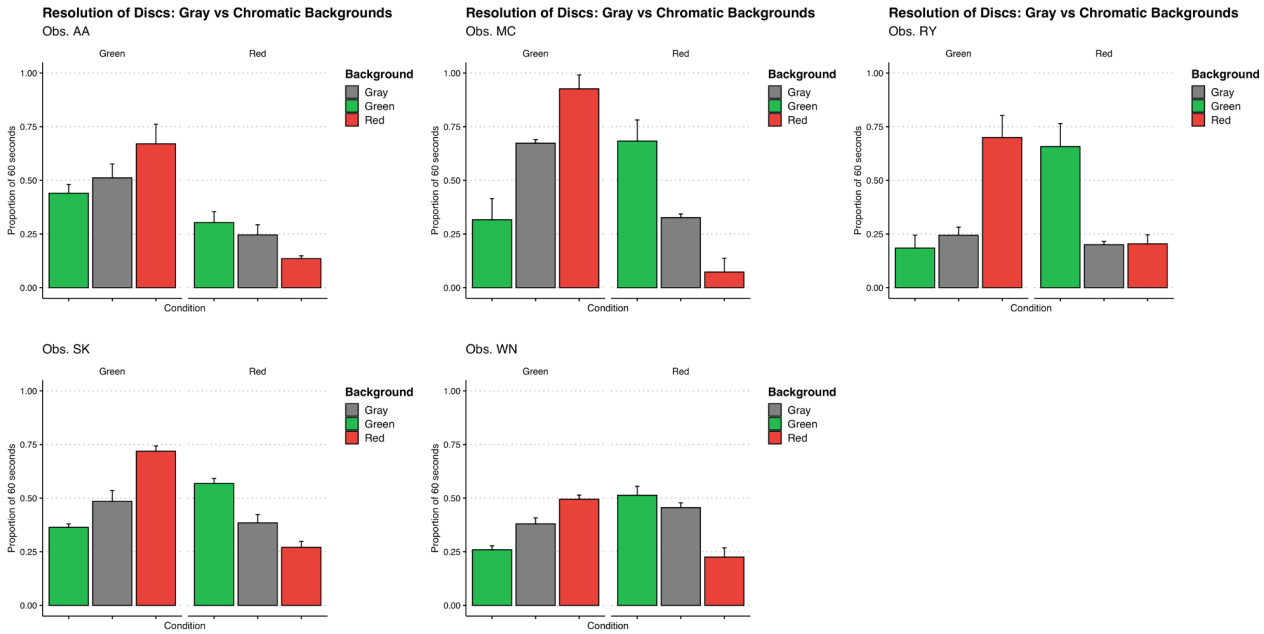

Figure 5.8: Planned contrasts for five subjects investigating P_{AF}. The vertical axis is the proportion of a 60-s trial that each percept was seen. The top horizontal axis groups results by resolved color. Finally, bar colors indicates the background color for each measurement.

Nine of the ten possible staircases (two per subject) were observed. This pattern (n = 10, k = 9, $p = 1/6$) of result has the one-tailed binomial probability of $p < 0.001$ of occurring under the null hypothesis. This provides strong evidence consistent with divisive normalization, assuming it acts continuously across chromaticity space and does not require identical representations.

5.3.5 Independence Predictions: Conditions A-D

As described in the general methods, independence predictions were calculated using top and bottom trials (Section 2.3.1). As in Experiment 2, the primary manipulation was the stable region adjacent to rivalrous regions. Comparisons between observations and independence predictions cannot index the extent to which a stable background influences the resolution of rivalrous regions. These predictions can only indicate the expectation under an independence model that top and bottom regions will resolve together. The manipulation of stable background chromaticity was known to increase the statistical dependencies between rivalrous and background regions. In line with a normalization pool explanation of interocular grouping, it was expected that single-grating trials used to calculate independence predictions would show very similar resolution rates due to the influence of the background. Since the joint probability of two equally likely independent events is always less than the probability of one of these events alone, it was expected that these comparisons would be rarely significant, but likely in the predicted direction, where observations occur more often than their predictions.

Condition A: Observations vs. Predictions

Of the 20 planned orthogonal contrasts (four per observer), five were statistically significant (Obs. SK, p's < 0.05; Obs. WN, p's < 0.001). Of the 20 comparisons, 19 were clearly in the predicted direction (Figure 5.9). One comparison ("Difference Green" for Obs. SK) is in the predicted direction, but the difference was small, so it was counted as a failure for calculating the chance probability ($p < 0.001$) of observing 19 (k) successes on 20 trials (n).

Condition B: Observations vs. Predictions

Of the 20 planned orthogonal contrasts (four per observer), one was statistically significant (Obs. WN, $p < 0.05$). Of the 20 comparisons, all 20 were in the predicted direction (Figure

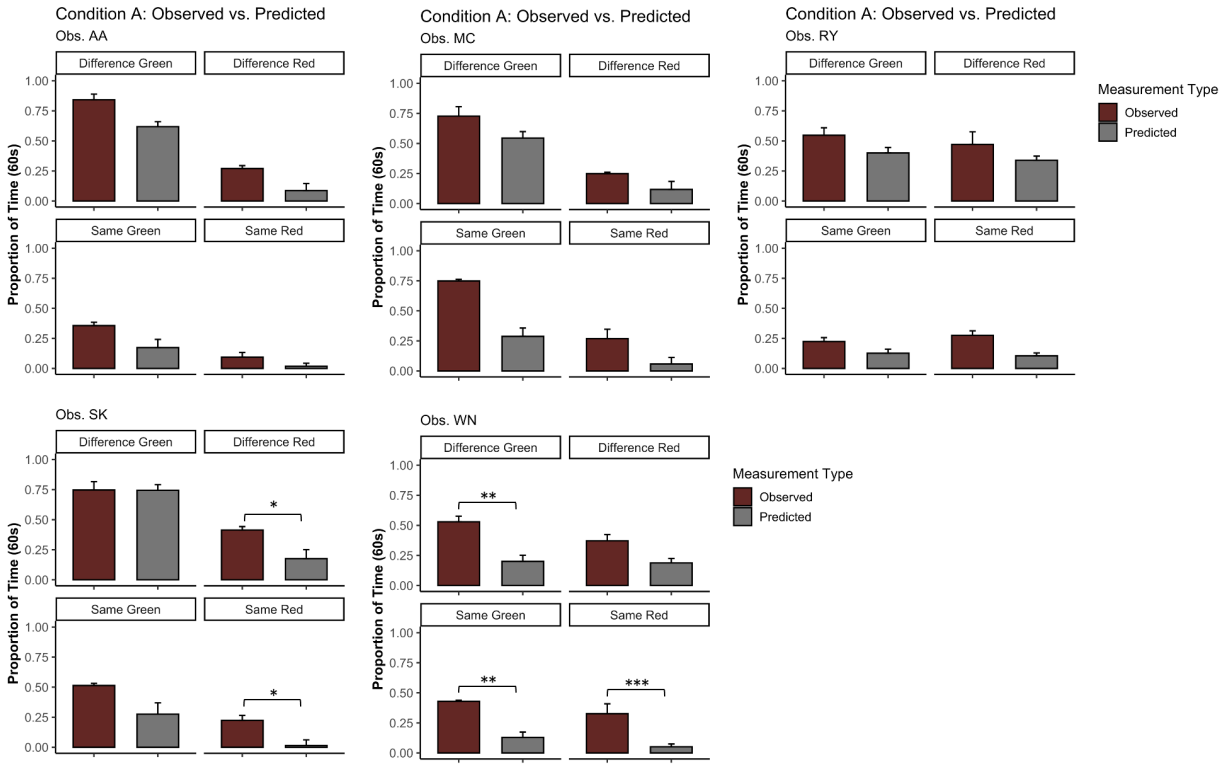

Figure 5.9: Planned contrasts for five subjects comparing observations in Condition A to their independence predictions. The vertical axis is the proportion of a 60-s trial that each percept was seen. Bar colors indicate the measurement type ("Observed" or "Predicted"). The top horizontal axes organize bars by response type ("Difference" or "Same") and background color ("Green" or "Red"). Brackets indicate a significant contrast, where *, **, and *** indicate significance at $p < 0.05$, $p < 0.01$, and $p < 0.001$, respectively.

5.10). The chance probability of observing 20 (k) successes on 20 trials (n) is $p = (0.5)^{20}$.

Condition C: Observations vs. Predictions

Of the 20 planned orthogonal contrasts (four per observer), five were statistically significant (Obs. SK, p <0.01; Obs. WN, p's < 0.05). Of the 20 comparisons, again all 20 were in the predicted direction (Figure 5.11). The chance probability of observing 20 (k) successes on 20 trials (n) is $p = (0.5)^{20}$.

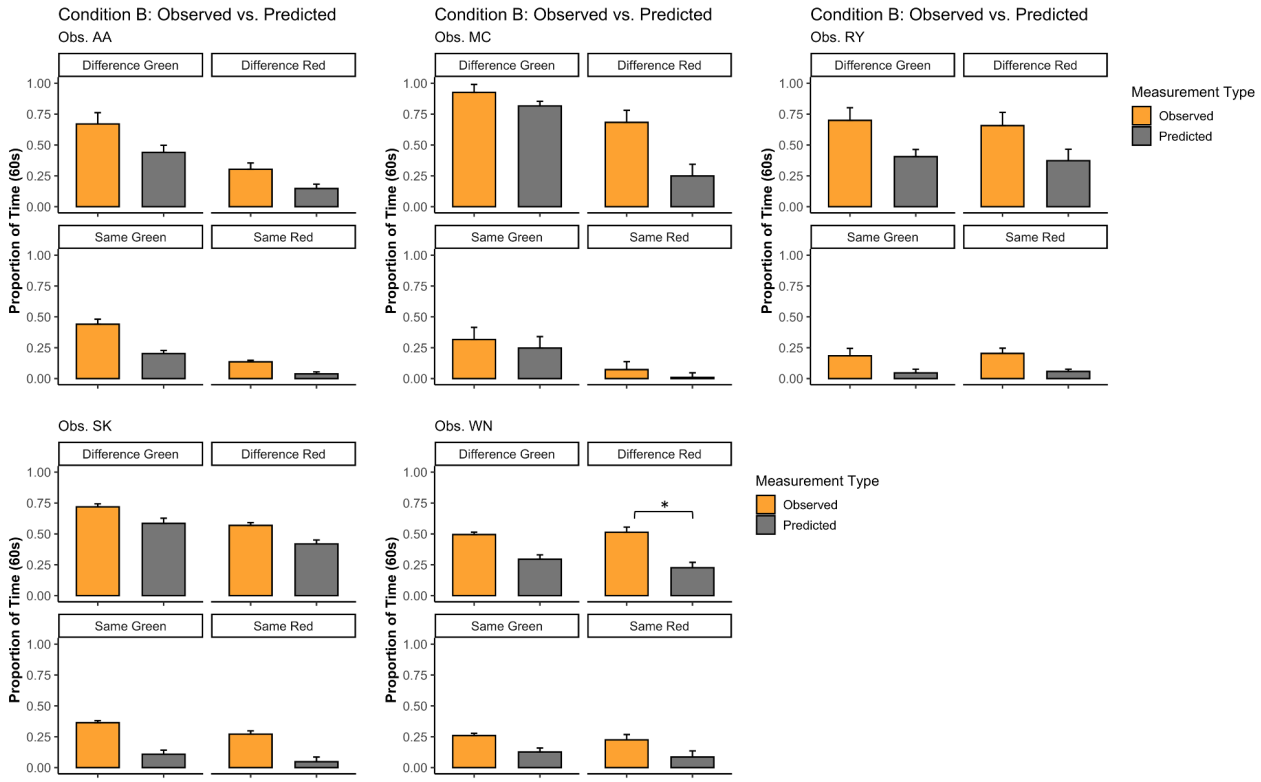

Figure 5.10: Planned contrasts for five subjects comparing observations in Condition B to their independence predictions. The vertical axis is the proportion of a 60-s trial that each percept was seen. Bar colors indicate the measurement type ("Observed" or "Predicted"). The top horizontal axes organize bars by response type ("Difference" or "Same") and background color ("Green" or "Red"). Brackets indicate a significant contrast, where *, **, and *** indicate significance at $p < 0.05$, $p < 0.01$, and $p < 0.001$, respectively.

Condition D: Observations vs. Predictions

Of the 20 planned orthogonal contrasts (four per observer), four were statistically significant for a single observer (Obs. WN, p's < 0.05). All 20 comparisons were in the predicted direction (Figure 5.11). The chance probability of observing 20 (k) successes on 20 trials (n) is $p = (0.5)^{20}$.

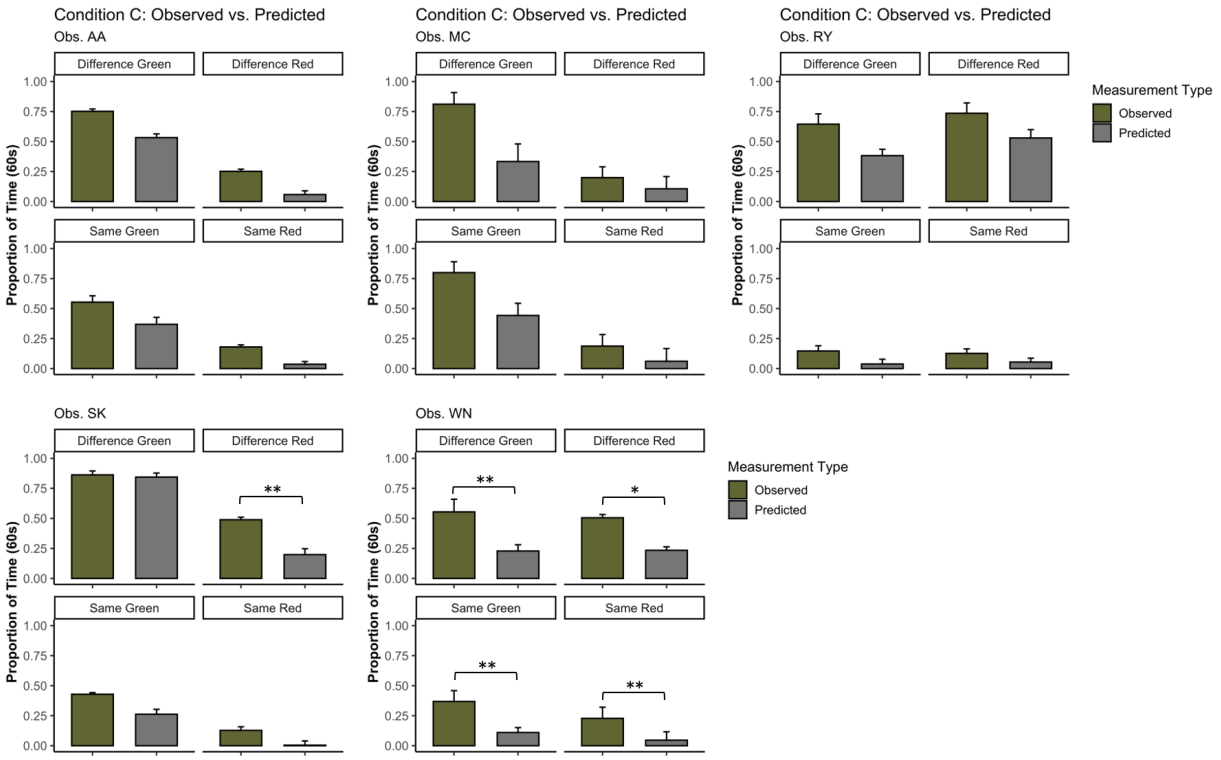

Figure 5.11: Planned contrasts for five subjects comparing observations in Condition C to their independence predictions. The vertical axis is the proportion of a 60-s trial that each percept was seen. Bar colors indicate the measurement type ("Observed" or "Predicted"). The top horizontal axes organize bars by response type ("Difference" or "Same") and background color ("Green" or "Red"). Brackets indicate a significant contrast, where *, **, and *** indicate significance at $p < 0.05$, $p < 0.01$, and $p < 0.001$, respectively.

5.4 Experiment 3 Discussion

The results from Experiment 3 provided evidence consistent with the hypothesis that the strength of the chromatic signal modulates a divisive-normalization mechanism and is not strongly selective for patterned stimuli (P_{AB}) or the degree of coherency between figure and background patterns ($P_{AC|BD}$). Another explanation for these results could be that divisive normalization primarily acts on single-opponent cells' activity, which integrates over spatiochromatic variations. The comparison between Conditions A (all checks) and E (checks on a space-averaged background) failed to find evidence that the chromatic signal being acted on is pattern-selective. Finally, the comparison between Conditions A and F supported the

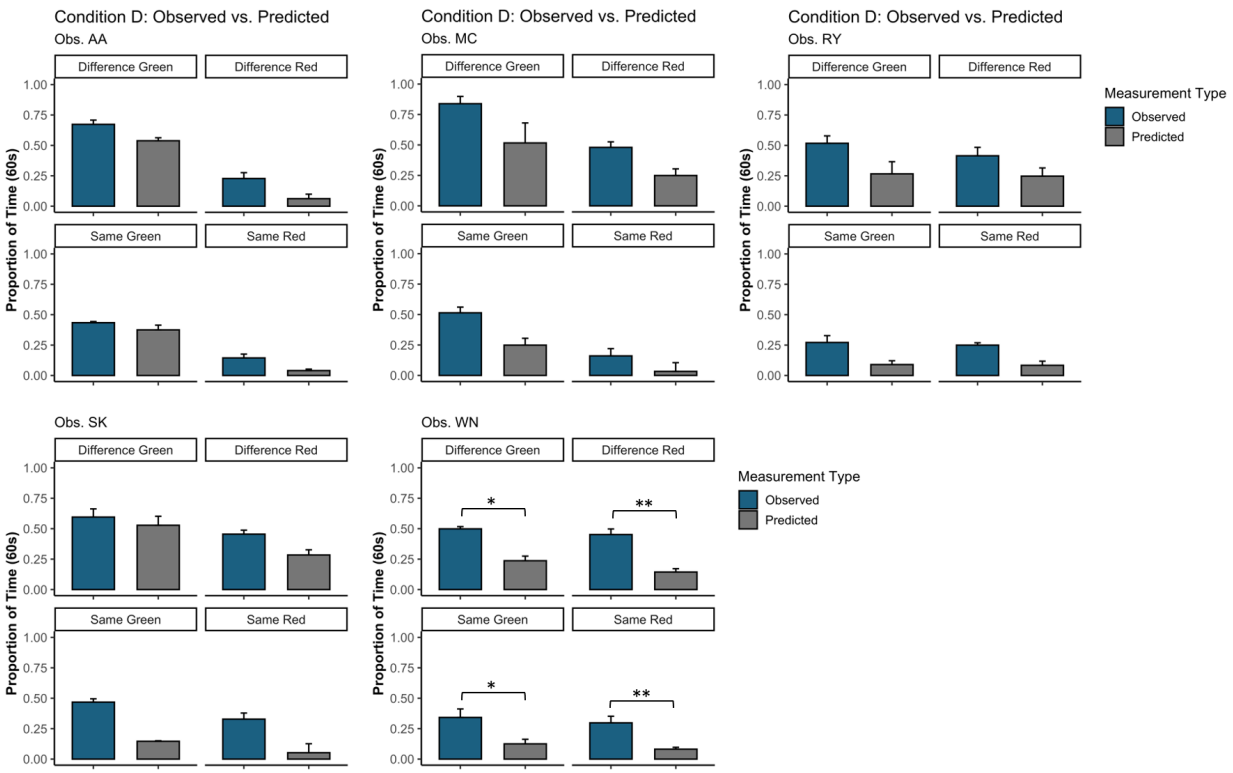

Figure 5.12: Planned contrasts for five subjects comparing observations in Condition B to their independence predictions. The vertical axis is the proportion of a 60-s trial that each percept was seen. Bar colors indicate the measurement type ("Observed" or "Predicted"). The top horizontal axes organize bars by response type ("Difference" or "Same") and background color ("Green" or "Red"). Brackets indicate a significant contrast, where *, **, and *** indicate significance at $p < 0.05$, $p < 0.01$, and $p < 0.001$, respectively.

hypothesis that a normalization process acts on continuous signals, and links between similar regions may be modulated by their relative distances in chromaticity space.

The stimuli used to evoke responses from single-opponent and double-opponent cells may have favored single-opponent cells in two ways: (1) patterned stimuli had less rivalrous signal, as grey phases were dichoptically stable and (2) their response may have been attenuated by the relatively neutral effect of an equal-energy stimulus. Also, a 2-D Fourier analysis of checkered patterns showed that power was oriented along both diagonals. Since double-opponent cells are thought to be orientation-selective, power in both directions may have

further divided the pools of neurons by the conjunction of their preferred orientation and color. Experiment four was designed to test a new hypothesis related to the influence of luminance-defined annuli.

CHAPTER 6

EXPERIMENT 4

6.1 Rationale

The final experiment attempted to rectify an asymmetry in the suitability of earlier (Experiments 2 and 3) stimuli for testing hypotheses about cell type. In particular, by using all chromatic square-wave gratings (2 cpd), the amount of rivalrous signal and the strength of the total chromatic signal are held constant across stimuli with uniform and patterned stimuli. If normalization happens primarily at the level of double-opponent cells with oriented RFs, the normalization effect should be stronger when the background shares the same pattern as rivalrous regions.

A new hypothesis H_4 posits that luminance-defined annuli may influence normalization pools, such that signals from within annulus regions are normalized less strongly by the background since the luminance edge is a cue to figure-ground segregation (Schnabel et al., 2018). The primary prediction under H_4 divisive normalization imposed by the background on rivalrous regions without annuli will be stronger than the same stimuli with annuli. Without the presence of annuli, percepts can resolve to apparent figure-region (uninterrupted background pattern).

6.2 Stimuli

For all conditions, rivalrous figures subtended 1.5° of visual angle. Stimuli (Conditions B & C) with black annuli (0.25 cd/m^2) had increased visual angle to 1.75°. All stimuli were presented inside square-shaped fusion boxes with subtended 4.5° of visual angle, set to be brighter than the gratings near 20 cd/m^2. The peripheral background was black at 0.25 cd/m^2. The rivalrous chromaticities were defined using lsY values of [0.72, 0.3, 15] for red-appearing (called "red"), [0.61, 0.3, 15] for green-appearing (called "green") regions, [0.70,

1.7, 15] for magenta-appearing (called "magenta"), and [0.63, 1.7, 15] for cyan-appearing (called "cyan"). The bottom and top regions on single-grating trials were a spatially uniform grey [0.665, 1.0, 14.95]. All trials were presented in ISR at 3.75 Hz (Christiansen et al., 2017; Logothetis et al., 1996). Additionally, the first 10 seconds of each 70-second trial were discarded to reduce possible stimulus onset effects. This experiment used 3 conditions (A-C) to make three planned comparisons.

6.2.1 Conditions

Rivalrous regions were always a two cpd square-wave grating with red/green and magenta/cyan rivalry. At any given moment, one eye's image is of a red and cyan grating, and the other eye's image is of a magenta and green grating. These chromaticities were selected to maximize chromatic contrast between rivalrous pairs and between phases. Two factors varied between conditions: (1) the presence of luminance-defined annuli (Conditions B & C) and (2) background pattern, which could be uniform (Condition C) or a square wave grating (Conditions A & B). Each trial type had two single-grating conditions (Section 2.3.1) used to calculate independence predictions for each region, yielding eight single-grating trials.

Condition A: No Annuli

Condition A's stimulus configuration (Figure 6.1) was of (45° *or* 135°) rivalrous square wave gratings in red/green and magenta/cyan without annuli on a stable square wave background (either red/cyan or green/magenta). This yielded four trial counterbalances for this condition: (1) rivalrous red/green and magenta/cyan 45° gratings on a stable red and cyan 45° background, (2) rivalrous red/green and magenta/cyan 135° red and cyan 135° background, (3) rivalrous red/green and magenta/cyan 45° gratings on a stable green and magenta 45° background, and (4) red/green and magenta/cyan rivalrous 135° gratings on a stable green and magenta 135° background.

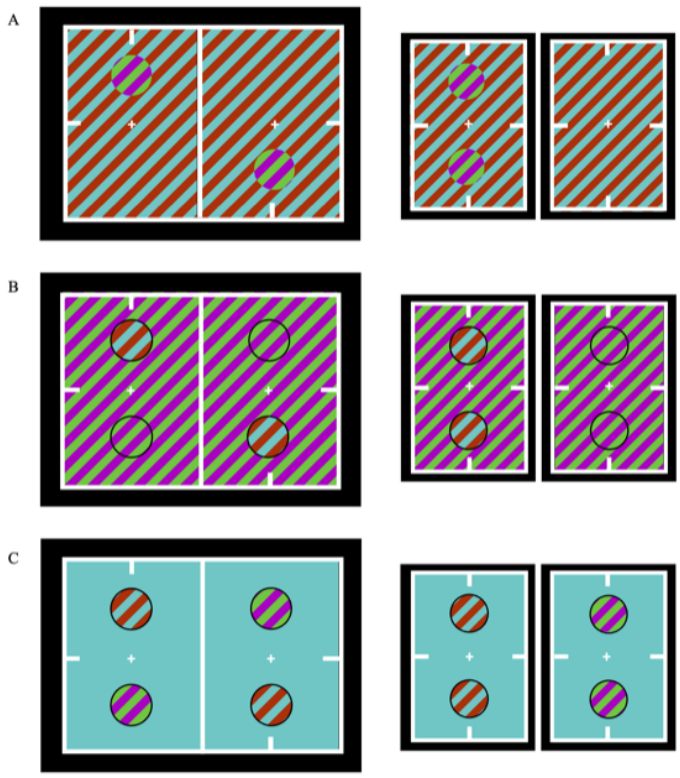

Figure 6.1: Conditions and percepts. Left: left and right eye images for Conditions A, B, and C. Right: measured percepts for each condition.

Condition B: Annuli

Condition B (Figure 6.1 B) was identical to Condition A except figures were presented *with* luminance-defined annuli. As before, this yielded four trial counterbalances for this condition: (1) rivalrous red/green and magenta/cyan 45° gratings on a stable red and cyan 45° background, (2) rivalrous red/green and magenta/cyan 135° red and cyan 135° background, (3) rivalrous red/green and magenta/cyan 45° gratings on a stable green and magenta 45° background, and (4) red/green and magenta/cyan rivalrous 135° gratings on a stable green and magenta 135° background.

Condition C: Uniform Background

Condition C's stimulus configuration ((Figure 6.1 C); only 45° cyan depicted) entailed identical rivalrous gratings with annuli as Condition B but with a uniform background (red, green, cyan, or magenta). This yielded eight trial counterbalances for this condition, two orientations (45° and 135°) for each of four background colors (red, green, cyan, or magenta). Each of these trial counterbalances had two single-grating trials, yielding 16 trials in this condition.

6.3 Results

Analyses were conducted within subjects using planned orthogonal contrasts. Since all predictions were directional, a non-parametric group analysis considered the one-tailed binomial probability of the observed results by chance under the null hypothesis (H_0). The one-tailed binomial probability $\Pr(X \geq k) = \sum_k^n \binom{n}{k} p^k (1-p)^{n-k}$ of k or more successes on n trials under H_0.

6.3.1 P_{AB}: Comparison between Conditions A & B

The prediction (P_{AB}) under H_4 was that the presence of luminance-defined annuli might reduce the extent to which stable regions divisively normalize a rivalrous signal. Stimuli without annuli (Condition A) should evoke more difference-enhanced percepts and fewer similarity-enhanced percepts relative to the same stimulus with annuli (Condition B).

Of the 20 contrasts performed (four per observer), five produced statistically-significant evidence (Figure 6.2) consistent with more divisive normalization on ambiguous gratings without annuli (Condition A). Despite this, every observer *always* resolved more difference-enhanced percepts in Condition A (no annulus) relative to the same stimulus with annuli (Condition B). This pattern of results has the probability of $p<0.001$ of occurring by chance

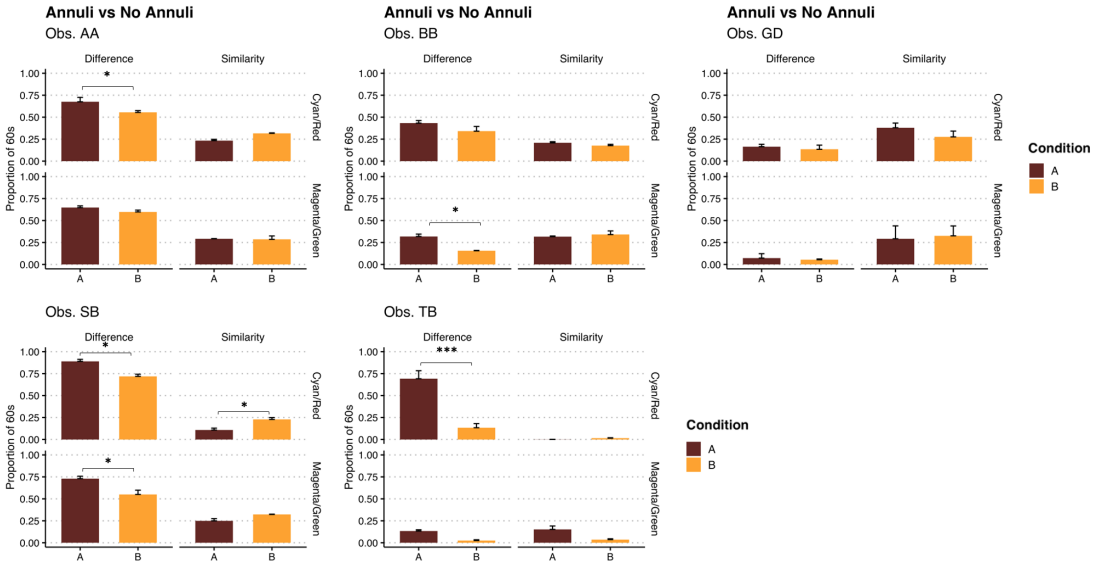

Figure 6.2: Planned contrasts for four subjects investigating P_{AB}. The primary vertical axis is the proportion of a 60-s trial that each percept was seen. The top horizontal axis groups results by percept type ("Difference" or "Similarity"). The right vertical axis groups results by stable background colors ("Cyan/Red" or "Magenta/Green"). The bottom horizontal axis and bar color indicate the Condition (A or B). Brackets indicate a significant contrast, where *, **, and *** indicate significance at $p < 0.05$, $p < 0.01$, and $p < 0.001$, respectively

under the null hypothesis. These results provide statistically-significant evidence supporting that luminance-defined annuli alter divisive normalization strength.

6.3.2 P_{BC}: Comparison between Conditions B & C

The hypothesis related to cell type was that if double-opponent cells drive a normalization process, an all-chromatic square wave background should impose more normalization than a uniform background. Experiments 2 and 3 provided evidence consistent with a normalization mechanism acting on rivalrous signals is influenced by chromatic signal strength and acts continuously across chromaticity space. One consideration for the comparison between Conditions B and C is that a uniform background (one of four chromaticities) should still impose normalization continuously on rivalrous regions. Meaning that a stimulus with a cyan background may be resolved by cyan signals imposing relatively more normalization on both

cyan and green signal than either magenta or red signals, and vice versa. A possible perceptual consequence is a similarity-enhanced percept of either a magenta and red grating or a cyan and green grating. Notably, while these percepts were possible (and verbally reported by observers) but not measured, taken together with the evidence that uniform backgrounds *usually* impose more divisive normalization, the expectation is that group differences will be minor, but that Condition A may evoke more difference-enhanced percepts.

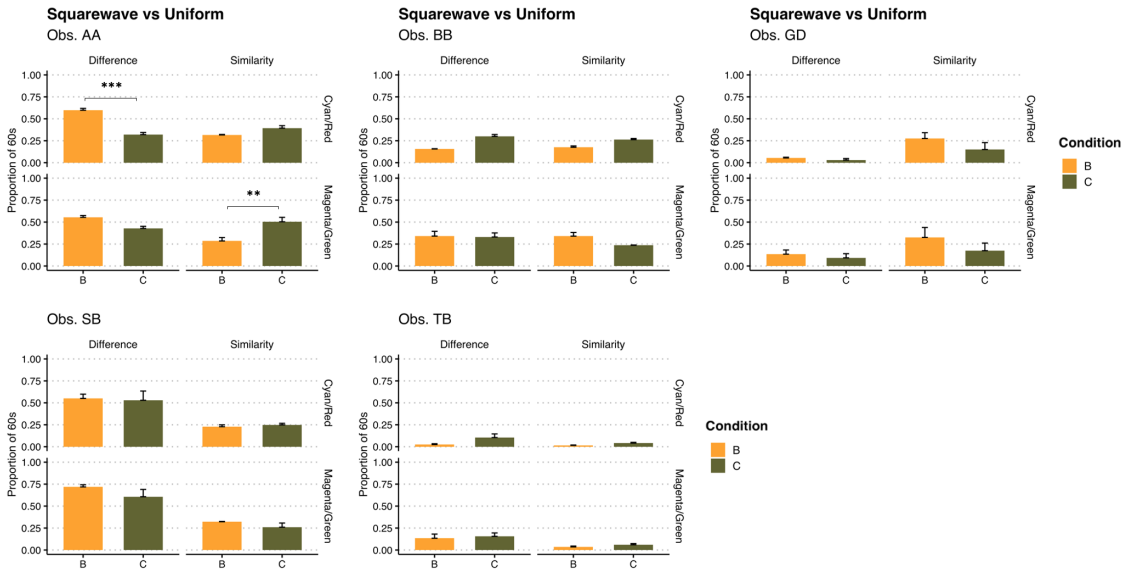

Figure 6.3: Planned contrasts for four subjects investigating P_{BC}. The primary vertical axis is the proportion of a 60-s trial that each percept was seen. The top horizontal axis groups results by response type ("Difference" or "Similarity"). The right vertical axis groups results by the chromatic grating colors ("Cyan/Red" or "Magenta/Green"). Finally, the bottom horizontal axis and bar color indicate the Condition (B or C).

Of the eight contrasts conducted, none achieved statistical significance. Additionally, the difference between condition means was small and irregular. These results are interesting because similar conditions from Experiments 2 and 3 were consistent with divisive normalization. This may be due to the addition of an all-chromatic square wave grating where every phase is a different rivalrous pair. In terms of a pooled divisive normalization hypothesis, an all-chromatic rivalrous grating may further increase the number of neural pools acting on the rivalrous region, effectively reducing the strength of each signal component.

6.3.3 Independence Predictions: Conditions A-C

Condition A: Observed vs. Predicted

Of the 20 planned orthogonal contrasts (four per observer), none was statistically significant, but 19 were in the predicted direction (Figure 6.4). This pattern of results has the chance probability (p <0.001) of observing 19 (k) successes on 20 trials (n).

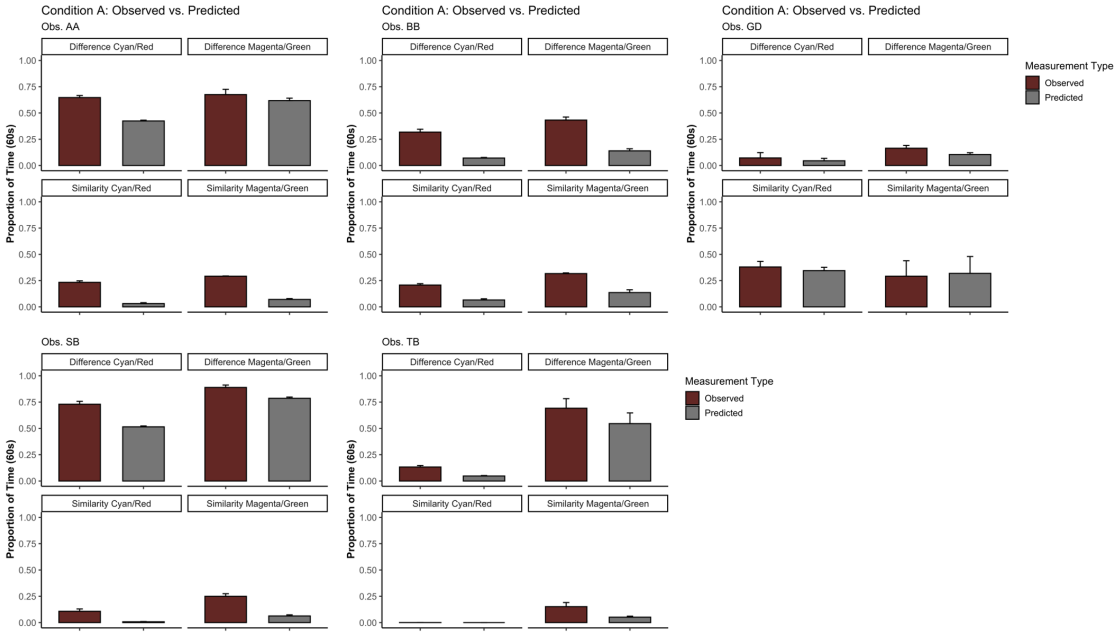

Figure 6.4: Planned contrasts for five subjects comparing observations in Condition A to their independence predictions. The vertical axis is the proportion of a 60-s trial that each percept was seen. Bar colors indicate the measurement type ("Observed" or "Predicted"). The top horizontal axes organize bars by response type ("Difference" or "Same") and background color ("Cyan/Red" or "Magenta/Green").

Condition B: Observed vs. Predicted

Of the 20 planned orthogonal contrasts (four per observer), none was statistically significant, but all 20 were in the predicted direction (Figure 6.5). This pattern of results has the chance probability of observing 20 (k) successes on 20 trials (n) is $p = (0.5)^{20}$.

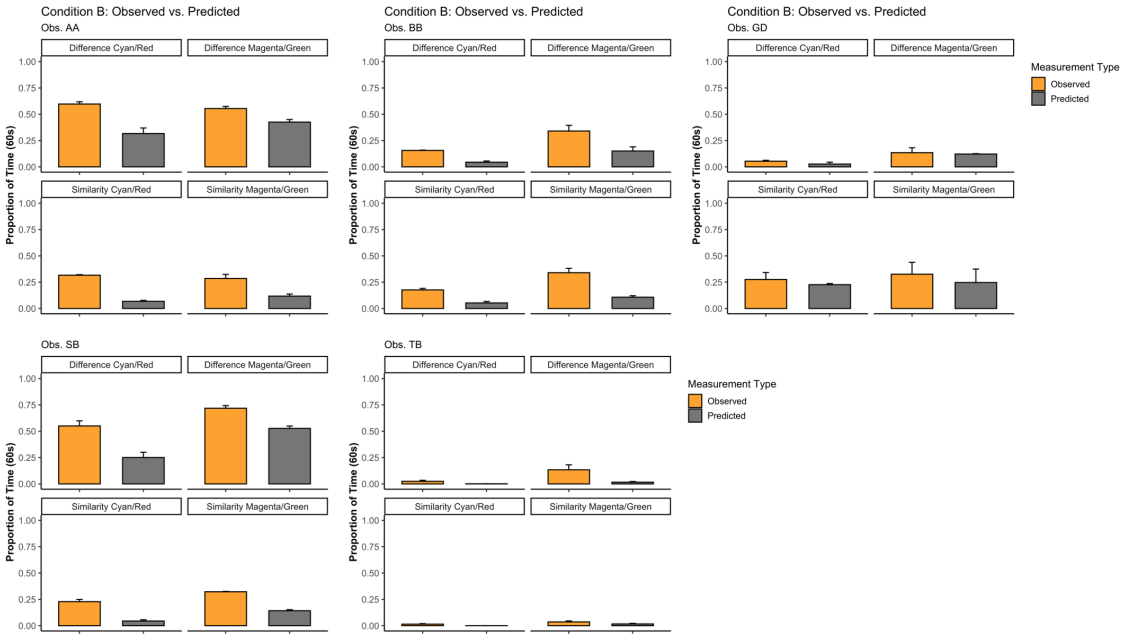

Figure 6.5: Planned contrasts for five subjects comparing observations in Condition B to their independence predictions. The vertical axis is the proportion of a 60-s trial that each percept was seen. Bar colors indicate the measurement type ("Observed" or "Predicted"). The top horizontal axes organize bars by response type ("Difference" or "Same") and background color ("Cyan/Red" or "Magenta/Green").

Condition C: Observed vs. Predicted

Of the 20 planned orthogonal contrasts (four per observer), one was statistically significant (Obs. AA, $p < 0.05$), 18 were in the predicted direction (Figure 6.6) and one observer (GD) showed the reversed pattern ("Difference Cyan/Red" and "Difference Magenta/Green") where predictions were greater than the corresponding observations. This pattern of results has the chance probability ($p < 0.001$) of observing 18 (k) successes on 20 trials (n).

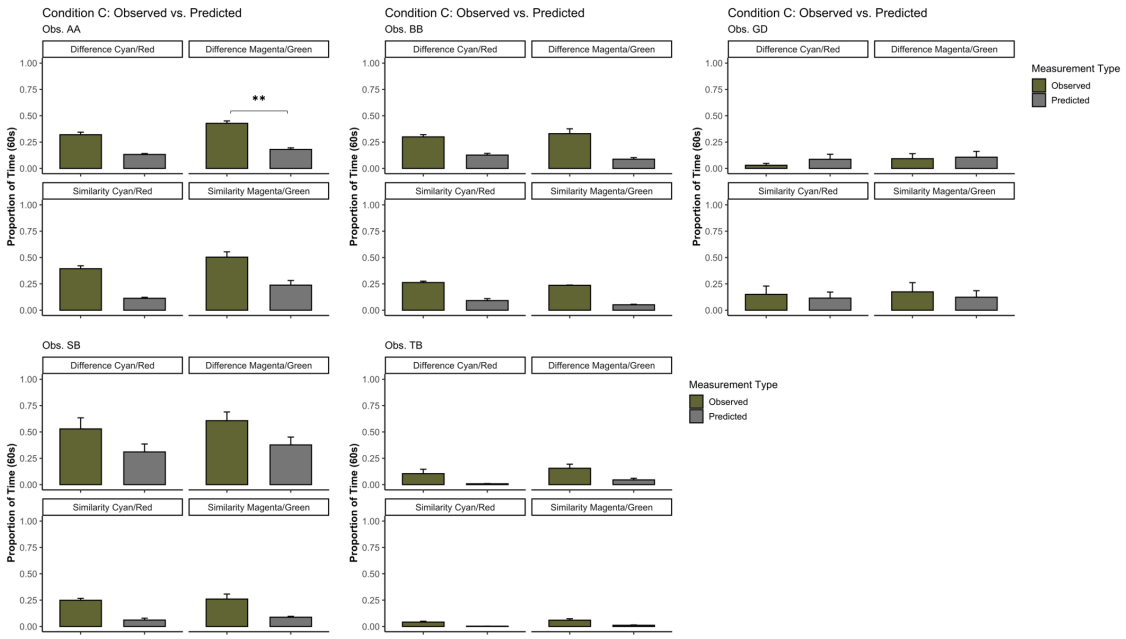

Figure 6.6: Planned contrasts for five subjects comparing observations in Condition C to their independence predictions. The vertical axis is the proportion of a 60-s trial that each percept was seen. Bar colors indicate the measurement type ("Observed" or "Predicted"). The top horizontal axes organize bars by response type ("Difference" or "Same") and background color ("Cyan/Red" or "Magenta/Green").

6.4 Discussion

The results from Experiment 4 provide evidence consistent with a divisive-normalization mechanism that is modulated by the presence of bounding annuli such that the background imposed more divisive strength on rivalrous signals without annuli. The hypothesis H_4 for this was that luminance edges served as a cue to figure-ground segregation, which may reduce the divisive strength of the background because of differential processing of background and figure signals. Specifically, signals being enhanced as figures are not thought to be divisively normalized with the neurons responding to suppressed background regions (Schwartz and Coen-Cagli, 2013). Annuli make it easier to segregate a figure from its background and keep the figure stably segregated from the background regardless of their resolved color. In the

absence of annuli, the visual signal may lose the representation of a figure altogether, and this impedance to figure-ground processing may evoke more divisive normalization. Since these trials led to the perceptual experience of an object disappearing intermittently from perception, an attentional effect may have contributed to increased divisive normalization strength. This perspective aligns with divisive normalization models of attention, where attention to a region reduces the divisive normalization strength in the attended region (Lee and Maunsell, 2009; Reynolds and Heeger, 2009; Schwartz and Coen-Cagli, 2013; Verhoef and Maunsell, 2017).

The second comparison addressing the hypothesis about cell type did not produce statistically significant or reliable results. This is not to say that one cell type is strictly implicated over another, but rather that perceptual (behavioral) evidence of a particular driving cell type was not found. Another possible explanation for these inconclusive results will be discussed in the General Discussion (Section 7.1).

CHAPTER 7

GENERAL DISCUSSION

The visual system may leverage all available information in its signal to resolve the neural ambiguity caused by incomplete or conflicting visual input. For instance, there is ample evidence of a grouping mechanism that acts on neurally ambiguous regions of the visual field to form a coherent similarity-enhanced percept (e.g., Adams and Haire, 1958; Kovács et al., 1996; Alais and Blake, 1999; Ngo et al., 2000; Slezak and Shevell, 2018). An adaptive visual system may strike a balance between perceptual flexibility and perceptual stability. The experiments in this dissertation sought evidence that a divisive-normalization mechanism could support stable perception through similarity links that support efficient, grouped percepts. Evidence was sought that dynamic pooled-normalization supports perceptual flexibility by changing the normalization pool by which a neural response was adjusted. It was posited that an attention-directed divisive-normalization mechanism flexibly pools neural responses depending on the context and observer goals. This dissertation found evidence that supports one of Barlow's seminal ideas, the "linking features" hypothesis, that holds features are non-topographically linked by similarity (Barlow, 1981).

7.1 Summary of Results

Experiment 1 provided novel evidence that difference-enhanced percepts can be evoked using rivalrous stimuli (Peiso and Shevell, 2020). In this case, it was hypothesized that a divisive-normalization mechanism would act disproportionately on the signal component that is shared between rivalrous regions, allowing the unique information in each region to dominate perception. In this case, difference-enhanced percepts dominated perception for every observer (Figure 3.5). Moreover, only one subject showed significantly more similarity-enhanced percepts than was predicted by chance (Figure 3.4). The total dominance durations

of the intermediate percepts provided evidence that the chromatic signal plays a driving role in ambiguity resolution at isoluminance; specifically, regardless of orientation, red and green grating percepts were always reported for longer total average dominance durations than those with a shared color above and below fixation. This provided preliminary evidence suggesting that a normalization mechanism may primarily act on a chromatic signal in comparison to spatial properties. Experiment 1 demonstrated that the visual system leverages contextual information, in this case, the presence of a second rivalrous region, to resolve ambiguous neural representations.

Experiment 1 was designed as a proof of concept and is published (Peiso and Shevell, 2020). The first experiment differed from the rest in a few ways: (1) it had only one experimental condition (and its color, position, and orientation counterbalances); thus, all planned comparisons were between percepts within this condition. (2) Additionally, Experiment 1 manipulated the dichoptic signal so that each of the rivalrous regions had a shared signal and a unique signal. The remaining experiments held the dichoptic signal constant in rivalrous regions and varied adjacent non-rivalrous regions. (3) Finally, the background surrounding rivalrous regions were luminance-defined. The remaining experiments primarily used chromatic backgrounds in isoluminance with rivalrous regions and luminance-defined bounding annuli. A replication of Experiment 1 should include an additional condition where rivalrous regions have the same rivalrous signal in both locations (i.e., no unique signals).

Experiment 2 sought evidence that a non-rivalrous background region contextualizes rivalrous signals and influences ambiguity resolution. The hypothesis was that a stable chromatic background can impose divisive normalization on the component of the rivalrous signal that is shared with the background. Experiment 2 showed this in two ways: (1) when the background was a stable (non-rivalrous) color, the rivalrous regions resolved to be different from the stable background more often than the same (Figure 4.3), and (2) when the background had the same rivalrous signal as the rivalrous grating, similarity-enhanced

percepts dominated perception (Figure 4.8). Additionally, Experiment 2 demonstrated that figure and background regions might evoke differential processing by comparing the resolution of rivalrous figures on stable backgrounds to stable figures on rivalrous backgrounds (Figure 4.4). The finding here was that stable backgrounds influenced the resolution of rivalrous figures, but stable figures had minimal influence on the resolution of rivalrous backgrounds. Since divisive normalization is thought to have an attention-driven component, evidence of this asymmetry supports the role of divisive normalization in figure-ground segregation (e.g., Schwartz and Coen-Cagli, 2013).

Experiment 3 provided evidence that the strength of the chromatic signal modulates divisive normalization. Experiment 3 corroborated Experiment 2 by replicating the main effect of a stable background on the resolution of rivalrous regions. Comparisons between uniform and checkered pattern stimuli supported the hypothesis that the chromatic signal's strength modulates the strength of divisive normalization (Figure 5.4). A comparison between checkered pattern and space-averaged checkered pattern backgrounds provided evidence that supports the possibility that a divisive-normalization mechanism acts to suppress signals from single-opponent cells (Figure 5.7), which integrate over patterned stimuli. If single-opponent cells are being moderated by divisive normalization, this may provide the redundancy reduction necessary for double-opponent cell responses, signaling chromatic contrast, to influence perception. Finally, comparisons between a "neutral" grey background stimulus and red- and green-appearing ones provided support for a divisive-normalization mechanism acting on a rivalrous chromatic signal to enhance-differences (Figure 5.8). Specifically, the frequency for resolving rivalrous disks as red or green was modulated by the stable (non-rivalrous) background color such that resolution of rivalrous gratings was biased towards resolving as the unique component (i.e., not shared with the background) of the rivalrous chromatic signal. Rivalrous gratings presented on a grey background, provided a baseline for resolution rates of rivalrous disks when neither rivalrous component was shared with the stable background.

Corroborating evidence has provided statistically significant support of interocular grouping for two different chromaticities that were made to appear the same using chromatic induction *and* chromaticities that were categorically similar but visually distinguishable (Slezak and Shevell, 2020).

Experiment 3 sought to answer some questions left by Experiment 2. One of these questions was whether the strength of the chromatic signal modulates divisive normalization strength. Here, strength was indexed by the space average of the pattern, such that a uniform chromatic (e.g., green-appearing) background will have more strength than an isoluminant square-wave grating that averages over grey-appearing and green-appearing regions. The spatial extent of the chromatic surround was held constant across conditions. Additional conditions with smaller chromatic surrounds could be useful comparison conditions to fully address the proposition that divisive normalization strength is modulated by chromatic signal strength that increases with stimulus area. In this case, if the background's size does not influence ambiguity resolution, this could suggest chromatically-contrasting edges and not the total spatial extent of spatiochromatic patterns, may drive normalization strength on rivalrous regions.

Experiment 4 introduced stimuli without non-rivalrous, grey-appearing regions and provided evidence that the strength of divisive normalization was modulated by the presence of the bordering annuli (Figure 6.2), which reduced the influence of the surround on rivalrous regions. The working hypothesis for this experiment was that the annular borders served as efficient cues for figure segregation, and that once a figure was segregated, its neural response was pooled differently than the background as a part of figure-ground segregation processes (Schwartz and Coen-Cagli, 2013). A complementary explanation is stimuli without annuli temporarily disappeared from perception appearing to be continuous with the background (i.e., no segregated figure), and this may have attracted additional attention-directed divisive normalization.

Finally, comparisons between background types (square-wave or uniform) yielded inconclusive results (Figure 6.3). This comparison between background types would have been more informative if two additional percepts had been measured. In addition to the measured percepts, rivalrous gratings could resolve to be magenta/red or cyan/green. These percepts were sometimes verbally reported in Conditions B (square-wave gratings with annuli) and C (uniform background). Including these percepts would provide the total time the grating regions resolved as the same or different color than the background. Experiment 4 observers were instructed only to report two percepts: cyan/red and magenta/green gratings. If the stable background was cyan, the measurements did not capture the amount of time the gratings appeared cyan/green or magenta/red. Experiment 3 provided evidence consistent with a divisive-normalization mechanism that acts on a continuous chromatic signal by showing a neutral isoluminant chromaticity evokes an intermediate normalization effect on regions in red/green chromatic rivalry. For instance, a rivalrous disk is the more likely to resolve as green with a stable red or grey surround than with a stable green surround. Furthermore, a rivalrous disk is most likely to resolve as green when presented with a stable red surround because neurons that were preferentially responding to red-appearing chromaticities formed a larger normalization pool and selectively attenuate the red-appearing chromatic component of the rivalrous signal. From this perspective, a cyan background should impose more normalization on both cyan- and green-appearing chromatic signals and less on magenta- and red-appearing signals. The most common percept predicted by this hypothesis for the rivalrous stimulus on a cyan background would be a magenta/red grating because of the increased normalization strength on cyan and green regions.

7.1.1 Independence Predictions Across Experiments

Across all four experiments, independence predictions were almost always lower than the corresponding experimental observations (96% of 336 total contrasts), which is as predicted.

However, only Experiment 1 achieved statistical significance on planned contrasts between predictions and observations. This may be due to a floor effect; Experiment 1 observers (three of four) rarely resolved percepts during single-grating trials (Figure 3.4). This dissertation's motivating theory offers a possible explanation: divisive normalization cannot act on a single rivalrous grating on a black background because no similarity links can form. Without similarity links there is minimal response pooling. In the absence of contextual influences, like a stable chromatic background (as in Experiments 2-4) or a shared and unique component between rivalrous regions (as in Experiment 1), the individual components of the rivalrous signal are normalized alone and relatively equally. Experiment 1's near-floor effects for independence predictions is consistent with a divisive normalization account of binocular rivalry (or in this case ISR). Conversely, Experiments 2-4 showed minor differences between the predictions calculated from single-region and experimental trials. The independence predictions in Experiments 2-4 were higher relative to Experiment 1, and only achieved statistical significance on 10% of the 220 planned contrasts. Even so, of the total contrasts performed across Experiments 2-4, only one was in the opposite direction of the prediction– the remaining violations were because observers rarely resolved difference-enhanced percepts on trials with rivalrous backgrounds (e.g., Figure 4.8) leaving near-zero observations and predictions. The key difference here is the manipulation of the background chromaticity gave the stimuli in Experiments 2-4 statistical dependencies between the rivalrous signal and the stable surround. The explanation suggested here is that the single-region stimuli in Experiments 2-4 still evoked divisive normalization due to the chromatic background. The theoretical implication is that interocular grouping results from a divisive-normalization mechanism that can act on the neural representations to evoke both similarity-enhanced and difference-enhanced percepts.

The pattern of independence-prediction results mentioned earlier can be contextualized by feature-integration theories of attention, which suggest that distributed attention auto-

matically extracts statistical dependencies or similarities from the visual scene (Treisman, 2006). Attention may not have the same ambiguity-reducing effect without any similarities to extract. Additionally, behavioral and brain imaging data may indicate distinct mechanisms for processing single objects and multi-object ensembles (e.g., Cant et al., 2015). At the single-unit level, a neuron's response is suppressed by a second spatially-discrete preferred stimulus within its receptive field. If one of these stimuli is attended to, the neuron's response resembles its maximal response to a single preferred stimulus in its receptive field (Treue and Maunsell, 1999). Evidence from this dissertation is consistent with attention's role in resolving ambiguity by biasing competition between neural representations through an attention-directed divisive-normalization mechanism (Lee and Maunsell, 2009; Reynolds and Heeger, 2009; Schwartz and Coen-Cagli, 2013; Verhoef and Maunsell, 2017). Since attention is commonly thought to aid in the spatial allocation of processing resources, a single, decontextualized object (e.g., Experiment 1 single-grating trials) may not evoke the same attentional processes.

Interocular grouping is the above chance co-resolution of identical percepts in separate rivalrous regions of the visual field. Interocular grouping is regarded as a process that acts on neural representations *and* a perceptual phenomenon. The evidence from the independence predictions across experiments supports the view of interocular grouping as a perceptual phenomenon. Specifically, the position here is that interocular grouping is caused by a divisive-normalization mechanism that aids in ambiguity resolution by biasing perception towards similarity-enhanced (grouped) percepts *or* difference-enhanced percepts. The stability of single-region trials in Experiments 2-4, relative to Experiment 1, provides additional evidence that a divisive-normalization mechanism acts on ambiguous chromatic representations.

7.2 An Updated Theoretical Framework

Divisive normalization models of attention suggest a cell's response is pooled differently depending on whether the stimulus or stimulus feature, in its receptive field, is being attended. When the stimulus in a cell's receptive field is unattended, its response is normalized by surrounding regions with a similar signal, but when the stimulus is attended, it is not normalized by the surrounding regions (Schwartz and Coen-Cagli, 2013). In addition to considering some posited attentional-driven effects, this dissertation's primary contribution was providing evidence that regions can be implicitly linked by similarity but, nonetheless, produce difference-enhanced percepts. This demonstrates that perception is not ubiquitously biased towards similarity by a grouping mechanism; further, a divisive-normalization mechanism is posited to pool responses based on mutual similarity. This dissertation assumed that the neural ambiguity evoked by binocular rivalry is resolved by well-known processes such as figure-ground segregation (Alais and Blake, 2005; Alexander, 1951; Leopold and Logothetis, 1996). While attention may be an important factor (Brascamp and Blake, 2012), a divisive-normalization mechanism may support figure-ground segregation in early vision by reducing the response evoked by the background's signal. Here, a divisive-normalization mechanism that attenuates a more common component of the visual signal may provide a mechanism for extracting figures from their grounds, as theorized by Gestalt cues of a smaller region encompassed by a larger region (Koffka, 1935).

The theoretical framework motivating the cell-type hypothesis required some refining. At the onset of these experiments, the hypothesis was that double-opponent cells, known to differentiate chromatic edges, would drive divisive normalization. Researchers have suggested that cone inputs to opponent sub-regions of double-opponent cells are not perfectly balanced in their response strength; however, this has been explained away as epiphenomenal (Conway, 2002). Consider the conjecture that the least biologically useful percept is one that has not yet been resolved. A double-opponent cell system having perfectly balanced

cone input strengths to opponent sub-regions might normally contribute to actionable percepts. However, in the case of ambiguous neural representations, especially those evoked by rivalrous stimuli presented in ISR, perfectly balanced cone input to all double-opponent sub-regions could result in uniform inhibition across all double-opponent cells. Uniformly inhibited double-opponent cells should not produce the rivalry dynamics reported here. It has been suggested that roughly equal cone inputs may support color-opponency (Conway, 2002). However, if all cell sub-regions produced equal strength responses, then a chromatically rivalrous stimulus could suspend perceptual resolution, functionally impeding the chromatic signal from reliably generating a percept over time. The relative equality between sub-region response strength may still cause a temporary suspension of ambiguity resolution, which may explain piecemeal or indescribable percepts. With this in consideration, unequal cone input to opponent sub-regions may aid in the evocation of a color experience, even under ambiguous stimulus conditions (e.g., ISR). Additional signal decorrelation may be afforded by the asymmetry in eye dominance that many cortical cells inherit from cells with asymmetrical influences from each eye (Tong et al., 2006), although this may not play as large of a role when stimuli are presented in ISR (Logothetis et al., 1996). Single-cell biases could be diminished or enhanced at the population level because an individual cell's response bias is integrated into pools of similarly-tuned cells, each having a multiplexed response profile (Macellaio et al., 2020; Carroll and Conway, 2021).

For example, consider two double-opponent cells with the same receptive field and similar sub-region response profiles but spatially-inverted sub-regions (Figure 7.1 B). In this example, one cell's L+/M- sub-region is spatially aligned with the other cell's L-/M+ sub-region, and the inverse is true for the second spatial region (L-/M+ aligned with L+/M-). Additionally, say these cells are straddling a region of space comprising the edge between a stable green-appearing (M) chromatic background and a chromatically-rivalrous (L/M) stimulus, such that one sub-region's receptive field lies in the stable background and the other within

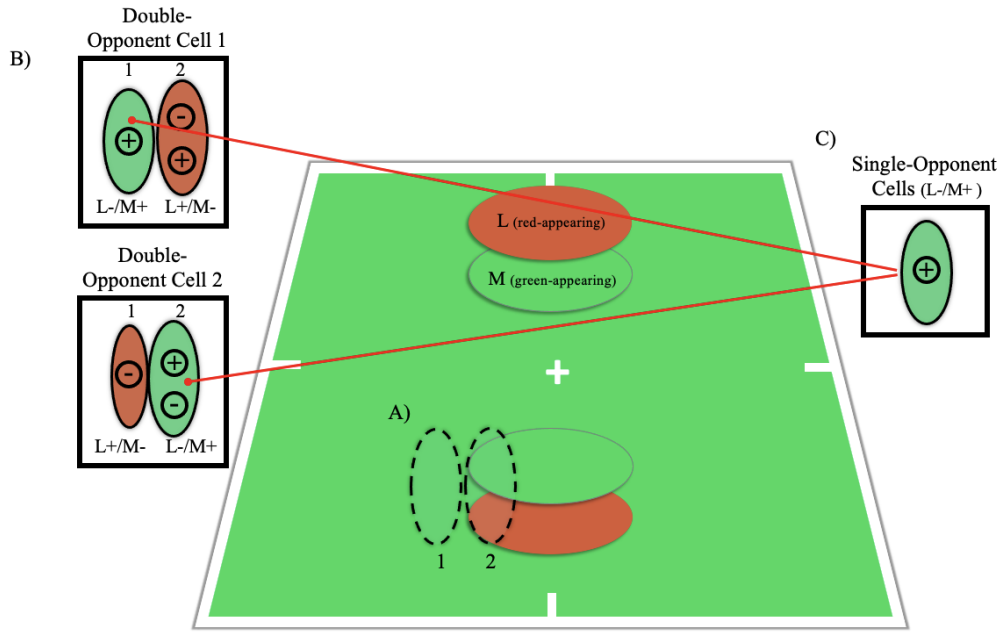

Figure 7.1: Schematic of updated theoretical framework. A) Depicts the receptive field shared by two theoretical double-opponent cells. The first sub-region (labeled 1) and the second sub-region (labeled 2) correspond to the sub-regions of both cells shown in B. B) Depicts two double-opponent cells (top: Cell 1 and bottom: Cell 2) with inverse spatiochromatic tuning but responding to the same region of the receptive field shown in A. C) Depicts one single-opponent cell (L-/M+) that represents the pool of single-opponent neurons responding to the uniform, green-appearing background. Red circle-capped lines indicate that divisive normalization is being imposed onto double-opponent sub-regions with similar tuning (i.e., L-/M+).

the rivalrous region (Figure 7.1 A). One cell has a sub-region (L-/M+) providing an elevated response to a stable green-appearing (M) background, and the other sub-region (L+/M-) produces an intermediate response to the rivalrous region (L/M). For the same receptive field, the second cell with the opposite spatial profile has a sub-region (L+/M-), providing a minimal response to a stable green-appearing background, and another sub-region (L-/M+) providing an intermediate response to the rivalrous region (L/M). The asymmetry between these two theoretical cells provides information about the contour as differential activity

across each cell's sub-regions.

Now consider the response of single-opponent cells (L-/M+) to a stable green-appearing (M) background (Figure 7.1 C). These cells should produce their maximal response to medium-wavelength chromaticities (i.e., green-appearing) and pool together similarly-tuned neural responses across the visual field, imposing normalization onto one component (green-appearing chromaticity) rivalrous signal. This attenuation of (L-/M+) single-opponent activity would then be inherited by the double-opponent cells that straddle the border between a stable background and a rivalrous region. The first cell will now have an attenuated sub-region (L-/M+) and intermediate response (L+/M-) to rivalrous regions. The second cell will show the same minimal response to the background and an attenuated response (L-/M+) to rivalrous regions. Therefore, the maximal response will be produced by the L+/M- sub-region. An L/M dichoptic signal will cause some intermediate effect on the L+/M- sub-region, but since the cone inputs are not perfectly balanced, cell responses will not drop to zero (Conway, 2002). Instead, for double-opponent cell sub-regions with slightly stronger L+ input, an L (red-appearing) signal, while double-opponent cell sub-regions with slightly stronger M- input are inhibited. The example cell in Figure 7.1 B (top) with a slightly larger L+/M- sub-region may be biased towards generating a red-appearing percept when probed with this stimulus. The generated L (red-appearing) signal is not stable; however, as the adaptation-level of neural populations maintaining red-color representations increases, attenuated L-/M+ may dominate perception. In addition to the temporal constraints provided to perception by adaptation, stochastic fluctuations in attention may temporarily increase the response gain for one of the possible color percepts. Nevertheless, the perceptual bias towards resolving a rivalrous disk as red-appearing on a green-appearing background is supported by unequal divisive normalization strength on component signals *and* by the unequal cone input to opponent sub-regions of double-opponent cells. A pooled divisive-normalization mechanism that acts on the most common chromatic signal could support the capacity of

double-opponent cells to rescue weaker signals that a common signal would otherwise drown out.

At the onset and throughout the execution of this project, there was an implicit assumption made that binocular rivalry is *solved* by binocularly-driven cortical cells. However, there is evidence of divisive normalization mechanisms in the retina, such as light adaptation and contrast normalization (e.g., Carandini and Heeger, 2012), and this may suggest a more parsimonious, retina-centered explanation. Specifically, each retina might divisively normalize the signal across its visual field independently through the coordinated activity of interneurons, and these pre-normalized monocular signals are then binocularly combined by binocularly-driven cortical cells. A retinal normalization mechanism followed by binocular summation by cortical cells could produce the same perceptual biases as the exclusively cortical model with fewer computational resources. An additional benefit of the retina-centered model is that the signals emerging from the retinae may always be relative to the image statistics of the eye's stimulus, and this may provide redundancy reduction and an improvement in SNR. This independent processing by each of the retinae may improve the efficacy of the later visual stages, where monocular signals are combined, by reducing the differences between the two eyes' signals that are related to the physics (e.g., aberration and light scatter) and biology (e.g., differences between cone mosaics and yellowing lenses) of the eyes while preserving rare signal components. The experiments presented herein used ISR presentation to reduce the influences of monocular mechanisms, so further experiments would be necessary to investigate retinal mechanisms.

The hypotheses here were constrained to simple chromatically-contrasting stimuli. In this case, binocular cells are considered to be the site of rivalrous representations, as this is where incompatible signals first meet. Other ambiguous representations, such as those caused by bistable figures (e.g., Necker cube), may be solved later by neural populations sensitive to object identity and spatial constraints. This idea is suggested by experimental evidence

that Necker cubes presented in chromatic rivalry resolve the two types of ambiguity, cube orientation and chromatic rivalry, relatively independently (Lange and Shevell, 2020). In this case, two chromatically-rivalrous Necker cubes were shown to produce similarity-enhanced color percepts and to perceptually group by orientation (Lange and Shevell, 2020). From the posited divisive normalization framework, neural pools drive the coordinated resolution of the Necker cubes' color through implicit similarity links. Separately, and later in the visual stream, neural populations representing the bistable Necker cubes' two 3-D orientations may be implicitly grouped by the bifurcation of their responses, providing inherent neural pools to be sampled by attention over time (Dieter et al., 2016), resulting in the perceptual grouping of Necker cube orientation (Adams and Haire, 1958) after the rivalrous chromatic signal has been resolved. Similarly, an experiment using complex stimuli, such as ambiguous objects or faces (e.g., Kovács et al., 1996), may require resolution and divisive normalization to act on neural populations that can be biased by expectations of holistic feature relations (Kovács et al., 1996) and semantic content retrieved from memory (Nichiporuk et al., 2017).

7.3 Future Directions & Concluding Remarks

Future research should consider disentangling the effects of the spatial extent of the background signal and background signal strength (e.g., saturation). The results presented here held the spatial extent of the background constant. Suppose a small-size background and a large-size background evoke similar perceptual results. In this case, similar results may suggest that normalization processes are acting locally and are not highly sensitive to global stimulus configuration, which is implicated in figure-ground segregation.

Additionally, there is evidence that color-opponent cortical cells encode temporal chromatic contrast, that is, producing an elevated response to chromatic changes, even if the change was from a preferred to a non-preferred stimulus (Conway, 2002; Carroll and Conway, 2021). The temporal encoding of chromatic contrast is thought to support color constancy

(Carroll and Conway, 2021). Stimuli presented in ISR inherently provide a temporal color contrast code for neurons to extract. None of the experiments in this dissertation employed standard binocular rivalry methods, where dichoptic stimuli are *not* swapped between the eyes. A standard rivalrous presentation would provide data to disentangle temporal effects, if any, from spatial effects. Previous work that found no statistically significant differences between ISR and standard binocular rivalry presentation only measured similarity-enhanced percepts under the conditions of equal normalization (e.g., Slezak and Shevell, 2018). Given the primary findings of this dissertation, differential results between standard binocular rivalry and ISR presentation for stimuli that evoke unequal normalization compared to equal cannot be ruled out. Moreover, the temporal mechanisms that support color constancy and change detection may act differentially on a signal that evokes unequal normalization compared to a signal that evokes equal normalization.

The experiments and guiding theoretical framework presented here have provided novel evidence that a divisive-normalization mechanism can act to resolve rivalrous neural representations. Additionally, evidence was found in support of the hypothesis that divisive normalization strength is modulated by chromatic signal strength (operationalized, here, as saturation). Finally, these findings extend existing evidence that divisive normalization underlies ambiguity resolution in binocular rivalry in achromatic, luminance-defined stimuli (Said and Heeger, 2013) to include patchwork stimuli presented in chromatic interocular-switch rivalry. This extension provided further support for a divisive-normalization mechanism that acts across the distributed visual hierarchy.

REFERENCES

Abbott, L. F. and Dayan, P. (1999). The effect of correlated variability on the accuracy of a population code. *Neural computation*, 11(1):91–101.

Adams, P. A. and Haire, M. (1958). Structural and conceptual factors in the perception of double-cube figures. *The American journal of psychology*, 71(3):548–556.

Alais, D. and Blake, R. (1999). Grouping visual features during binocular rivalry. *Vision research*, 39(26):4341–4353.

Alais, D. and Blake, R. (2005). Binocular rivalry and perceptual ambiguity. In Wagemans, J., editor, *The Oxford Handbook of Perceptual Organization*, volume 1093. Oxford University Press, Oxford, UK.

Alexander, L. T. (1951). The influence of figure-ground relationships in binocular rivalry. *Journal of Experimental Psychology: General*, 41(5).

Aschner, A., Solomon, S. G., Landy, M. S., Heeger, D. J., and Kohn, A. (2018). Temporal contingencies determine whether adaptation strengthens or weakens normalization. *Journal of Neuroscience*, 38(47):10129–10142.

Barlow, H. (2001). Redundancy reduction revisited. *Network: computation in neural systems*, 12(3):241.

Barlow, H. B. (1981). The ferrier lecture, 1980. *Proceedings of the Royal Society of London. Series B. Biological Sciences*, 212(1186):1–34.

Barlow, H. B. et al. (1961). Possible principles underlying the transformation of sensory messages. *Sensory communication*, 1(01).

Beaudoin, D. L., Borghuis, B. G., and Demb, J. B. (2007). Cellular basis for contrast gain control over the receptive field center of mammalian retinal ganglion cells. *Journal of Neuroscience*, 27(10):2636–2645.

Boynton, G. M. (2009). A framework for describing the effects of attention on visual responses. *Vision research*, 49(10):1129–1143.

Brascamp, J. W. and Blake, R. (2012). Inattention abolishes binocular rivalry: Perceptual evidence. *Psychological Science*, 23(10):1159–1167.

Brascamp, J. W. and Shevell, S. K. (2021). The certainty of ambiguity in visual neural representations. *Annual Review of Vision Science*, 7:465–486.

Braun, J. and Mattia, M. (2010). Attractors and noise: twin drivers of decisions and multistability. *Neuroimage*, 52(3):740–751.

Brown, J. M. and Plummer, R. W. (2020). When figure–ground segregation fails: Exploring antagonistic interactions in figure–ground perception. *Attention, Perception, & Psychophysics*, 82(7):3618–3635.

Buschman, T. J. and Kastner, S. (2015). From behavior to neural dynamics: an integrated theory of attention. *Neuron*, 88(1):127–144.

Bushnell, B. N., Harding, P. J., Kosai, Y., Bair, W., and Pasupathy, A. (2011). Equiluminance cells in visual cortical area v4. *Journal of Neuroscience*, 31(35):12398–12412.

Cant, J. S., Sun, S. Z., and Xu, Y. (2015). Distinct cognitive mechanisms involved in the processing of single objects and object ensembles. *Journal of Vision*, 15(4):1–21.

Carandini, M. and Heeger, D. J. (2012). Normalization as a canonical neural computation. *Nature Reviews Neuroscience*, 13(1):51–62.

Carandini, M., Heeger, D. J., and Movshon, J. A. (1997). Linearity and normalization in simple cells of the macaque primary visual cortex. *Journal of Neuroscience*, 17(21):8621–8644.

Carroll, J. and Conway, B. R. (2021). Color vision. *Handbook of Clinical Neurology*, 178:131–153.

Carter, O. and Cavanagh, P. (2007). Onset rivalry: brief presentation isolates an early independent phase of perceptual competition. *PloS One*, 2(4):e343.

Christiansen, J. H., D'Antona, A. D., and Shevell, S. K. (2017). Chromatic interocular-switch rivalry. *Journal of Vision*, 17(5):1–16.

Cohen, M. R. and Maunsell, J. H. (2011). Using neuronal populations to study the mechanisms underlying spatial and feature attention. *Neuron*, 70(6):1192–1204.

Conway, B. R. (2002). *Neural mechanisms of color vision: Double-opponent cells in the visual cortex*. Springer Science & Business Media.

Cronin, S. L., Spence, M. L., Miller, P. A., and Arnold, D. H. (2017). Bidirectional gender face aftereffects: Evidence against normative facial coding. *Perception*, 46(2):119–138.

Davidson, M. J., Alais, D., van Boxtel, J. J., and Tsuchiya, N. (2018). Attention periodically samples competing stimuli during binocular rivalry. *Elife*, 7:e40868.

Dieter, K. C., Brascamp, J., Tadin, D., and Blake, R. (2016). Does visual attention drive the dynamics of bistable perception? *Attention, Perception, & Psychophysics*, 78(7):1861–1873.

Dieter, K. C., Melnick, M. D., and Tadin, D. (2015). When can attention influence binocular rivalry? *Attention, Perception, & Psychophysics*, 77(6):1908–1918.

Dowling, J. E. (2010). Retina: An overview. In Squire, L. R., editor, *Encyclopedia of Neuroscience*, pages 159–169. Academic Press.

Drewes, J., Goren, G., Zhu, W., and Elder, J. H. (2016). Recurrent processing in the formation of shape percepts. *Journal of Neuroscience*, 36(1):185–192.

D'Zmura, M. and Lennie, P. (1986). Mechanisms of color constancy. *JOSA A*, 3(10):1662–1672.

Emery, K. J., Volbrecht, V. J., Peterzell, D. H., and Webster, M. A. (2017). Variations in normal color vision. vi. factors underlying individual differences in hue scaling and their implications for models of color appearance. *Vision Research*, 141:51–65.

Eyer, S. (2009). Translation from plato's republic 514b–518d ("allegory of the cave"). In *Ahiman: A Review of Masonic Culture and Tradition*, volume 1, pages 73–78. Plumbstone Books.

Garcia-Diaz, A., Fdez-Vidal, X. R., Pardo, X. M., and Dosil, R. (2012). Saliency from hierarchical adaptation through decorrelation and variance normalization. *Image and Vision Computing*, 30(1):51–64.

Geisler, W. S. (2011). Contributions of ideal observer theory to vision research. *Vision research*, 51(7):771–781.

Georgopoulos, A. P., Schwartz, A. B., and Kettner, R. E. (1986). Neuronal population coding of movement direction. *Science*, 233(4771):1416–1419.

Hohwy, J. (2012). Attention and conscious perception in the hypothesis testing brain. *Frontiers in psychology*, 3(96):1–14.

Hohwy, J., Roepstorff, A., and Friston, K. (2008). Predictive coding explains binocular rivalry: An epistemological review. *Cognition*, 108(3):687–701.

Huang, L., Wang, L., Shen, W., Li, M., Wang, S., Wang, X., Ungerleider, L. G., and Zhang, X. (2020). A source for awareness-dependent figure–ground segregation in human prefrontal cortex. *Proceedings of the National Academy of Sciences*, 117(48):30836–30847.

Jokisch, D. and Jensen, O. (2007). Modulation of gamma and alpha activity during a working memory task engaging the dorsal or ventral stream. *Journal of Neuroscience*, 27(12):3244–3251.

Jung, Y. and Chong, S. C. (2014). Effects of attention on visible and invisible adapters. *Perception*, 43(6):549–568.

Kanizsa, G. (1976). Subjective contours. *Scientific American*, 234(4):48–53.

Kim, I., Hong, S. W., Shevell, S. K., and Shim, W. M. (2020). Neural representations of perceptual color experience in the human ventral visual pathway. *Proceedings of the National Academy of Sciences*, 117(23):13145–13150.

Kim, Y.-J., Grabowecky, M., and Suzuki, S. (2006). Stochastic resonance in binocular rivalry. *Vision research*, 46(3):392–406.

Kirk, R. E. (2013). *Experimental Design: Procedures for the Behavioral Sciences*. Sage Publications, Thousand Oaks, California, USA, 4 edition.

Koffka, K. (1935). *Principles of Gestalt Psychology*. Harcourt, Brace and Company, New York, USA.

Kovács, I., Papathomas, T. V., Yang, M., and Fehér, A. (1996). When the brain changes its mind: Interocular grouping during binocular rivalry. In *Proceedings of the National Academy of Sciences*, volume 93, pages 15508–15511.

Kruger, P. B. (1979). Infrared recording retinoscope for monitoring accommodation. *American Journal of Optometry and Physiological Optics*, 56(2):116–123.

Kunkel, T. and Reinhard, E. (2010). A reassessment of the simultaneous dynamic range of the human visual system. In *In Proceedings of the 7th Symposium on Applied Perception in Graphics and Visualization*, pages 17–24, Los Angeles, USA.

Lamme, V. A. (1995). The neurophysiology of figure-ground segregation in primary visual cortex. *Journal of neuroscience*, 15(2):1605–1615.

Lange, R. and Shevell, S. K. (2020). Does feature integration affect resolution of multiple simultaneous forms of ambiguity? *JOSA A*, 37(4):105–113.

Lee, B. B., Martin, P. R., and Valberg, A. (1988). The physiological basis of heterochromatic flicker photometry demonstrated in the ganglion cells of the macaque retina. *The Journal of physiology*, 404:323–347.

Lee, J. and Maunsell, J. H. (2009). A normalization model of attentional modulation of single unit responses. *PloS One*, 4(2):e4651.

Lee, S. M., Slezak, E., and Shevell, S. (2018). Ambiguity contributes to grouping of color objects. *Journal of Vision*, 18(10):586–586.

Lehky, S. R. and Maunsell, J. H. (1996). No binocular rivalry in the lgn of alert macaque monkeys. *Vision research*, 36(9):1225–1234.

Leopold, D. A. and Logothetis, N. K. (1996). Activity changes in early visual cortex reflect monkeys' percepts during binocular rivalry. *Nature*, 379(6565):549–553.

Li, H. H., Rankin, J., Rinzel, J., Carrasco, M., and Heeger, D. J. (2017). Attention model of binocular rivalry. *Proceedings of the National Academy of Sciences*, 114(30):6192–6201.

Linden, D. E., Bittner, R. A., Muckli, L., Waltz, J. A., Kriegeskorte, N., Goebel, R., Singer, W., and Munk, M. H. (2003). Cortical capacity constraints for visual working memory: dissociation of fmri load effects in a fronto-parietal network. *NeuroImage*, 20(3):1518–1530.

Ling, S. and Carrasco, M. (2006). When sustained attention impairs perception. *Nature Neuroscience*, 9(10):1243–1245.

Logothetis, N. K., Leopold, D. A., and Sheinberg, D. L. (1996). What is rivalling during binocular rivalry? *Nature*, 380(6575):621–624.

Macellaio, M. V., Liu, B., Beck, J. M., and Osborne, L. C. (2020). Why sensory neurons are tuned to multiple stimulus features. *bioRxiv*.

MacLeod, D. I. and Boynton, R. M. (1979). Chromaticity diagram showing cone excitation by stimuli of equal luminance. *JOSA*, 69(8):1183–1186.

Meng, M. and Tong, F. (2004). Can attention selectively bias bistable perception? differences between binocular rivalry and ambiguous figures. *Journal of Visison*, 4(7):539–551.

Monnier, P. and Shevell, S. K. (2003). Large shifts in color appearance from patterned chromatic backgrounds. *Nature neuroscience*, 6(8):801–802.

Moradi, F., Koch, C., and Shimojo, S. (2005). Face adaptation depends on seeing the face. *Neuron*, 45(1):169–175.

Murray, N., Vanrell, M., Otazu, X., and Parraga, C. A. (2013). Low-level spatiochromatic grouping for saliency estimation. *IEEE transactions on pattern analysis and machine intelligence*, 35(11):2810–2816.

Nelson, R. A. and Palmer, S. E. (2007). Familiar shapes attract attention in figure-ground displays. *Perception & Psychophysics*, 69(3):382–392.

Ngo, T. T., Miller, S. M., Liu, G. B., and Pettigrew, J. D. (2000). Binocular rivalry and perceptual coherence. *Current Biology*, 10(4):134–136.

Ni, A. M. and Maunsell, J. H. (2019). Neuronal effects of spatial and feature attention differ due to normalization. *Journal of Neuroscience*, 39(28):5493–5505.

Nichiporuk, N., Knoblauch, K., Abbatecola, C., and Shevell, S. (2017). The lightness distortion effect: Additive conjoint measurement shows race has a larger influence on perceived lightness of upright than inverted faces. *Journal of Vision*, 17(10):245–245.

Olsen, S. R., Bhandawat, V., and Wilson, R. I. (2010). Divisive normalization in olfactory population codes. *Neuron*, 66(2):287–299.

Palmer, S. E. (2002). Perceptual grouping: It's later than you think. *Current Directions in Psychological Science*, 11(3):101–106.

Pasupathy, A. and Connor, C. E. (2002). Population coding of shape in area v4. *Nature neuroscience*, 5(12):1332–1338.

Peiso, J. R. and Shevell, S. K. (2020). Seeing fruit on trees: enhanced perceptual dissimilarity from multiple ambiguous neural representations. *JOSA A*, 37(4):255–261.

Peterson, M. A. (1999). Knowledge and intention can penetrate early vision. *Behavioral and Brain Sciences*, 22(3):389.

Peterson, M. A., Harvey, E. M., and Weidenbacher, H. J. (1991). Shape recognition contributions to figure-ground reversal: Which route counts? *Journal of Experimental Psychology: Human Perception and Performance*, 17(4):1075.

Pinna, B., Uccula, A., and Tanca, M. (2010). How does the color influence figure and shape formation, grouping, numerousness and reading? the role of chromatic wholeness and fragmentation. *Ophthalmic and Physiological Optics*, 30(5):583–593.

Poort, J., Self, M. W., Van Vugt, B., Malkki, H., and Roelfsema, P. R. (2016). Texture segregation causes early figure enhancement and later ground suppression in areas v1 and v4 of visual cortex. *Cerebral cortex*, 26(10):3964–3976.

Pylyshyn, Z. (1999). Is vision continuous with cognition?: The case for cognitive impenetrability of visual perception. *Behavioral and brain sciences*, 22(3):341–365.

Quian Quiroga, R. and Kreiman, G. (2010). Measuring sparseness in the brain: comment on bowers (2009). 117(1):291–297.

Reynolds, J. H. and Heeger, D. J. (2009). The normalization model of attention. *Neuron*, 61(2):168–185.

Ringach, D. L. (2010). Population coding under normalization. *Vision research*, 50(22):2223–2232.

Rokni, D., Hemmelder, V., Kapoor, V., and Murthy, V. N. (2014). An olfactory cocktail party: figure-ground segregation of odorants in rodents. *Nature neuroscience*, 17(9):1225–1232.

Roux, F. and Uhlhaas, P. J. (2014). Working memory and neural oscillations: alpha–gamma versus theta–gamma codes for distinct wm information? *Trends in cognitive sciences*, 18(1):16–25.

Rubin, E. (1915). *Synsoplevede figure: Studier i psykologisk analyse [Perceived figures: Studies in psychological analysis]*. Gyldendal, Nordisk forlag.

Said, C. P. and Heeger, D. J. (2013). A model of binocular rivalry and cross-orientation suppression. *PLoS computational biology*, 9(3):e1002991.

Sanchez-Giraldo, L. G., Laskar, M. N. U., and Schwartz, O. (2019). Normalization and pooling in hierarchical models of natural images. *Current Opinion in Neurobiology*, 55:65–72.

Schiller, P. H. and Lee, K. (1991). The role of the primate extrastriate area v4 in vision. *Science*, 251(4998):1251–1253.

Schnabel, U. H., Bossens, C., Lorteije, J. A., Self, M. W., Op de Beeck, H., and Roelfsema, P. R. (2018). Figure-ground perception in the awake mouse and neuronal activity elicited by figure-ground stimuli in primary visual cortex. *Scientific reports*, 8(1):1–14.

Schwartz, O. and Coen-Cagli, R. (2013). Visual attention and flexible normalization pools. *Journal of Vision*, 13(1):1–24.

Senoussi, M., Moreland, J. C., Busch, N. A., and Dugué, L. (2019). Attention explores space periodically at the theta frequency. *Journal of Vision*, 19(5):22–22.

Shapley, R. and Hawken, M. J. (2011). Color in the cortex: single-and double-opponent cells. *Vision research*, 51(7):701–717.

Shapley, R., Nunez, V., and Gordon, J. (2019). Cortical double-opponent cells and human color perception. *Current Opinion in Behavioral Sciences*, 30:1–7.

Shevell, S. K. (2019). Ambiguous chromatic neural representations: perceptual resolution by grouping. *Current Opinion in Behavioral Sciences*, 30:194–202.

Shevell, S. K. and Martin, P. R. (2017). Color opponency: tutorial. *JOSA A*, 34(7):1099–1108.

Shpiro, A., Moreno-Bote, R., Rubin, N., and Rinzel, J. (2009). Balance between noise and adaptation in competition models of perceptual bistability. *Journal of computational neuroscience*, 27(1):37–54.

Skottun, B. (2013). On using isoluminant stimuli to separate magno-and parvocellular responses in psychophysical experiments—a few words of caution. *Behavior research methods*, 45(3):637–645.

Slezak, E., Coia, A., and Shevell, S. (2018). Perceptual grouping of dichoptic plaids. *Journal of Vision*, 18(10):442–442.

Slezak, E. and Shevell, S. K. (2018). Perceptual resolution of color for multiple chromatically ambiguous objects. *JOSA A*, 35(4):B85–B91.

Slezak, E. and Shevell, S. K. (2020). Grouping ambiguous neural representations: neither identical chromaticity (the stimulus) nor color (the percept) is necessary. *JOSA A*, 37(4):A97–A104.

Solomon, S. G. and Kohn, A. (2014). Moving sensory adaptation beyond suppressive effects in single neurons. *Current Biology*, 24(20):R1012–R1022.

Solomon, S. G. and Lennie, P. (2005). Chromatic gain controls in visual cortical neurons. *Journal of Neuroscience*, 25(19):4779–4792.

Switkes, E. (2008). Contrast salience across three-dimensional chromoluminance space. *Vision research*, 48(17):1812–1819.

Teki, S., Chait, M., Kumar, S., von Kriegstein, K., and Griffiths, T. D. (2011). Brain bases for auditory stimulus-driven figure–ground segregation. *Journal of Neuroscience*, 31(1):164–171.

Tong, F., Meng, M., and Blake, R. (2006). Neural bases of binocular rivalry. *Trends in cognitive sciences*, 10(11):502–511.

Toppino, T. C. (2003). Reversible-figure perception: Mechanisms of intentional control. *Perception & psychophysics*, 65(8):1285–1295.

Treisman, A. (1962). Binocular rivalry and stereoscopic depth perception. *Quarterly Journal of Experimental Psychology*, 14(1):23–37.

Treisman, A. (1985). Preattentive processing in vision. *Computer vision, graphics, and image processing*, 31(2):156–177.

Treisman, A. (2006). How the deployment of attention determines what we see. *Visual cognition*, 14(4-8):411–443.

Treisman, A. M. and Gelade, G. (1980). A feature-integration theory of attention. *Cognitive psychology*, 12(1):97–136.

Treue, S. and Maunsell, J. H. (1999). Effects of attention on the processing of motion in macaque middle temporal and medial superior temporal visual cortical areas. *Journal of Neuroscience*, 19(17):7591–7602.

van Ee, R. (2009). Stochastic variations in sensory awareness are driven by noisy neuronal adaptation: evidence from serial correlations in perceptual bistability. *JOSA A*, 26(12):2612–2622.

Van Essen, D. C., Anderson, C. H., and Felleman, D. J. (1992). Information processing in the primate visual system: an integrated systems perspective. *Science*, 255(5043):419–423.

Vanmarcke, S. and Wagemans, J. (2015). Rapid gist perception of meaningful real-life scenes: Exploring individual and gender differences in multiple categorization tasks. *i-Perception*, 6(1):19–37.

Verhoef, B.-E. and Maunsell, J. H. (2017). Attention-related changes in correlated neuronal activity arise from normalization mechanisms. *Nature neuroscience*, 20(7):969–977.

Wachtler, T., Sejnowski, T. J., and Albright, T. D. (2003). Representation of color stimuli in awake macaque primary visual cortex. *Neuron*, 37(4):681–691.

Wang, X.-J., Liu, Y., Sanchez-Vives, M. V., and McCormick, D. A. (2003). Adaptation and temporal decorrelation by single neurons in the primary visual cortex. *Journal of neurophysiology*, 89(6):3279–3293.

Wark, B., Lundstrom, B. N., and Fairhall, A. (2007). Sensory adaptation. *Current opinion in neurobiology*, 17(4):423–429.

Webster, M. A. (2015). Visual adaptation. *Annual review of vision science*, 1:547.

Webster, M. A. and Mollon, J. (1995). Colour constancy influenced by contrast adaptation. *Nature*, 373(6516):694–698.

Werner, A. (2014). Spatial and temporal aspects of chromatic adaptation and their functional significance for colour constancy. *Vision research*, 104:80–89.

Wertheimer, M. (1938). Laws of organization in perceptual forms. In Ellis, W. D., editor, *A source book of Gestalt psychology*. Kegan Paul, Trench, Trubner & Company. (Original work published in 1923 as Untersuchungen zur Lehre von der Gestalt II, in Psychologische Forschung 4, 301–350).

Wilson, H. R., Blake, R., and Lee, S.-H. (2001). Dynamics of travelling waves in visual perception. *Nature*, 412(6850):907–910.

Wolfe, J. M. (2020). Visual search: How do we find what we are looking for. *Annual review of vision science*, 6(1):539–562.

Womelsdorf, T., Fries, P., Mitra, P. P., and Desimone, R. (2006). Gamma-band synchronization in visual cortex predicts speed of change detection. *Nature*, 439(7077):733–736.

Wyszecki, G. and Stiles, W. (1982). *Color Science*, volume 8. Wiley, New York.

Zhang, Y., Meyers, E. M., Bichot, N. P., Serre, T., Poggio, T. A., and Desimone, R. (2011). Object decoding with attention in inferior temporal cortex. *Proceedings of the National Academy of Sciences*, 108(21):8850–8855.

Zohary, E. (1992). Population coding of visual stimuli by cortical neurons tuned to more than one dimension. *Biological cybernetics*, 66(3):265–272.